UNIVERSITY OF CALGARY

A Model to Predict the Undrained Response of Loose Gassy Sand

by

Shanmugalingam Mathiroban

A THESIS

SUBMITTED TO THE FACULTY OF GRADUATE STUDIES

IN PARTIAL FULFILMENT OF THE REQUIREMENTS FOR THE

DEGREE OF MASTER OF SCIENCE

DEPARTMENT OF CIVIL ENGINEERING

CALGARY, ALBERTA

DECEMBER, 2004

UNIVERSITY OF CALGARY

FACULTY OF GRADUATE STUDIES

The undersigned certify that they have read, and recommend to the Faculty of Graduate Studies for acceptance, a thesis titled "A Model to Predict the Undrained Response of Loose Gassy Sand" submitted by Shanmugalingam Mathiroban in partial fulfillment of the requirements for the degree of Master of Science in Geotechnical Engineering.

Joseph L. H. Grozic

Dr. J.L.H.Grozic, Department of Civil Engineering (Supervisor)

R.G. Wan

Dr. R.G.Wan, Department of Civil Engineering

M. Pooladi-Darvish

Dr. M.Pooladi-Darvish, Department of Chemical and Petroleum Engineering

14 Dec 04

Date

ABSTRACT

Submarine slopes in deltaic environments often consist of loose sand containing gas bubbles within voids. It has been speculated that the presence of gas bubbles is one of the causes of submarine slope instability problems. This thesis studies the effect of presence of gas bubbles on undrained behaviour of loose sand.

The presence of gas bubbles increases the compressibility of the pore fluid. Accordingly, gassy soil can be considered as saturated soil with compressible pore fluid. Gassy soils exhibit both volumetric strain and pore pressure changes during undrained shearing. This response has been found to be due to the partial (internal) drainage, a phenomenon that occurs due to the increased compressibility of the gas-water mixture.

An elasto-plastic stress-strain model for sand has been modified to account for the effect of increased compressibility that results in volumetric strain and pore pressure change during an undrained shearing of loose gassy sand. This has been achieved by coupling volumetric strain due to gas compression/expansion and dissolution/ex-solution with volumetric strain during the yielding of sand. The model simulation shows that presence of gas bubbles increases the undrained shear strength of soil, and this increase is retarded by excess pore pressure that is associated with gassy soil.

ACKNOWLEDGEMENT

I would like to express my sincere gratitude to my supervisor, Dr. Jocelyn L.H.Grozic, for her guidance in academic research, encouragement in career development and her tireless effort in founding the gas hydrate research laboratory with brand new testing equipments. Above all, I admire her personal involvement and generosity with her students, thank you Dr.Grozic.

I would like to thank Dr. S.M.R. Imam for providing me with the digital version of the basic model and also for his useful suggestions. I would also like to thank Dr.R.Wan and Dr.R.C.K.Wong from the Department of civil engineering for helping me with this research endeavour.

I gratefully acknowledge the financial support provided by Natural Science and Engineering Research Council of Canada (NSERC) and teaching assistantship provided by the Department of civil engineering, University of Calgary. I am also grateful to the Faculty of Graduate studies for giving me this opportunity and awarding me the Graduate Travel Award. Young Engineers' Award for the year 2004, given by Calgary Chapter of Canadian Geotechnical Society (CGS), which gave me the opportunity to present my research in a national conference, is also gratefully appreciated.

I would also like to thank my friends, colleagues and research group-mates who helped me during this past two years for my research. A special thanks to my fellow graduate students for the useful discussions on research topics.

Finally, I would like to express my deepest gratitude to all my family members and friends for their initiation to pursue graduate studies and their genuine interest in my academic career; especially to my wife, and to my uncle Dr.S.Premasri. I do not have words either to describe or to acknowledge my parents' aspiration for my academic achievements.

To my mathematics teacher, 'Vector' Velautham

TABLE OF CONTENTS

LIST OF TABLES

LIST OF FIGURES

LIST OF SYMBOLS, ABBREVIATIONS, AND NOMENCLATURE

A	Skempton's pore pressure parameter
ASTM	American Society for Testing of Materials
B	Skempton's pore pressure parameter
BSR	Bottom Simulating Reflector
CANLEX	Canadian Liquefaction Experiment
CDS	Constant Deviatoric Stress
CU	Consolidated Undrained
C_C	Coefficient of Compression or slope of e vs ln(p) plot
CO_2	Carbon Dioxide
c_u	Undrained shear strength of soil
d	Incremental
e	Void ratio
e_r	Reference void ratio
e_{ss}	Steady state void ratio
e_μ	Value of normalised void ratio corresponding to inter-particle friction angle in $\mathrm{Sin}\varphi_p$ vs e_μ graph.
FRD	Fraser River Delta
G	Elastic shear modulus
H	Henry's coefficient of solubility constant
h	Henry's volumetric coefficient of solubility constant
K	Elastic bulk modulus

k_f	Variation of the maximum friction angle at failure with current state parameter
km	Kilometer
k_m	Variation of peak friction angle with void ratio
kPa	Kilopascal
k_{PT}	Variation of friction angle at phase transformation with current state parameter
LCC	Limiting Compression Curve
M_d	Mass of dissolved gas
M_p	Stress ratio at which peak value of q occurs
M_f	Stress ratio at failure
NC	Normal Consolidation
NGI	Norwegian Geotechnical Institute
n	An elastic parameter
n_0	Initial porosity
P	Absolute pressure of gas
PT	Phase Transformation
P-UESP	Peak point of Undrained Effective Stress Path
P-YS	Peak point of Yield Surface
P_g	Absolute pressure of gas
p	Mean normal effective stress
p_a	Atmospheric pressure
p_c	Consolidation pressure
p_f	Size of the yield surface, if current state is the failure state

q	Deviator stress
S	Degree of water saturation ($S = \frac{V_w}{V_v}$); accordingly, 1-S is the degree of gas saturation
SEM	Scanning Electronic Micrograph
T	Surface tension
UESP	Undrained Effective Stress Path
u	Pore pressure
u_a	Pore air pressure
u_w	Pore water pressure
V	Volume
V_d	Volume of dissolved gas
V_g	Volume of gas
V_{fg}	Volume of free and dissolved gas
V_T	Volume of soil
V_{Tg}	Volume of total gas
V_v	Volume of voids
V_w	Volume of water
YS	Yield Surface
1-D	One Dimensional
β	Compressibility parameter of sand in Imam's (1999) model
β_g	Compressibility of gas
β_T	Compressibility of soil skeleton
β_w	Compressibility of water

Γ	Intercept of the line of best fit in void ratio vs logarithmic mean stress space.
ε_1	Major principle strain
ε_3	Minor principle strain
ε_a	Axial strain
ε_v	Volumetric strain
ε_q	Deviatoric strain
η	Stress ratio, p/q
λ	Slope of the line of best fit in void ratio vs logarithmic mean stress space.
ρ_v	Average pore size
σ'	Effective stress
σ'_1	Effective major principle stress
σ'_3	Effective minor principle stress
φ_{cv}	Friction angle at constant volume
φ_f	Friction angle at failure state
φ_m	Mobilised friction angle
φ_{PT}	Friction angle at phase transformation
φ_μ	Intrinsic friction angle
ψ	State parameter

CHAPTER 1

INTRODUCTION

The scope of geotechnical engineering has been broadened due to increased development activities in the near and offshore. In recent years, offshore development activities such as construction of sea floor infrastructures (e.g. communication cables, oil pipe lines, and offshore platforms) and the search for oil and gas reserves in increasingly deep water have widened the horizon of geotechnical engineering in marine environments. Constructions of marine infrastructures, as well as oil and gas development activities, require an evaluation of potential submarine geohazards. In this context, submarine landslides have become a major concern for developers which has instigated renewed research on submarine slides.

While studying the causes of submarine landslides, researchers found the presence of occluded gas bubbles in the vicinity of most slide areas (for example, Fraser River delta, British Columbia; Mississippi River delta, Lousiana; Cape Fear land slide, North Carolina; and Storregga submarine mass movement, Norwegian continental margin). An attempt to associate the presence of free gas in bubble form to submarine mass movement resulted in several views, some of which are even contradictory. In order to understand the behaviour of marine sediments, a few experiments have been carried out on re-constituted soil that contains discrete gas bubbles.

Experiments were carried out in University of Oxford, University of Alberta and in the Norwegian Geotechnical Institute (NGI) to study the influence of free gas in marine sediments. A deviation of this type of soil from a saturated soil response was observed where the undrained shear strength of soil with free gas was found to increase or decrease compared to saturated soil. At the same time, several models were proposed to predict the behaviour of soil that contains occluded gas bubbles, none of which addressed all aspects of marine sediments (such as gas solubility, surface tension and excess pore pressure) at the same time. This study focuses on incorporating the effect of gas bubbles on the undrained behaviour of sand using an existing model developed for saturated loose sand by Imam (1999). A Model has been developed to predict the response of loose gassy sand that contains discrete gas bubbles within the soil voids – a three phase continuum mostly found in deltaic environments. Imam (1999)'s elasto-plastic stress-strain model has been selected as the base model. The model results show that the undrained shear strength of loose sand is increased due to presence of discrete gas bubbles. The results also indicate that the excess pore pressure that exists in marine sediments influences the response of loose gassy sand during undrained shearing. This model can be used to predict the instability potential of deltaic slopes, and hence safe and economic offshore development activities can be planned and executed.

1.1 Definition of gassy soil

Soil mechanics is the study of the behaviour of particulate materials with particular emphasis to strength behaviour, volume change and flow through porous media. At the early stages of development of soil mechanics, study was confined to two broad categories:

dry soil (solid particles and air) and wet soil (solid particles and water). The study on wet soil (normally with water) progressed rapidly with Terzaghi's principle of effective stress, which states that 'upon application of total stress to a soil continuum, the stress taken by soil skeleton is the difference between total stress and pore water pressure'. This can be expressed in mathematical form as:

$$\sigma' = \sigma - u \qquad [1.1]$$

where σ = total stress, u = pore water pressure and σ' = effective stress or average inter-granular stress. Terzaghi's principle is based on negligible particle contact area. Materials for which particle contact area can not be neglected (for example, in the case of cemented particles), Equation (1.1) needs modification to account for contact area.

Successful application of the principle of effective stress to saturated soil prompted several researchers to study the behaviour of unsaturated soil and come up with a similar expression. Unsaturated soil is a three-phase system; pore voids occupied by water and air along with the soil skeleton. These soils are commonly encountered in geotechnical engineering situations such as earth fill dams, highways and airport runways where evaporation of water makes the soil unsaturated. Being in contact with atmospheric air, pore air pressure is usually at atmospheric pressure and pore water pressure is negative with respect to pore air pressure, denoted by 'suction pressure' or 'matric suction'. In extending the effective stress concept to unsaturated soil, several equations have been proposed, out of which the expression suggested by Bishop (1959) gained widespread reference. Bishop (1959) proposed effective stress for unsaturated soil as:

$$\sigma' = (\sigma - u_a) + \psi(u_a - u_w) \qquad [1.2]$$

where u_a = pore air pressure and ψ = material parameter that is related to degree of saturation of the soil. Dependency of this parameter on various factors such as soil type and wetting and drying cycle resulted in researchers suggesting different expressions effective stress for unsaturated soil (e.g. Fredlund and Morgenstern 1977). Nevertheless, Equation (1.2) is widely used in practice. For soil with water content higher than optimum or at higher degree of saturation, ψ is closer to unity and pore fluid pressure is approximately equal to pore water pressure.

Recently, with the exploration of oil and gas from deep ocean beds and development activities in offshore environments, a new class of soil emerged in geotechnical engineering, gassy soil. Though gassy soil consists of three phases (soil, water and gas) like unsaturated soil, the following two distinct characteristics of this soil made it different from engineering behaviour of unsaturated soil:

(i) Compared to the air-water mixture in unsaturated soil, large amounts of gas are dissolved in the pore fluid of gassy soils due to the high solubility of the guest gas (mostly methane) at the in situ pressure of the marine environment. In case of unsaturated soil, air solubility in water at atmospheric pressure and room temperature is very low.

(ii) Unlike in unsaturated soil, the gas phase is discontinuous in gassy soil; gas exists either in dissolved form or as free gas in the form of occluded bubbles and large cavities. Upon reduction of pore pressure to near atmospheric pressure (in the case of ship board sampling, for example), a large amount of gas is released.

Sobkowikz (1982) used the term GASSY SOIL to denote this type of soil*. Abundance of dissolved gas is the main feature of the gassy soil. Methane is the commonly encountered gas in marine environments because of bacterial and thermal activity in organic rich sediment. Other than methane, carbon dioxide, hydrogen sulphide and ethane have also been traced in marine sediments.

---

* There exists a discrepancy between Sobkowicz's definition of gassy soil and what has been considered as gassy soil by researchers from University of Oxford. According to Sobkowicz's definition, soil matrix that gives response 'A' (as in Figure 2.2) upon undrained unloading is known as gassy soil. But, Wheeler (1988) considered gassy soil as bubbles in occluded form either within pore voids (Type C soil, see Figure 1.1a) or as large cavities spanning soil skeleton (Type D soil, see Figure 1.1b) irrespective of how it behaves in undrained unloading. Type C soil is a three phase continuum in which gas phase is discontinuous and liquid phase is continuous.

In analyzing behaviour of gassy soil, Wheeler (1988) suggested two different types of gassy soil for coarse grained soil and fine grained soil. Accordingly, free gas exists in deltaic environment (Chillarige et al. 1997) and oil sand tailings pond (Fourie et al. 2001) due to biogenic activity; bubbles exist within the pore voids without influencing the solid surface. Type D soil exists predominantly in fine grained soils, most commonly found in deep sea environments. In Type D soil, gas bubbles are larger than the pore voids and bubbles span soil skeleton, making a contact angle that depends on the difference between pore gas pressure and pore water pressure.

Detecting the presence of gas in marine sediments has advanced from early visual observation of gas exsolution during shipboard sampling to geo-physical techniques. At early stages, core expansion of deep sea samples were observed when reduced to or exposed to atmospheric pressure. In estuaries and deltas, the presence of biogas was inferred from bubbles evolving from bottom to top. Now acoustic penetration techniques are being used to detect the presence of gas in sediments and to analyse the structure and behaviour of gassy soil. Based on reflection of acoustic signal transmitted from sonar devices, properties and constituents of sub sea sediments can be inferred. The presence of gas bubbles in soil significantly affects the acoustic signal attenuation and based on acoustic speed, volume fraction of gas bubble can be estimated (Sills et al. 1991).

1.2 Need for the study

Organic materials buried to depth millions of years ago are the major source of gas in deep marine sediments. Over the time with geological changes such as high pressure and low temperature, these materials are converted in to hydrocarbon products, mostly methane – a process known as 'thermogenic activity'. At a particular pressure-temperature regime (see Figure 1.2), methane-water mixture forms a solid, ice-like crystalline compound known as gas hydrate. Upon sea level change or increase in global temperature, gas hydrate dissociates, releasing free gas to the deep sea bed. On the other hand, availability of abundant organic rich sediment in estuaries and deltaic environment favors bacterial activity, generating biogas, mostly methane – a process known as 'biogenic activity'.

Though the presence of gas is not common in land, there are several cases where the presence of gas has been reported to cause engineering challenges. The presence of gas bubble has been detected in the vicinity of major submarine slope failure areas. Some of the reported case histories in which the presence of gas bubbles within soil has been established are given below:

1.2.1 Gas in oil sands:

Early discovery of gassy soil occured in the oil sands during drilling and excavation. The Athabassca region in Northern Alberta, Canada is enriched with oil sand – 'a dense uncemented fine grained sand with gas saturated bitumen' (Dusseault 1979). Hardy and Hemstock (1963) were the first to report the effect of gas exsolution during sampling (or pressure reduction) that resulted in shear strength reduction. Dusseault (1979) observed core expansion in the oil rich zone of the core sample compared to the oil free zone where no radial expansion was observed. Other than core expansion, excessive heave and softening of oil sand upon excavation for foundation, settlement upon loading (Hardy and Hemstock 1963) and delayed instability of oil sand slopes due to time dependent behaviour of gas in oil sand (Dusseault and Morgenstern 1978) has also been reported.

All the phenomena described above are evidence of the gas saturated bitumen in the oil sands. Upon unloading below liquid-gas saturation pressure (see section 1.4(b)), the gas expands, causing overall volume expansion and pore pressure generation. Recently, experiments conducted on Syncrude oil sand tailings as a part of Canadian Liquefaction Experiment (CANLEX) project highlighted evidence of discrete gas bubbles within voids below phreatic surface (Fourie et al. 2002). Scanning Electron Micrograph (SEM) images showed that these bubbles are small (0.001mm – 0.05mm) compared to average pore size of tailings sand. Though the gas was found to be predominantly air, bio gas, mostly methane and carbon dioxide were significantly higher than available in the atmosphere. It was speculated that the reason for this elevated carbon dioxide and methane concentration was due to bacterial activity that uses residual hydrocarbons as an energy source.

1.2.2 Gas in estuarine and deltaic environments:

Biogas, mostly methane occurs in marine sediments owing to oxygen free environment and sediment being enriched with organic matter that favors anerobic digestion. Methane (as dissolved gas or free gas, occluded within sediments) exists in shallow water for a long period of time (Hulbert and Bennet 1975), since methane oxidation is possible in aerobic environment only (Byron, 1974), see Figure (1.3).

Several deltaic slope instability problems have been linked to presence of occluded gas within deltaic sediments. In the early investigation of submarine slope failures (such as Howe island flow slide, British Columbia; and submarine slope failures in Norwegian fjords), liquefaction susceptibility of loose sand was suggested as the reason for slope failure (Terzaghi 1956; and Bjerrum 1971). Later, it was found that presence of gas bubble is **one of the** reasons for submarine slope failures (Chillarige et al. 1997). Three major deltaic slope failures have been demonstrated here, where the presence of occluded gas bubbles within pore void has been suggested as a reason for slope instability.

- Fraser River delta, British Columbia, Canada.

  Five major slides have been reported in Fraser River delta between 1970 and 1985 (McKenna et al. 1992). Fraser River in British Columbia carries approximately 88% of the sediment bearing water (Mckenna et al., 1992) to the delta in west cost of Vancouver, with average sedimentation rate of 2.16 cm/year. The delta hosts several infrastructure facilities like ferry terminal, communication cables and shipping and fishing facilities. In addition to loose sand deposit, evidence of free methane gas, with degree of saturation ranging from 85% to 100% has been detected (Christian et al. 1997). Mean tidal variation of 2.6 m with a maximum of 5.4 m has been reported. Though the delta lies within one of the most seismically active area in Canada, no seismic activity was recorded for the recent submarine landslide in 1985. In analyzing the instability of Fraser River delta, Christian et al. (1997) concluded that residual pore pressure in the sediment during tidal draw down due to the existence of free gas could have led to the triggering of these flow slides. Figure (1.4) shows 75% attenuation and a 1 hour phase lag of pore pressure variation at 5m below sea bed, measured at Fraser River delta, which may be due to the increased compressibility of the sea bed and the time dependent behaviour of free gas.

- Klamath River delta, California, United States.

The Klamath River in western United States, California contributes a high sedimentation rate (about 3.56×10^6 metric tons per year) to the delta. Following the earthquake on November 8, 1980, sediment failure and a large quantity of released gas in the delta was detected. Field and Jennings (1987) suggested that there was a relationship between the observed gas seeps and the liquefaction failure.

- Missisippi River delta, California, United States.

The Mississippi River is the largest river system in North America with an average water discharge of 15,400 m^3/s to the delta in the coast of Lousiana, Gulf of Mexico. 210 to 680 million tons per year of sediments are discharged to the delta, 90% of which is fine sand (Coleman et al. 1990). The delta is highly susceptible to submarine slope failure due to powerful hurricanes that develop in the Gulf of Mexico and traverse through the Mississippi River delta. The destruction of one offshore platform and damage to two others during a submarine landslide during hurricane 'Camillee' in 1969 drew increased attention to this issue from both industrialists and academics. In addition to excess pore pressures, large concentrations of gasses (due to abundant fine-grained organic matter) have been suggested as a triggering mechanism for the submarine slope failures (Coleman et al. 1990).

1.2.3 Gas in the deep seabed:

Organic sediments buried and trapped under the deep ocean bed millions of years ago are responsible for methane due to biogenic activity in the deep seabed. When a methane-water mixture is subjected to a particular temperature-pressure regime (Figure 1.2), i.e., low temperature and high pressure, the mixture forms a solid crystalline structure known as gas hydrate (Claypool and Kaplan 1974). Gas hydrate cannot exist below a certain depth from seabed because the temperature increase due to the geo-thermal gradient exceeds the gas hydrate stability zone in temperature-pressure regime. Below this depth, methane exists in gaseous form*.

---

* This phenomenon of gas hydrate layer with under lying methane gas in deep sea appears as a Bottom Simulating Reflector (BSR) on the seismic profile, since the hydrate layer and free gas have differing seismic reflection characteristics.

While gas hydrate has been thought of as a potential energy source, numerous deep sea failures have been reported where decomposition of gas hydrate has been thought of as the cause of failure. Hydrate decomposition may be due to a sea floor lowering or an increase in temperature due to global warming. For illustration purposes, the following failure case histories have been presented.

- Cape Fear landslide, North Carolina.

  The Cape Fear landslide on the North Carolina continental shelf of Carolina Trough was discovered in 1970 with echo-sounder profiles and cores. Carolina Trough was formed following the initial drifting of African and North American continent 140 millions years ago (Popenoe et al. 1990). In the vicinity of the Carolina Trough, the free gas trapped beneath the gas hydrate layer was reported based on interpretation of the seismic reflection profile. Decomposition of gas hydrate layer due caused by post global warming or sea level lowering has been suggested as a reason for this submarine landslide (Popenoe et al. 1990)

- Storregga slide, Norwegian continental margin, Norway.

  The Storegga submarine slides occurred thousands of years ago on the continental slope off the coast of western Norway near Scotland (Figure 1.5); three major submarine landslides occured within 30,000 years. Earthquakes, together with gas released from the decomposition of gas hydrates are considered to be the most likely triggering mechanisms for the slides (Mienert et al. 2003).

In addition to being a threat to marine infra structures and oil and gas development offshore, submarine landslides are a huge threat to coastal habitats and eco-system. The surge wave generated due to submarine landslides in deltaic fronts travels upstream of the river and causes flooding. In the same manner, a huge wave (known as 'Tsunami') can be generated due to the impulsive vertical motion of the sea water column during deep sea slope failures. For example, a Tsunami wave generated due to the Storregga submarine slide hit the northern coast of Scotland.

1.2.4 Gas trapped in land.

Like bio gas buried in the deep sea bed, there are situations encountered in which trapped bio gas caused problems on land. Upon excavation for engineering works, gas expands and causes serious problems. Excessive heave during an excavation up to 10m depth for Alto Lazio nuclear power plant foundation in Italy was observed. The underlying silty sand was found to contain carbon dioxide gas in solution within the pore fluid; the degree of saturation of the pore fluid was found to be about 95%. During a borehole investigation at Sarnia area in Southwestern Ontario, Canada, venting of gas from the soil pores was observed (Dittrich et al. 2002). In addition, contaminant landfills are found to include or generate biogas. This has been a concern in designing confinement capacity of landfills as well as settlement characteristics (Sills and Conzalez 2001).

The failure case histories listed above emphasizes the importance of understanding the failure potential of soils containing free gas in occluded form. The objective of this study is to develop a model that can predict the undrained response of loose gassy sand.

1.4. Terminology used:

Most of the engineering terminologies used in this thesis are commonly used in classical soil mechanics practice; however, due to the subject matter there are some special terms that will be explained here.

(a) Partial drainage:

Based on the flow boundary condition applied to the soil element under consideration, most of the conventional soil mechanics problems are confined to 'drained' and 'undrained' analysis. 'Drained condition' refers to the situation in which pore fluid is permitted to enter/exit through the boundary and the term 'undrained condition' refers to the flow boundary condition in which pore fluid is not permitted to enter/exit the system. In practice, short term analysis corresponds to the undrained condition and long term analysis corresponds to the drained condition. In conventional saturated soil mechanics, the pore fluid (most of the time water) is assumed to be incompressible whereby Skempton's B parameter is approximated to be equal to unity in undrained loading. Due to presence of gas bubbles, there will be drastic change in compressibility of a gas-liquid mixture. This leads to volumetric strain as well as pore pressure development, the one similar to drainage controlled shearing (where drainage is controlled such that to allow for some volumetric strain) of saturated soil. Vaid and Eliadorani (1988) referred to this as partial drainage shearing. The phenomena of volume change and pore pressure change in gassy soil under undrained loading is **analogous to partial drainage** loading of saturated soil.

(b) Volumetric coefficient of solubility (h):

When partially miscible gas and liquid is in equilibrium, a certain amount of gas molecules dissolve into the liquid. The amount of gas that will be dissolved in the liquid is governed by Henry's law, which states that the volume of dissolved gas is proportional to the volume of liquid at a constant temperature and pressure.

Fredlund and Rahardjo (1993) used the piston and porous stone analogy (see Figure 1.6) to explain this phenomenon. The system consists of a porous stone at the base that corresponds to liquid and a frictionless piston for applying pressure. Porous stone has a fixed volume of pores (v_d) which mimics the Henry's volumetric coefficient of solubility ($h = v_d/V$). Above the porous stone, the gas is in equilibrium and there is an imaginary valve at the boundary between gas and liquid. Upon application of load to the piston while the valve is closed, the free gas volume decreases according to Boyle's law. If we open the valve, gas diffuses in to the pores according to Henry's law. Upon application of further load, eventually all the gas will diffuse into the porous stone. This pressure is known as the liquid-gas saturation pressure.

(c) Dissolved gas saturation:

From section (b) above, it is understood that the solubility coefficient of the liquid-gas mixture (h) determines the maximum amount of gas that can be dissolved in a fixed volume of water at any pressure. The pressure at which this occurs is known as the 'liquid-gas saturation pressure' ($P_{l/g}$) or the 'bubble pressure'. Dissolved gas saturation is the ratio of the amount of gas dissolved to the maximum amount of gas that can dissolve (Rad et al. 1994). Depending on whether ambient pressure (P) is less than or greater than liquid-gas saturation pressure ($P_{l/g}$), free gas will exist or the liquid will be 'under saturated' with gas.

1.5 Thesis objective.

The case histories presented in this chapter depict the importance of understanding the role of gas bubbles in slope instability problems. Several experiments have been carried out in the recent past to understand the behaviour of gassy soil. These experimental findings concluded that undrained shear strength of gassy soil is increased or decreased depending on gas pressure (Wheeler 1988), confining pressure (Wheeler 1988), and initial void ratio with respect to steady state void ratio (Rad et al. 1994; and Grozic 1999).

The objective of this thesis is to develop a numerical model that can predict the undrained response of loose gassy sand where gas bubbles are entrapped within pore voids (Type C soil) or for gassy soil with degrees of water saturation less than 85%.

1.6 Scope of the thesis.

The scope of the thesis is limited to coarse-grained soils that contain free gas in occluded form. Field studies show that in deltaic environments bubbles produced during bacterial activity are small enough to be confined within pore voids without making contact with soil skeleton (i.e. Type C soil) and degrees of water saturation are above 85%. The effect of occluded gas bubbles will be incorporated into an existing elasto-plastic stress-strain model. Only the equilibrium behaviour of gassy soil will be considered, which means that Boyle's law and Henry's law effects are assumed to be time independent. Though the model is developed for the conventional triaxial space only, the response for other loading conditions can be predicted by incorporating the appropriate form of the flow rule and hardening rule. The Model parameters for both Ottawa sand and Fraser River sand are selected/estimated from previous studies and experimental observations.

In addition, the thesis is limited to behaviour of gassy soil in 'undrained' response where no fluid is allowed to flow in and out of the system, but with compressible fluid.

1.7 Outline of the thesis

The case histories of submarine slope failure described previously depict the necessity of understanding the role of gas bubbles on the liquefaction potential of sandy slopes. Most of these failures have been found to occur in undrained conditions or due to short term external perturbations like sudden tidal drawdown or high sedimentation rates. Only a handful of previous studies have been undertaken in order to understand the role of gas bubbles/cavities in undrained loading and unloading. ***Chapter 2*** illustrates the previous studies (both experimental and numerical) case by case, discusses special features of the studies and reviews the results. The gap between experimental observation and numerical studies is highlighted and the aim of the research is briefly explained at the end of this chapter.

As stated in section (1.5), the developed model is limited to loose sand. Both experimental observation and model predictions show that loose sand exhibits a definite peak behaviour during undrained loading. Several stress-strain models have been proposed to predict the behaviour of sand. ***Chapter 3*** describes the basic elements of an elasto-plastic stress-strain model proposed by Imam (1999) to predict the liquefaction potential of loose sand. A brief description on how to determine the model parameters is given at the end, with particular emphasis on Fraser River sand.

In this thesis, Type C soil (see Figure 1.2(b)) has been modeled by idealizing it as saturated soil with a compressible pore fluid. The effect of a compressible pore fluid is that both volume change and pore pressure development occurs during 'undrained' loading- a condition known as partial(internal) drainage. In ***Chapter 4***, the gassy soil effect has been incorporated into the model described in ***Chapter 3*** by coupling the volumetric strain due to gas compression and according to Boyle's law and ex-solution/dissolution according to Henry's law with the volumetric strain in the model. The developed model was calibrated against the experimental result for loose gassy Ottawa sand reported by Grozic (1999). Due to a limited availability of experimental data the model is compared with other reported result for loose gassy Ottawa sand. Finally, the response of loose gassy Fraser River sand is simulated.

Chapter 5 summarizes the thesis and presents a general discussion and conclusion pertaining to the behaviour of gassy soil. The validity of the assumptions is discussed and recommendations for future work are outlined.

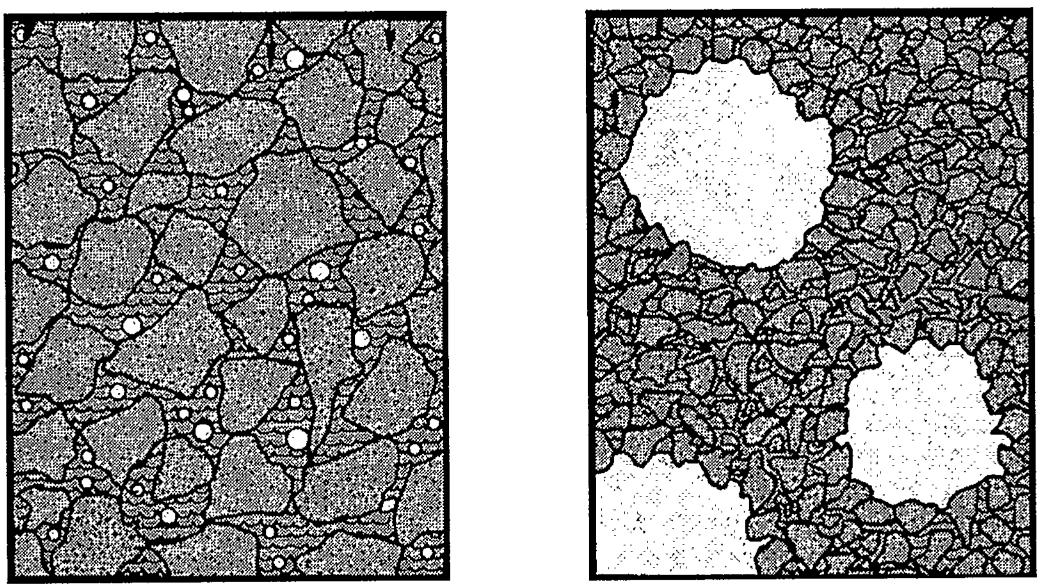

(a) (b)

Figure 1.1 - Possible structures of gassy soil (a) in coarse grain soil, bubbles are smaller than average pore voids within pore voids and hence contained within voids; (b) in fine grain soil, spanning soil skeleton (after Wheeler 1988). Note that Figures are in different scales.

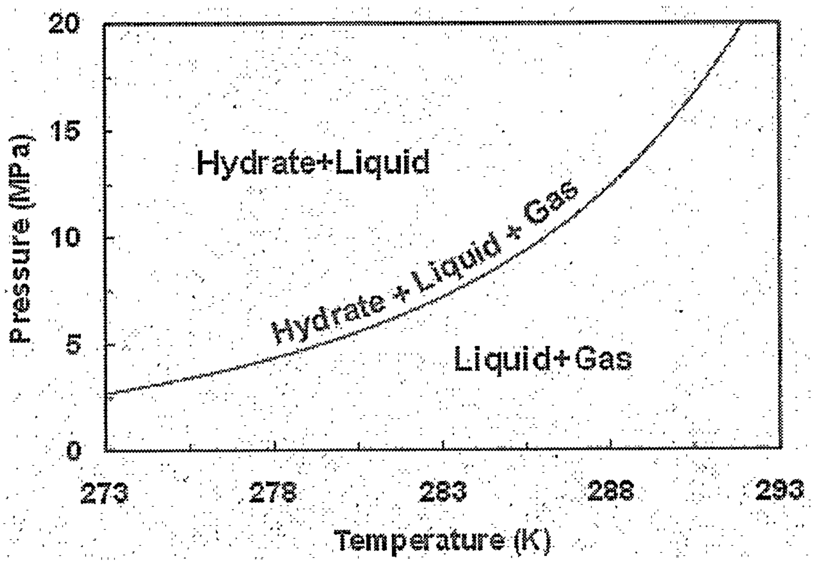

Figure 1.2 - Pressure-temperature regime for stability of gas hydrate (Centre for gas hydrate research: http://www.pet.hw.ac.uk/research/hydrate/hydrates_where.html).

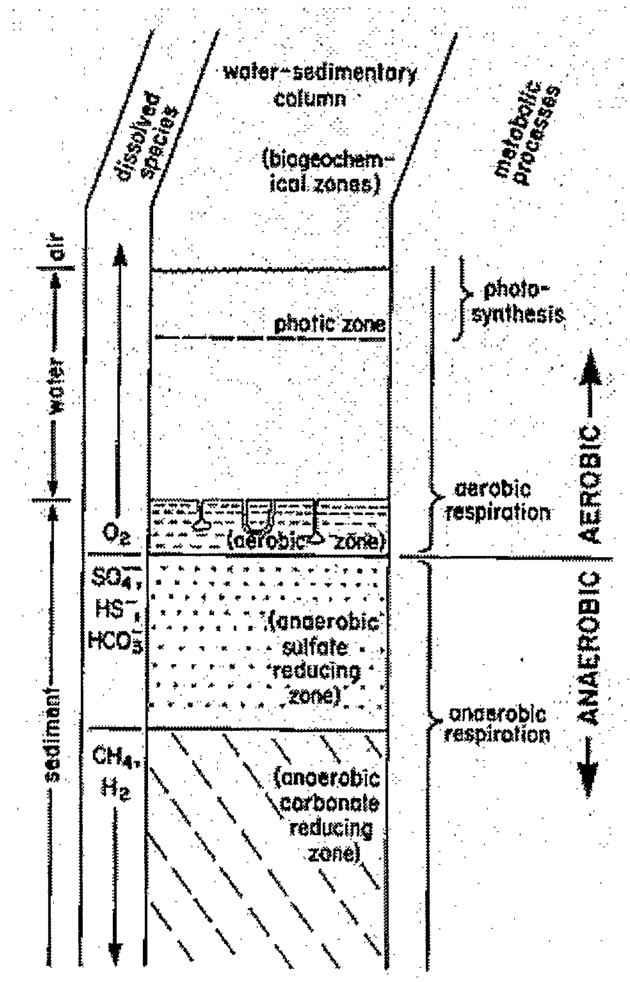

Figure 1.3 - Typical cross section of a marine, organic rich sedimentary environment that favors bacterial activity (adopted from Claypool and Kaplan 1972). Gas bubbles, mostly methane, released due to anerobic oxidation in this environment are trapped within sediments due to high sedimentation rate in deltas and silt content in the upper layers.

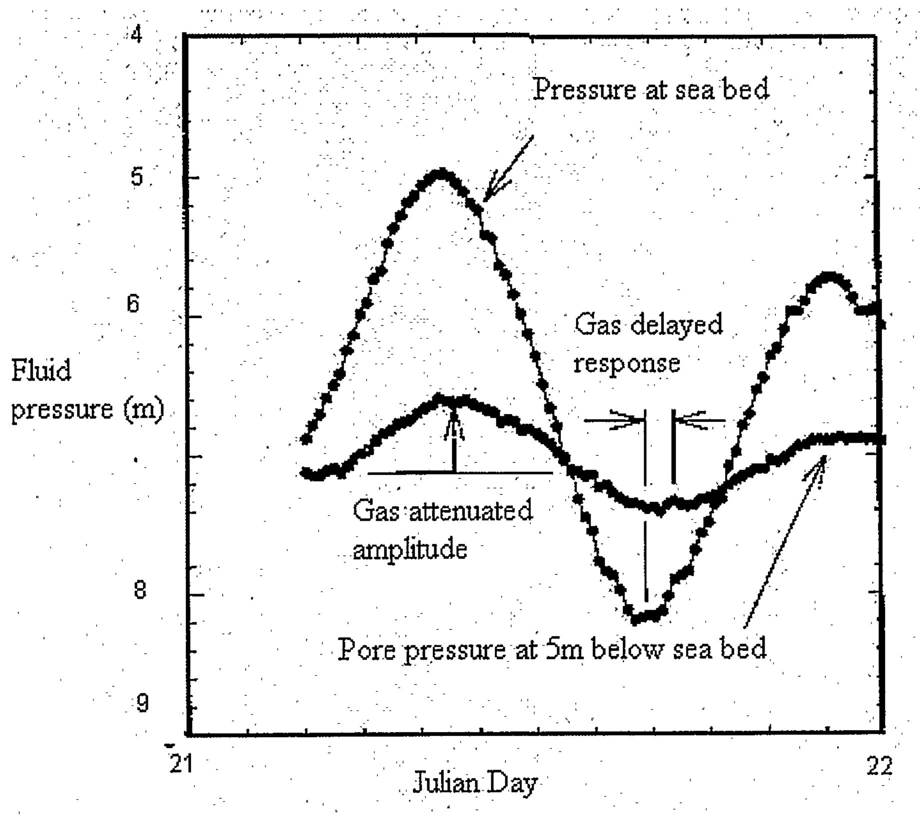

Figure 1.4 – Residual pore pressure in gassy sea bed; measured 5m below sea bed in Fraser River delta, British Columbia (after Christian et al. 1997).

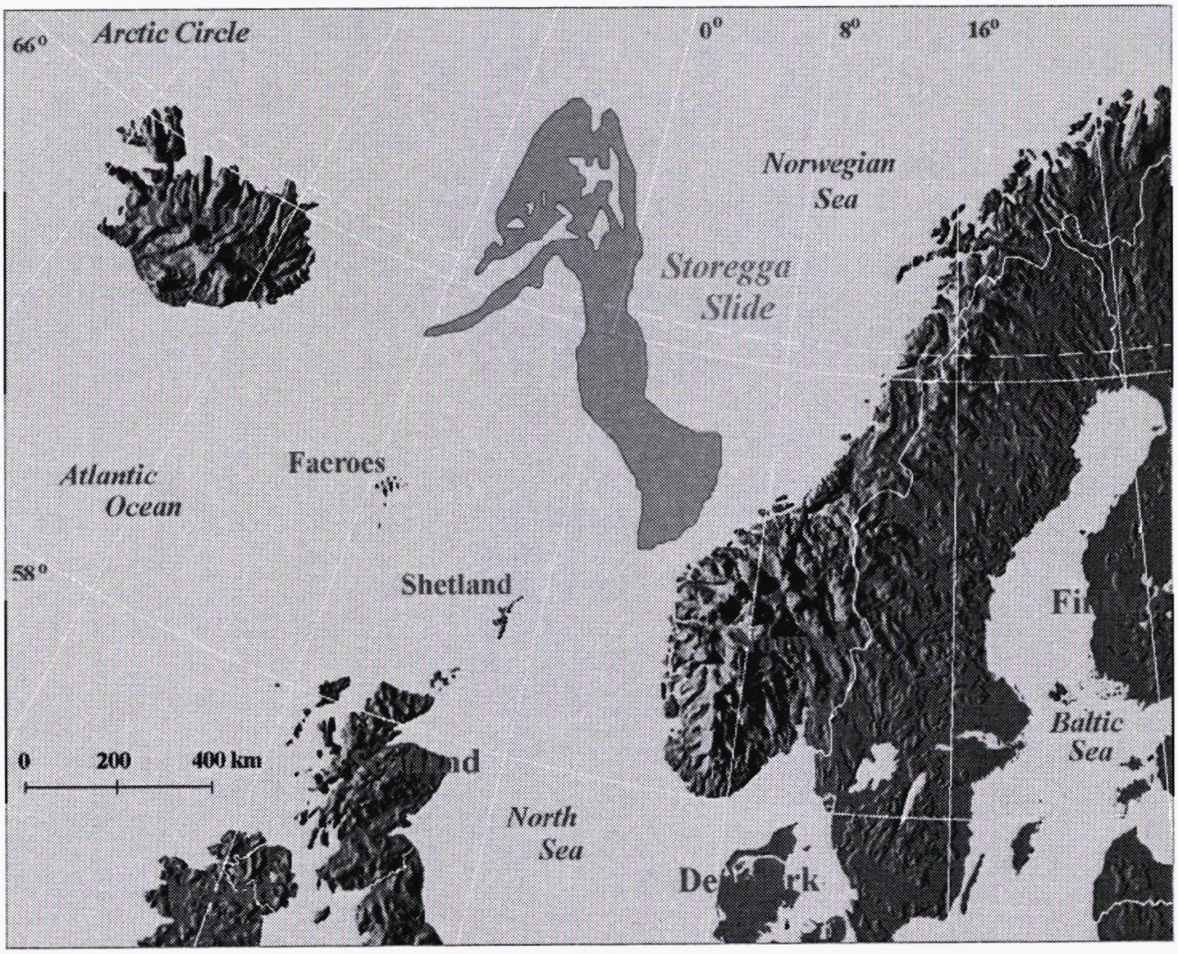

Figure 1.5 – Map that shows Storregga slide area in Norwegian continental margin; three major slides have been reported that involve unconsolidated sediments *(www.soc.soton.ca.uk/CHD/poseidon/overview)*.

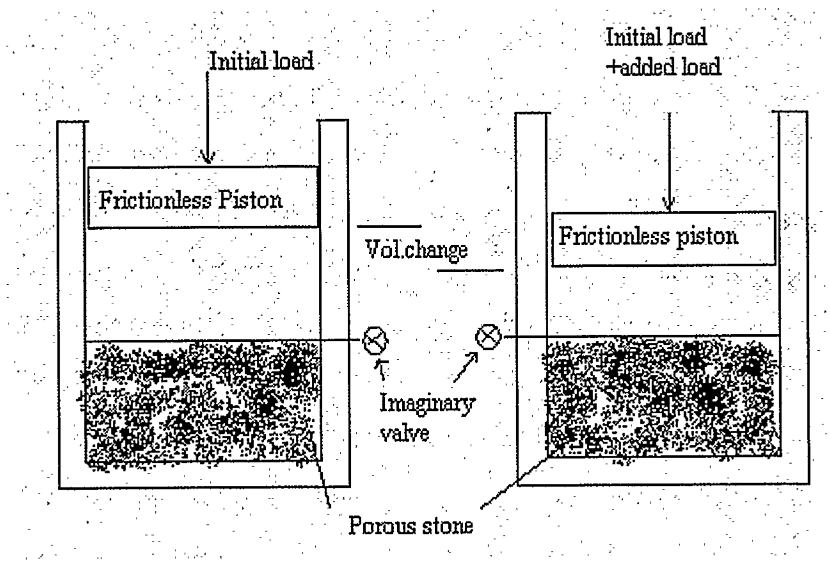

Figure 1.6 - Piston and porous stone analogy to understand Henry's law or solubility coefficient of gas-liquid mixture; fixed volume of pores in the porous stone represent the volumetric coefficient of solubility for a particular gas-liquid mixture, 0.02 times volume of water for air-water mixture (adopted from Fredlund and Rahardjo 1993).

CHAPTER 2

UNDRAINED BEHAVIOUR OF GASSY SOIL

2.1 Introduction.

The stability analysis of slopes, bearing capacity estimation of foundations and deformation analysis of retaining walls and embankments requires knowledge about the stress-strain behaviour of soil under appropriate drainage conditions. In conventional soil mechanics, two types of analysis are performed based on how quickly the dissipation of excess pore pressure occurs. Short term or undrained analysis is carried out in cases where the rate of loading is very much higher than the rate of pore pressure dissipation. On the other hand, if the pore pressure dissipation is quick enough or the loading rate is slow compared to excess pore pressure dissipation rate, drained or long term analysis is carried out.

It is evident from Chapter 1 that most of the submarine slope failures are due to tidal variation, sea level change and offshore development activities; dissipation of excess pore pressure is hindered in this environment due to various factors such as impermeable silt content and/or high sedimentation rate in deltas (Terzaghi 1956) and impermeable gas hydrate layer in deep seabeds (Coleman et al. 1991). This necessitates the undrained analysis on marine sediments where the pore fluid is either saturated with gas or contains free gas as occluded bubbles. The presence of free gas in marine sediments is speculated to be one of the causes of submarine slope instability problems (e.g. Fraser River delta, British

Columbia; Mississippi River delta, California; Cape Fear landslide, North Carolina; and Storregga submarine slump, Norwegian continental margin).

Both experimental and numerical studies have been carried out in the past to understand the behaviour of gassy soil during undrained loading. A few numerical models have been proposed up to now. Even the proposed models did not address all aspects of the problem, such as solubility of gas, compressibility, surface tension and excess pore pressure at the same time. This resulted in a gap between experimental observation and numerical prediction. In this chapter, the undrained analyses that have been carried out in the past, both experimental and numerical, are reviewed. Some important conclusions from the analyses are drawn which shall contribute to the modeling of loose gassy sand for undrained loading described in Chapter 4.

2.2 Review of experimental studies on gassy soil.

Prior to laboratory experiments, core expansions on ship board samples were the only source to study the behaviour of gassy soil upon unloading. Sobkowikz (1982) was the first one to perform an undrained unloading experimental study on gassy soil. Ottawa sand with carbon dioxide saturated pore fluid was subjected to 1200-1300 kPa confining pressure and 600 kPa back pressure (which was greater than liquid-gas saturation pressure), then the confining pressure was reduced by increments of 100 kPa. A mathematical formulation of the pore pressure response (based on compressibility of pore fluid and soil skeleton) as well as the experimental study showed that upon unloading, Skempton's B-parameter was close to zero due to gas exsolution from gas-saturated pore fluid. This is evident from Figure (2.1) in which the pore pressure remains close to the liquid-gas saturation pressure during the unloading exercise because evolving gas bubbles provided the energy for the pressure to be maintained at this equilibrium pressure. Further knowledge in the microscopic processes of gas exsolution in porous media of closed system is needed to develop a theory on gas exsolution-pressure relationship. As noted by Sobkowikz (1982), 'our understanding of the process as well as the complex boundary conditions in the pores of a soil is too rudimentary to develop a general theory'. Most recently, Wong (2003) proposed a model to predict the short term and long term pore pressure response parameter due to time dependent gas exsolution process by considering the kinetics of gas exsolution. This model was based on the assumption of instantaneous and homogeneous bubble growth. Both studies centered on the undrained unloading case owing to the geographical location of both researchers; gas exsolution from oil sand and heavy oil upon reduction of confining pressure that results in 'sand production' is a major concern to the oil and gas industry in Alberta, Canada.

The main outcome from Sobkowicz's observations was that a clear boundary between unsaturated soil and gassy soil was drawn where it is the behaviour of the soil that distinguishes a gassy soil from an unsaturated soil, rather than the constituents of the soil matrix (see Figure 2.2). It should be noted that Sobkowicz's boundary between unsaturated soil and gassy soil differs from other contemporary researchers' explanation for gassy soil (e.g. Wheeler 1988). Sobkowicz's definition for gassy soil was purely based on the unloading response of the soil.

The gassy soil response shown in Figure (2.2) was entirely due to the relative compressibilities of the pore fluid and soil skeleton. Though there are some earlier works on the effect of the compressibility of the liquid-gas mixture on the soil behaviour, (Dusseault 1979; and Schuurman 1966), Sobkowicz's finding was a significant breakthrough in understanding the undrained behaviour of gassy soil during unloading.

While gas exsolution upon unloading was experimentally studied in laboratory by Sobkowicz, several researchers studying the in situ strength of marine sediments from pressurerised core samples found that the ship board strength was less than the in situ strength; this decrease in strength was attributed to gas exsolution (Silva and Brandes 1998; and Esrig and Kirby 1997). In studying the in situ shear strength variation with depth in the Mississippi River delta by acoustical penetration, Whelan et al. (1977) found that gas bubbles cause depressed shear strength gradients as well as significant attenuation and scattering of the acoustical signal. The depressed shear strength can occur in several ways, including minimization of grain to grain contact and creation of buoyancy force to counteract hydrostatic and overburden pressure (Whelan et al. 1977).

Different researchers have given different views as to how gas bubbles contribute to slope instability, some of which are:

(i) Disruption of the sediment fabric during gas exsolution (Silva and Brandes 1988)

(ii) Increase in the void ratio due to bubble growth (Esrig and Kirby 1997)

(iii) Excess pore pressure associated with gas bubble and minimisation of grain to grain contact (Whelan et al. 1977)

An extensive experimental investigation on reconstituted gassy sample was first carried out at the University of Oxford and reported by Wheeler (1988). Synthesised fine grained gassy samples were prepared in Combwich estuarine mud, Somereset, England using the Zeolite chemical, which has a strong affinity to water molecules compared to methane. Scanning electron microscope (SEM) images showed that the prepared sample was similar to a Type D gassy soil, as shown in Figure (1.1b). Though it was argued that the process of sample preparation mimics bubble nucleation and growth in marine environments, the pore fluid in laboratory prepared samples would not be gas saturated whereas marine sediments contain gas saturated pore fluid. In order to compare the result with actual marine sediments, Henry's law effect on this type of soil needs to be studied.

Isotropically consolidated undrained triaxial tests were carried out on the sample. As shown in Figure (2.3) undrained shear strength plotted against the degree of saturation at the start of the shearing for different combination of consolidation pressure and back pressure. Wheeler (1988) concluded that the undrained shear strength of gassy soil is influenced by both consolidation pressure and back pressure. The undrained shear strength can either be increased or decreased due to the presence of gas bubbles depending on cavity expansion/contraction, bubble flooding and localized consolidation. Bubble flooding is said to occur when the difference between the gas pressure and the pore water pressure exceeds a certain limit where as localized consolidation is the effect of stress concentration around the bubble cavities.

An analytical study was carried out by Wheeler (1988) to search for the micro-mechanical behaviour of gassy soil which might explain the observed laboratory behaviour. Wheeler (1988) developed a conceptual model in which a continuum was considered as 'large isolated gas bubbles surrounded by saturated soil matrix' (Figure 2.4). It was argued that the surrounding soil matrix behaves as work hardening or work softening material depending on whether bubble cavities shrink or expand. Cavity shrinkage/expansion depends on whether the stress difference ($p-u_g$) is positive or negative. Two other microscopical phenomena: bubble flooding and localised consolidation were also suggested as the reasons for the increased undrained shear strength observed in some cases. These will be discussed in further detail later in this chapter.

An important observation was drawn from one dimensional consolidation tests carried out on synthesised gassy soil by Sills et al. (1991). The consolidation tests consisted of fine gassy samples prepared by the Zeolite technique described earlier and thus resulted in a microstructure similar to a Type D soil. Figure (2.5) shows the water void ratio plotted against ($\sigma-u_w$). At time zero, total stress was applied while drainage was closed; the very small change in void ratio of the sample was found to be equal to the change in gas void ratio and void ratio change was attributed entirely to gas compression (according to Boyle's law). Subsequently, when the drainage valve was opened, the change in sample void ratio was found to be equal to the change in water void ratio; no change in gas void ratio was observed. Since the pore fluid in the sample prepared using the Zeolite technique would not be gas saturated, Henry's constant would have no role in this experiment.

Sills et al (1991)'s experiment led to the following conclusions:

- Gas void ratio change occurs due to change in total stress and is not altered by dissipation of excess pore pressure during consolidation.
- For any gas content, water void ratio is a function of the difference between total stress and pore water pressure (σ-u_w)*.

Sills and Conzalez (2003) carried out one dimensional self-weight consolidation tests on gassy samples prepared using a different technique. The samples were prepared by culturing methanogenic bacteria in the Rotterdam harbor mud under anaerobic condition. The main conclusion of this experiment was that the shearing resistance of gassy soil is greatly influenced by the strength of the saturated soil matrix surrounding the bubble cavity, rather than gas bubbles (note that in this discussion, Sills and Conzalez (2003) considered gassy soil as Type D soil).

A series of drained tests carried out by Sills et al. (1991) on gassy samples prepared using the Zeolite technique supported the above conclusion. The main conclusion from these tests was that the presence of undissolved gas has no significant influence on the drained

---

*For gassy soil, Sills et al. (1991) called the stress difference σ-u_w as 'operative stress' rather than 'effective stress', since it can not determine both shearing resistance and deformation behaviour of gassy soil, according to Terzaghi's definition of effective stress.

strength of normally consolidated fine soil; it depends on the stiffness of the saturated soil matrix that surrounds the bubble cavity (see Figure 2.6). Sills et al. (1991) suggested that the presence of cavities causes stress concentrations that results in localised consolidation around the cavities which strengthen the surrounding area; hence, localised consolidation and the weakening effect might be equalised. Observation from both drained and undrained test suggested that gas bubbles influence the compressibility of the pore fluid; not the shear resistance of the surrounding soil matrix.

Rad et al. (1994) also carried out triaxial experiments on gassy sand but adopted a different sample preparation method: gas saturated pore water was allowed to percolate through a saturated specimen at a pore pressure above the liquid-gas saturation pressure. Then, the pore pressure was reduced resulting in generation of gas bubbles. Tests were performed on dense gassy sand in which both volume change and pore pressure variation was observed. In saturated dense sand, tendency to expand in volume caused a reduction in pore pressure that resulted in increased shear strength during undrained shearing. However, dense gassy sand exhibited a reduction in shear strength compared to saturated soil (see Figure 2.7a). Rad et al. (1994) suggested that 'the possibility for volumetric expansion and thus partial (internal) drainage and less intense pore pressure reduction is the reason behind the observed reduction in shear strength'. Rad et al. (1994)'s observation agreed with Grozic (1999)'s observation **on loose gassy sand** where volumetric strain due to gassy soil resulted in increased undrained shear strength compared to saturated soil with same consolidation pressure and void ratio.

The response of dense gassy sand for different pore pressure levels was also tested by Rad et al. (1994). Figure (2.7b) shows the response of dense gassy sand for different pore pressure levels. Higher pore pressure means less partial (internal) drainage according to Boyle's law; that means higher undrained shear strength of dense gassy sand.

In the late 90s, Grozic (1999) performed an extensive experimental study on loose gassy sand at the University of Alberta. Grozic (1999) prepared gassy samples by reducing the backpressure of the samples, which contained pore fluid saturated with gas; thus both isotropic consolidation and gas exsolution from the pore fluid was achieved simultaneously. Loose gassy sand exhibited a definite peak behaviour to strain hardening response depending on the degree of saturation* before shearing (see Figure 2.8). The main conclusion of the laboratory work was that loose gassy sand shows a definite peak behaviour if the initial degree of saturation is above 88% and shows a strain hardening response if the initial degree of saturation is below 88%. Though this 'cut-off' degree of saturation is a subjective value, this finding concludes that gas content drastically changes the undrained response of gassy soil.

---

* Throughout this thesis, degree of saturation or degree of water saturation will be referred to the ratio of volume of water voids to the volume of total voids (see Figure 4.3), as used in classical soil mechanics. The term 'degree of gas saturation' will be used to refer to the ratio of volume of gas voids to total volume of voids.

As noted earlier, Grozic (1999) observed increased undrained shear strength due to the presence of gas bubbles, compared to a saturated soil. Figure (2.9a) shows the deviation of a gassy soil response from a saturated soil response for a consolidated undrained triaxial (CU) test. While the saturated soil showed a decrease in mean stress (p) throughout shearing, the gassy soil responded with an increase in mean stress at the early stages of shearing. This is due to volumetric strain introduced in gassy soils. Change in mean effective stress is given by,

$$dp=K..\, d\varepsilon_v^e$$

where K = bulk modulus and $d\varepsilon_v^e$ = incremental elastic volumetric strain.

For a saturated sample (2.9b) elastic volumetric strain is algebraically equal to plastic volumetric strain. At small strain level (i.e. before peak is attained), plastic volumetric strain (hence elastic volumetric strain) is very small. This results in less reduction in mean normal stress and gives nearly a vertical effective stress path. In gassy soil, there will be volumetric strain due to gas compression and ex-solution/dissolution which results in a positive elastic volumetric strain; accordingly, there will be an increase in mean stress initially.

The same trend has been observed by Kvalstad et al. (2003) who performed CU test on Laponite and African Congo slope clay; the gassy sample from Congo slope clay was prepared in the same manner as described by Grozic (1999).

2.3 Numerical study on gassy soil response

Wheeler (1988)'s conceptual model (Figure 1.1) opened the way to numerical studies on gassy soil. In an attempt to find the theoretical undrained shear strength of gassy soil, Wheeler (1988) conceptualized the continuum as 'bubble cavities surrounded by saturated soil matrix' (Figure 2.4b). The model represented Type D soil which was under study in the University of Oxford at the time Wheeler proposed this model. Micro level phenomena like bubble flooding, localized consolidation and bubble shrinkage/expansion in bubble cavity level were analysed qualitatively and an upper and lower bound values for undrained shear strength of gassy soil were proposed. Wheeler (1988) argued that in the course of shearing, u_g- u_w becomes negative due to differing compressibility values of gas and water. This leads to bubble flooding, a process by which the void ratio of saturated soil matrix is decreased. An upper bound value for the undrained shear strength was derived assuming complete bubble flooding. In the same manner, localized consolidation around the bubble cavities due to stress concentration also increased the shear strength.

Assuming the saturated soil matrix to be a rigid perfectly plastic material, Wheeler (1988) argued that due to post yield behaviour of the soil matrix, depending on whether the bubble cavities shrink or expand, it behaves as a work hardening or work softening material despite matrix being perfectly plastic after yield. It was demonstrated that cavities would shrink or expand depending on whether the stress difference (p- u_g) is positive or negative. These three scenarios led Wheeler (1988) to propose the following relation for undrained shear strength of gassy soil (C_u), in which (C_u) is equal to half of the applied deviator stress:

$$\frac{c_u}{(c_u)_{sat}} = f\left[f_0, \frac{\sigma_3 - u_{g0}}{(c_u)_{sat}}, \frac{u_{g0} + p_a}{(c_u)_{sat}}, \frac{He_{m0}}{1+e_{m0}}, \frac{2T}{R_c (c_u)_{sat}}, \frac{1+e_{m0}}{\lambda} \right] \quad [2.1]$$

where c_u = undrained shear strength of gassy soil, e_{m0} = matrix void ratio, f_0 = bubble fraction, H = Henry's law constant, p_a = atmospheric pressure, R_c = critical radius of curvature of the meniscus, T = surface tension, u_{g0} = initial gas pressure, λ = slope of the critical state line in $e - \log_e(p - u_w)$ space for a saturated soil, and σ_3 = all around pressure.

Based on the continuum model proposed by Wheeler (1988), Pietruzczak and Pande (1996) developed a constitutive model for both Type C and Type D soil in tensor form. The effect of gas cavity inclusion was incorporated into an already developed elasto-plastic deviatoric hardening model for the drained behaviour of sand. The mathematical formulation incorporated the average pore/bubble size (ρ_v) as an independent material parameter:

$$\rho_v = n/(\gamma_d S_f) \quad [2.2]$$

where γ_d is the dry density of the soil and S_f is the specific surface area of the soil. This means that the model predicts different undrained responses for fine and coarse sand, though the degree of saturation at the start of shearing is same. While no comparison with reported experimental results has been given, the numerical prediction was against experimental observation on dense sand reported by Esrig and Kirby (1997) (see Figure 2.10).

In analyzing the flow liquefaction potential of loose gassy sand, Atigh and Byrne (2003) modified an elasto-plastic model to incorporate the effect of gassy soil by considering gassy soil response in undrained condition as equivalent to saturated soil response in partially drained condition. Accordingly, the undrained loading of a gassy sample that results in contractive volumetric strain was considered as an outflow state in a partially drained condition and vise versa. Atigh and Byrne (2003) did not discuss the effect of the pore pressure level on the undrained behaviour of gassy soil, observed by Esrig and Kirby (1997) and the effect of solubility of gas on pore liquid, as observed by Rad et al. (1994). In an attempt to model the undrained behaviour of loose gassy sand, Grozic (1999) modified an elasto-plastic model proposed by Imam (1999). Though the model predicted the general trend of gassy sand, Grozic (1999) noted that there exist a discrepancy between prediction and observation at the initial stages of loading.

The model proposed in this research focuses on incorporating the effect of increased compressibility of gas-liquid mixture, type of gas and pore pressure level into an existing model developed for loose sand.

2.4 Conclusion:

Core expansion of Athabassca oil sands and marine sediments during sampling prompted experimental studies on gassy soils. Based on the unloading response of these types of soil, Sobkowikz (1982) defined what is gassy soil. Later, several experiments were carried out on gassy soil with respect to loading stress path (Wheeler 1988; Rad et al. 1994; Grozic

1999; and Sills et al. 2003). The general conclusion from these observations is that the undrained response of gassy soils is influenced by an increased compressibility of the gas-water mixture. The increased compressibility of the pore fluid results in volume change as well as pore pressure change during undrained shearing.

Grozic (1999) performed undrained triaxial tests on loose gassy sand and observed that loose gassy sand exhibits a wide range of responses from peak behaviour to strain hardening, depending on the gas content (see Figure 2.8). Grozic (1999) further noted that the undrained response of gassy soil significantly varies from that of saturated soil with the same void ratio and confining pressure. This variation was eminent at the initial stages of shearing when strain levels are low (see Figure 2.9). A modified model to predict gassy soil response by incorporating Boyle's law and Henry's law effect was not able to capture this initial deviation.

The gap between experimental observation and model prediction by Grozic (1999) has been reduced by this research. This has been achieved by coupling the volumetric strain due to gas compression/exsolution (according to Boyle's law and Henry's law) into an existing model for loose sand. The volumetric strain due to gas compression/exsolution is calculated assuming an equilibrium response of gassy soil. Pore pressure and solubility dependency of gassy soil, observed by Rad et al. (1994) has also been addressed in this model.

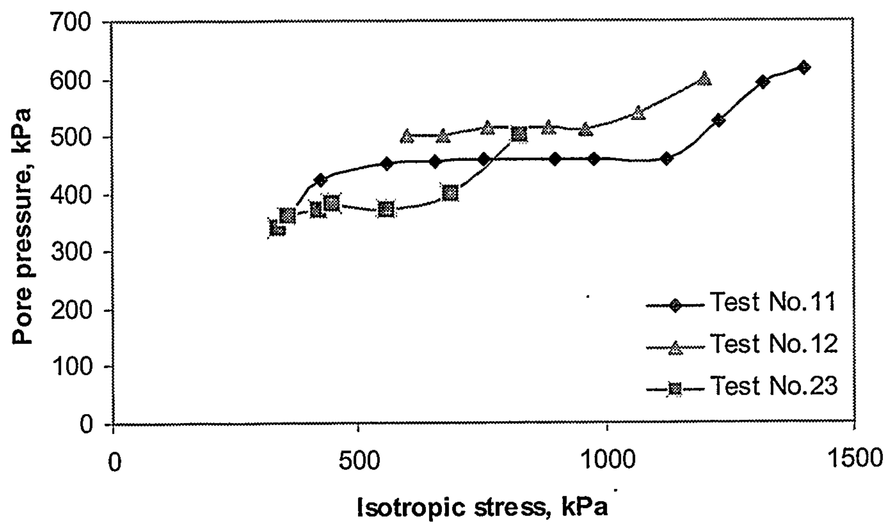

Figure 2.1 - Pore pressure response during an isotropic unloading experiment on gassy soil (Sobkowicz 1982). Note that pore pressure remains unchanged at liquid-gas saturation pressure.

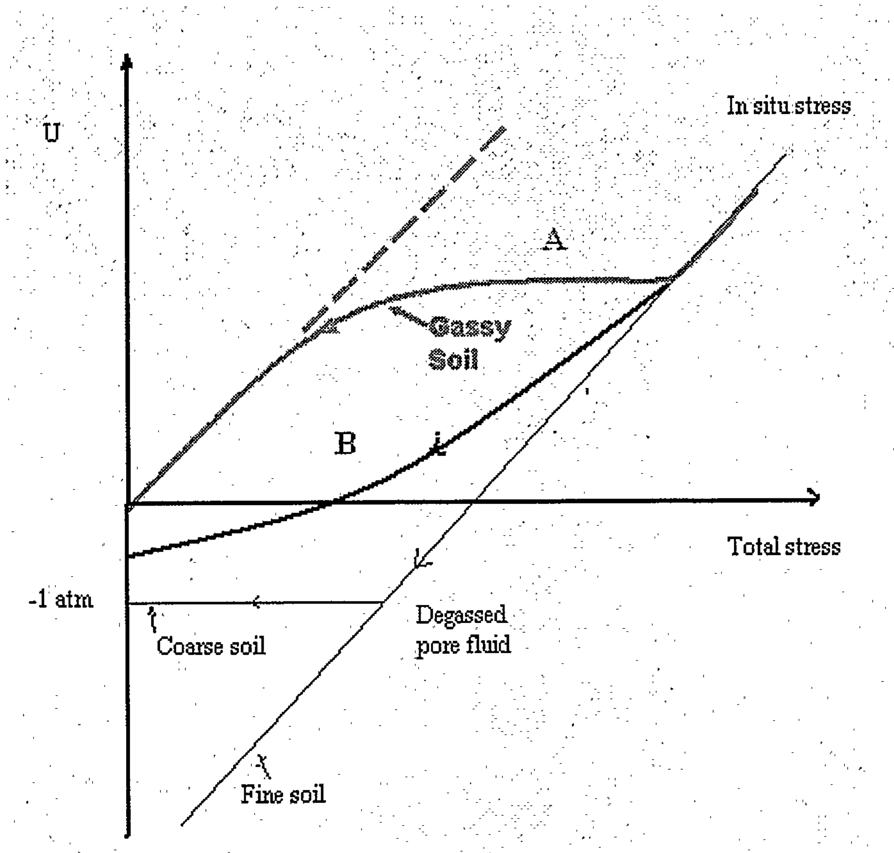

Figure 2.2 - Comparison of undrained equilibrium behaviour of gassy soil upon loading with unsaturated soil. Sobkowicz (1982) used this response (response A) to define a gassy soil.

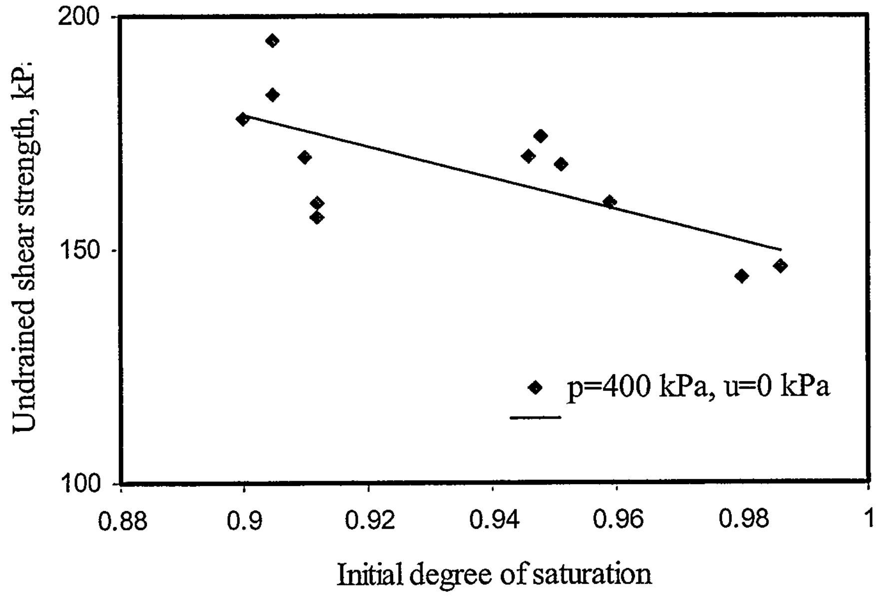

(a)

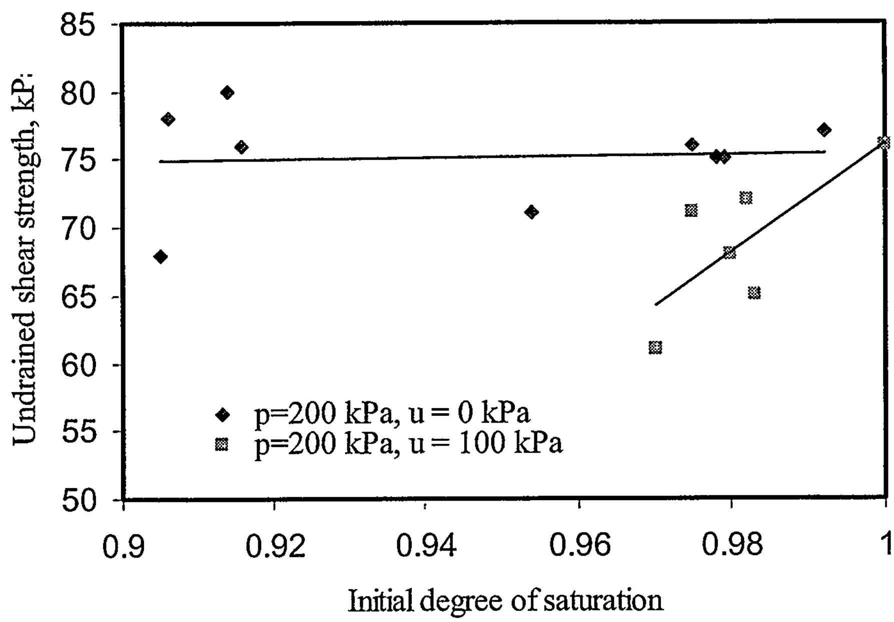

(b)

Figure 2.3 - Undrained shear strength against degree of saturation at start of shearing for different combinations of consolidation and back pressure (adopted from Wheeler 1988).

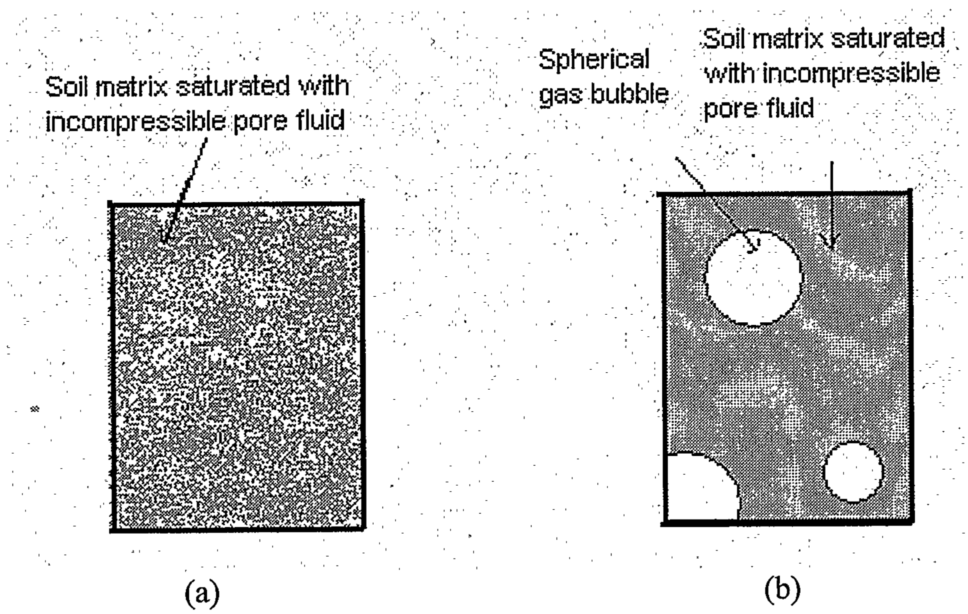

Figure 2.4 - Conceptual models for (a) Type C gassy soil (Thomas 1989) and (b) Type D gassy soil (Wheeler 1988). Model (a) considers gassy soil as saturated soil with compressible pore fluid, similar to Double spring model proposed by Dusseault (1979); model (b) considers gassy soil as saturated soil (with incompressible water) that contains embedded gas cavities.

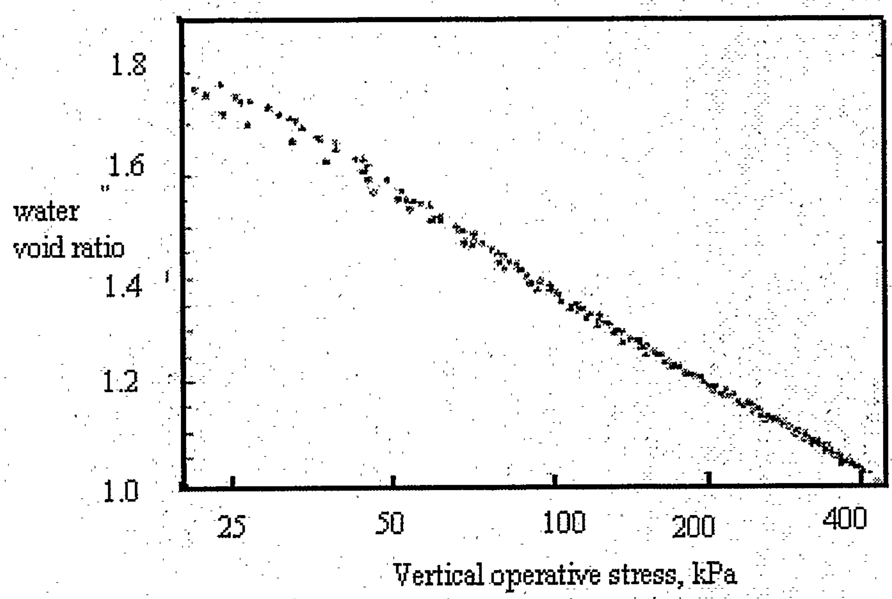

Figure 2.5 - Water void ratio plotted against operative stress in a 1-D consolidation test for different samples with varying degree of saturation. Gassy samples were similar to Type D soil (Sills et al. 1991).

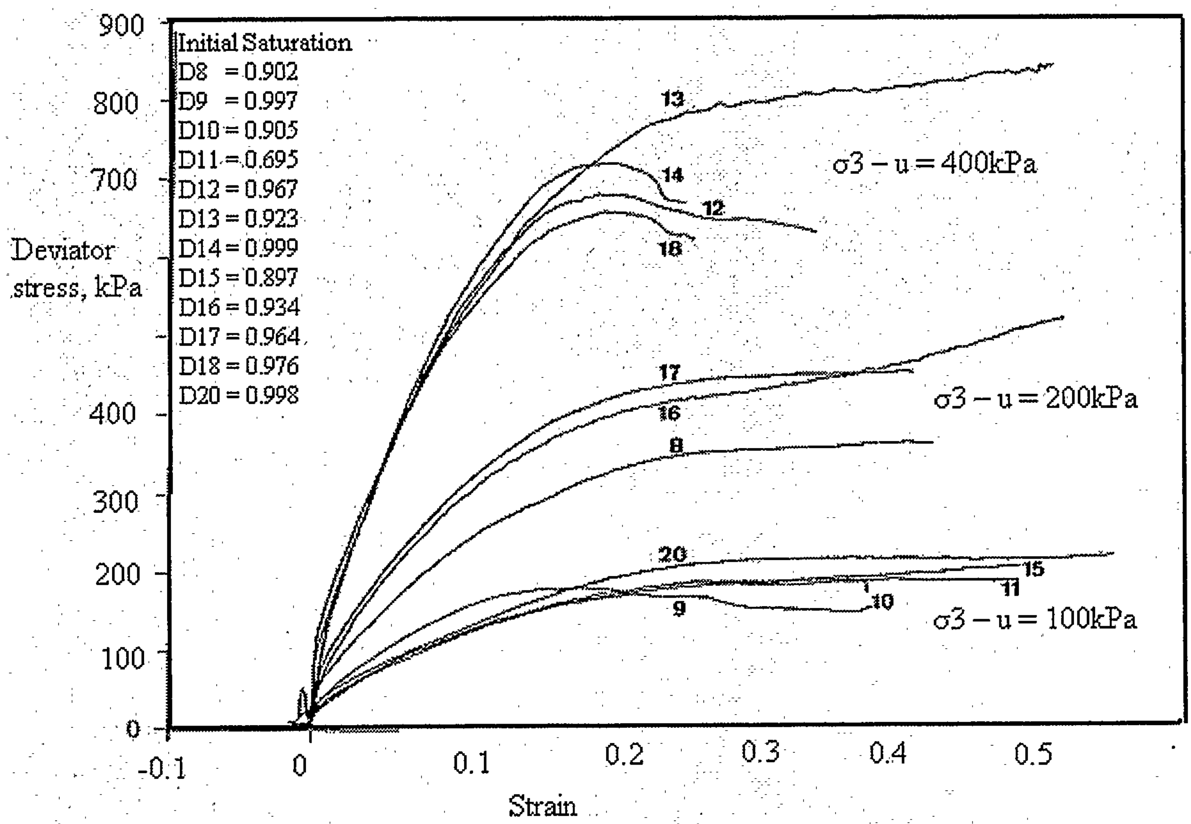

Figure 2.6 - Stress-strain response of gassy soil for drained triaxial testing; notice that gas content has no effect on the drained shear strength of gassy soil (Sills et al. 1991).

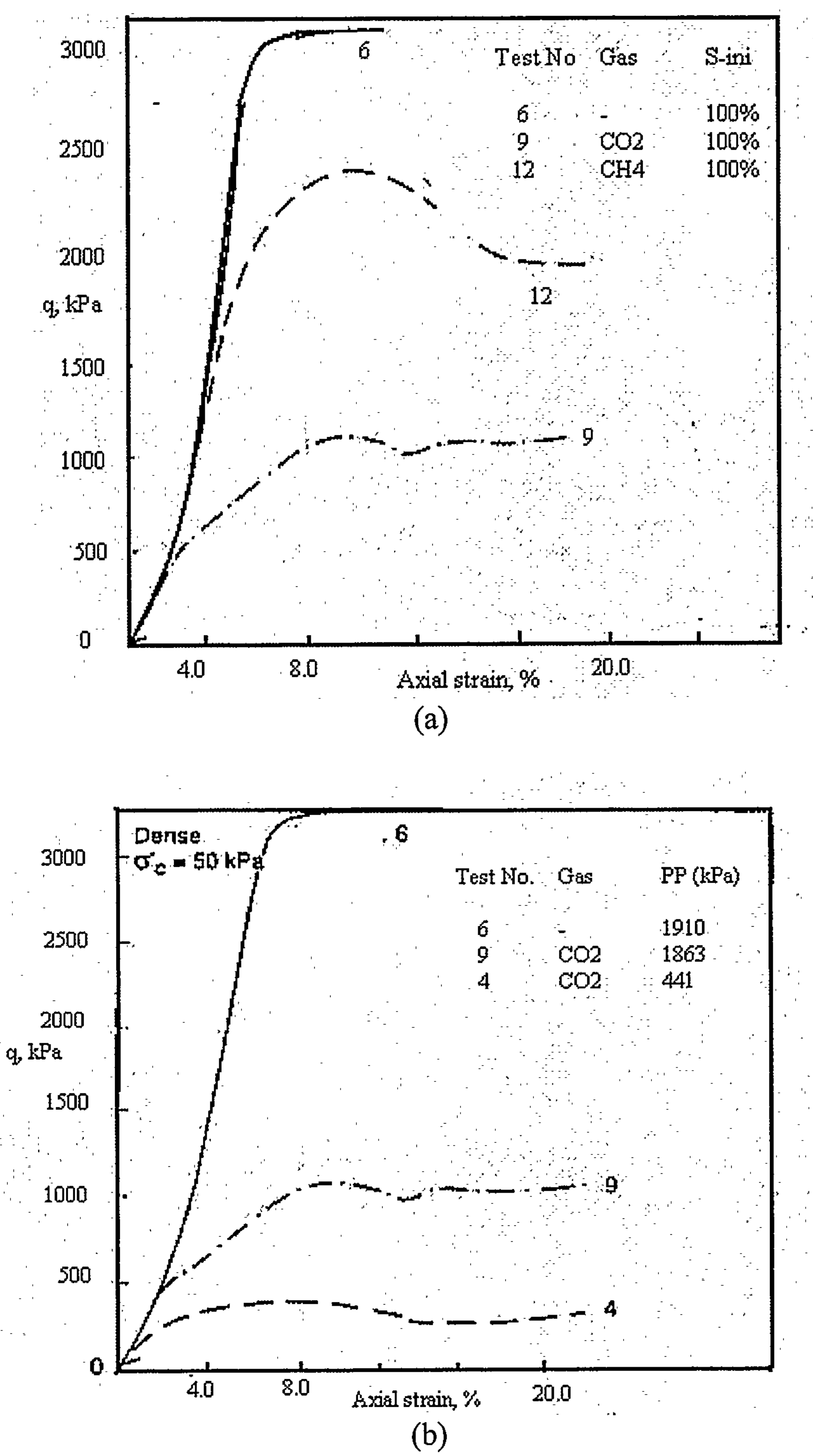

Figure 2.7 - Behaviour of dense gassy sand upon undrained shearing in triaxial cell. Note the effect of gas type on the response; deviation from saturated soil response has been attributed to partial (internal) drainage. (adopted from Rad et al. 1994).

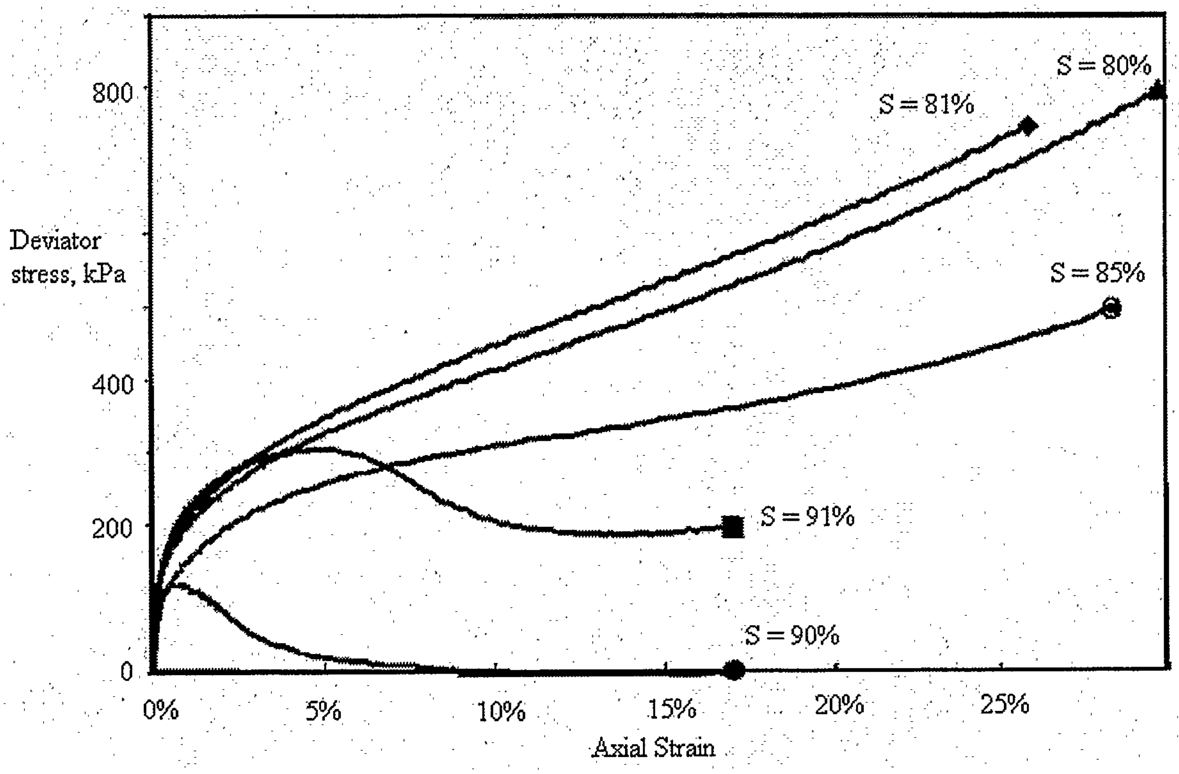
S = 80%
S = 81%
800
Deviator stress, kPa
S = 85%
400
200
S = 91%
S = 90%
0
0%
5%
10%
15%
20%
25%
Axial Strain

(a)

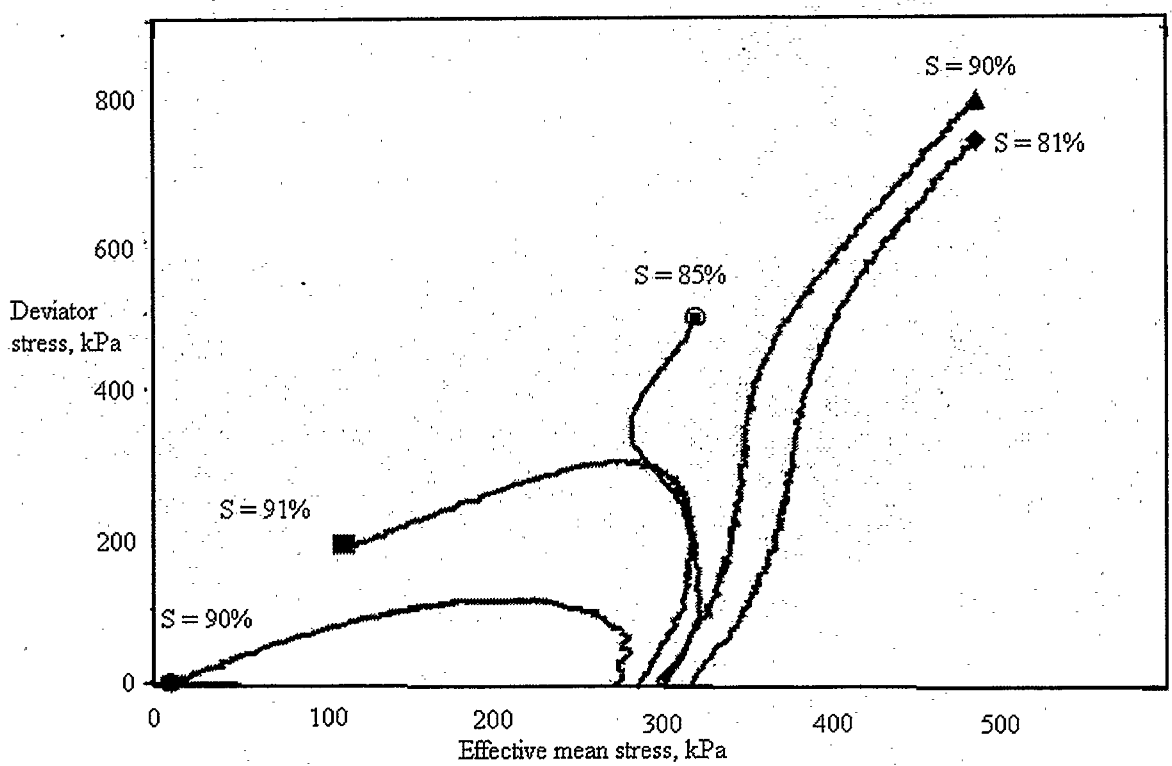
S = 90%
S = 81%
800
600
S = 85%
Deviator stress, kPa
400
S = 91%
200
S = 90%
0
0
100
200
300
400
500
Effective mean stress, kPa

(b)

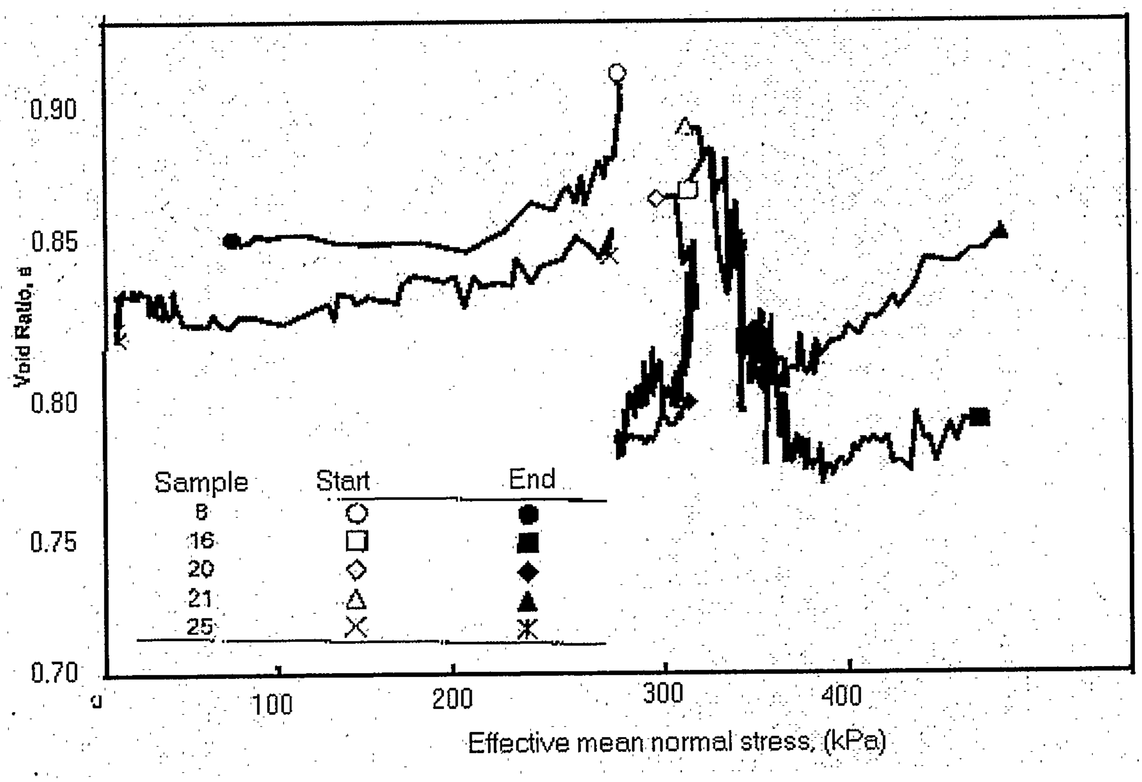

(c)

Figure 2.8 – Wide range of response of gassy specimen for different initial degree of water saturation (a) in stress-strain space, (b) in p-q space and (c) in void ratio – mean effective stress space (Grozic 1999).

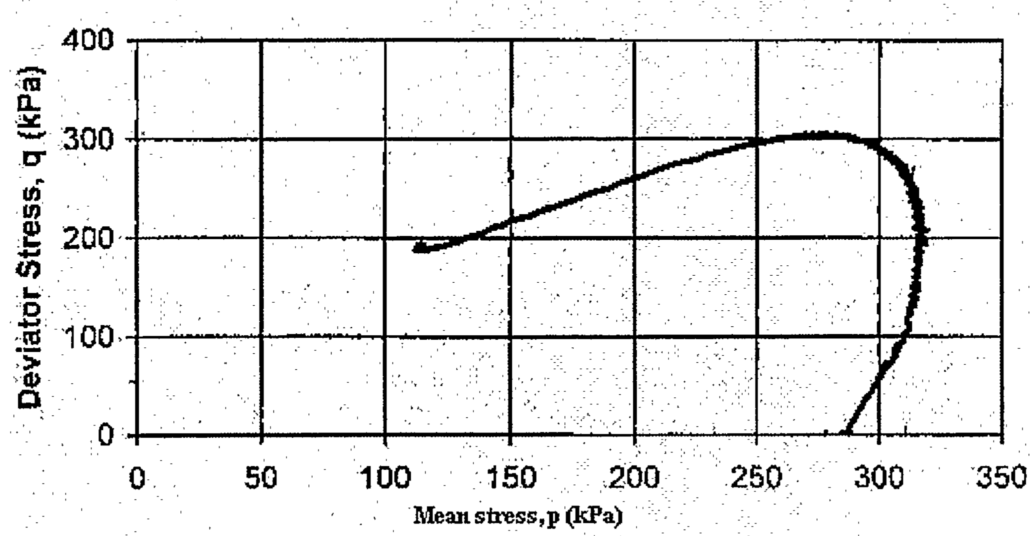

(a)

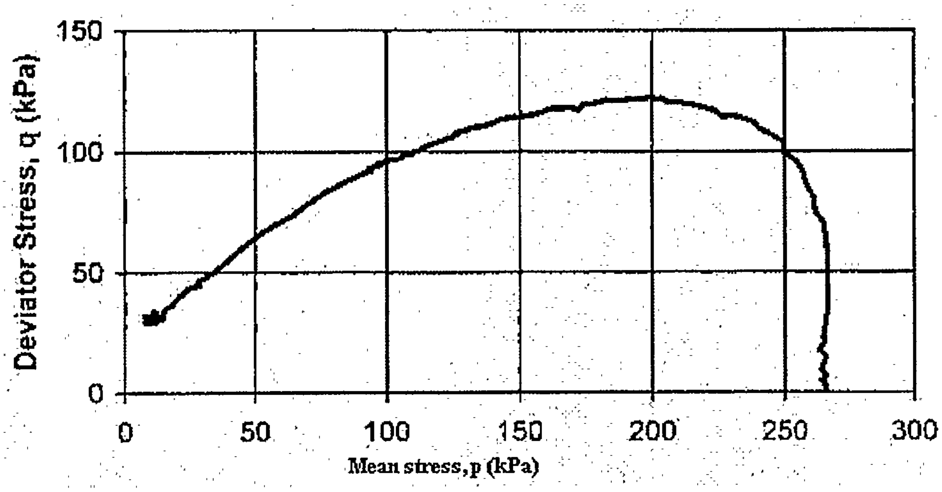

(b)

Figure 2.9 – (a) Response of loose gassy sand in p-q space; initial mean effective stress of 286 kPa, void ratio of 0.92 and degree of saturation of 80% and (b) response of saturated loose sand for initial mean stress of 266 kPa, void ratio of 0.9 (Grozic 1999).

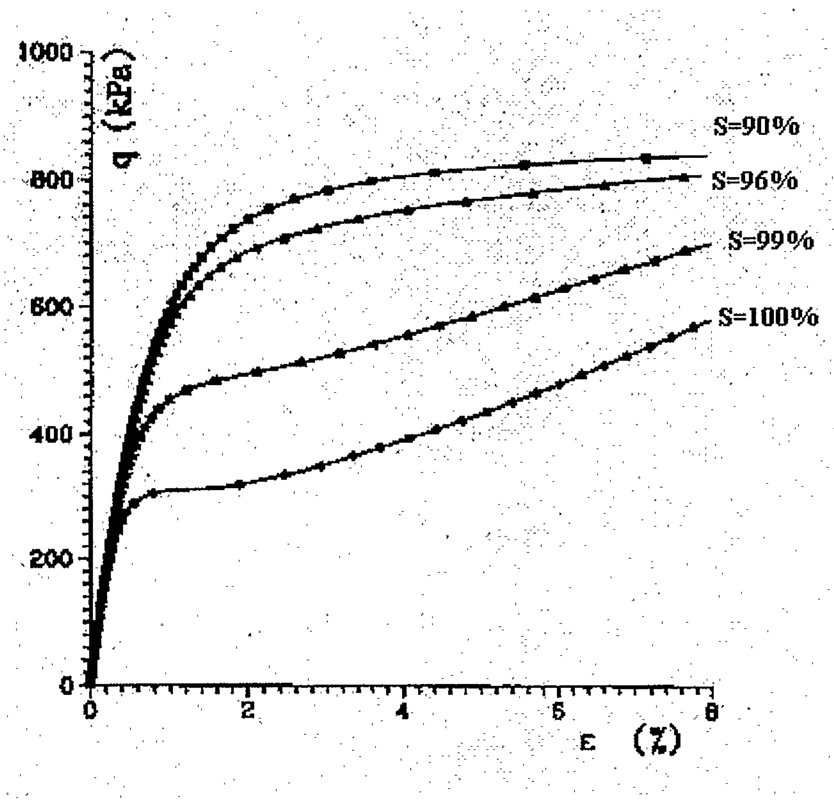

Figure 2.10 - Numerical prediction of dense gassy sand in p-q space (Pietruszczak and Pande 1996). Note that this is against Esrig and Kirby (1997)'s observation that gas bubbles in dense sand decreases the undrained shear strength.

CHAPTER 3

AN OVERVIEW OF ADOPTED MODEL FOR LOOSE SAND

3.1 Introduction

Instability problems in sub-aqueous and deltaic environments received considerable attention in the past and because of that the study of the behaviour of loose sand gained momentum. For example, in analyzing the slope failures of Norwegian fjords, Bjerrum et al. (1971) concluded that the existence of loose sand contributes to the initiation of the slope failure. Glacial water and post glacier river deposits resulted in enormous amount of sub-aqueous loosely compacted fine sands in these fjords which resulted in subsequent flow slides. Terzaghi (1956) studied the role of granular media in the mechanism of sub-marine flow slides after a flow slide in a delta front at the north shore of Howe island, British Columbia, which occurred in August 22, 1955. The slide occurred immediately after an extreme low tide condition.

During shearing, sand exhibits either volume contraction or dilation and reaches a particular void ratio (known as 'critical void ratio'), depending on whether it is loosely packed or densely packed. During undrained shearing, as volume change is restricted, the tendency to change in volume is transformed to either pore water pressure increase or decrease. Several undrained experimental studies on loose sand found that loose sand will strain soften due to the generation of high pore pressures. This results in a decrease in effective stress, loss of shear strength, and inability to carry shear load all of which contribute to the phenomenon known as 'liquefaction'. In analysing the mechanisms of submarine landslides, Morgenstern (1967) attributed the structure of loose sedimentary deposits to liquefaction failure and found that the failure mode was consistent with the failure mode of loose sand in undrained shearing. Identifying different mechanisms of liquefaction, Robertson (1994) reffered this as 'flow liquefaction' – loss of shearing resistance or development of large strains due to transient or monotonic loading.

Numerous elastic-plastic constitutive models have been developed to understand the behaviour of sand, both loose and dense and to predict liquefaction susceptibility. This chapter describes the basic elements of an elasto-plastic stress-strain model and elaborates on the model developed by Imam (1999). A brief description on how to determine model parameters is also given at the end of this Chapter, with particular emphasis on Fraser River sand.

3.2 Basic features of a constitutive model

The basic elements of an elastic-plastic constitutive model are yield surface, flow rule and hardening rule.

The process of yielding can be explained with the aid of Figure (3.1), which shows the typical stress-strain curve for an annealed copper wire. OA_1 shows the loading path and

A_1B_1 is the unloading path. The load path of the wire for a simple tension is not re-traced upon unloading and the wire is left with an irreversible/plastic deformation (strain component OB_1) when the load is completely removed. When the wire is re-loaded up to or below the maximum past load (A_1), the wire shows basically an elastic response in which recoverable or reversible deformation occurs. Once the past maximum load is exceeded, this elastic response vanishes and further irreversible/plastic deformation (B_1B_2) is introduced. This process of under going irreversible or plastic deformation is called yielding and the maximum past load (A_1) is known as the yield point. If the stress point A_1 keeps on increasing, then the material is said to harden; if it remains constant, the material is said to be perfectly plastic and if it decreases, it is said to behave in a strain softening manner. An elastic-plastic model can describe this behaviour more accurately.

If the current stress state of the soil lies within the yield surface (for that particular maximum past pressure), the behaviour can be described by elastic parameters. Section (3.3.4) discusses elastic parameters for loose sand adopted in Imam's (1999) model.

3.2.1. Yield surface

The existence of a unique Normal Consolidation (NC) line for fine grained soil made it simple for developing a stress-strain model for clays. Roscoe et al. (1969) developed a simple model, known as 'Cam Clay model' for fine grained soil based on critical state soil mechanics. However, the absence of a unique relationship between void ratio and consolidation pressure is a major challenge in developing constitutive models for sand compared to clay.

The simple yield locus proposed for granular soil is a family of straight lines radiating from the origin of the stress space that corresponds to a constant stress ratio, $\eta=q/p$, where $q=(\sigma_1-\sigma_3)/2$ and $p=(\sigma_1+\sigma_2+\sigma_3)/3$ (Lade and Duncan 1976). To overcome the experimental deviation for increasing pressure and inability to predict plastic deformations along proportional loading, Lade (1977) later introduced a capped yield surface to capture the behaviour over a wide range of confining pressure. Even this model showed deviation from experimental results at small strain levels.

3.2.2 Plastic potential or flow rule.

Calculation of plastic deformation is the most essential component of an elasto-plastic model. Plastic deformations depend on the stress state at which yielding of soil occurs; not the stress path by which that stress state was achieved. In general, yielding is associated with change in plastic volumetric strain and change in plastic shear strain. With the assumption of co-axiality, ie, direction of principal stresses and direction of principal strain increments are parallel, the plastic strain increment vector can be drawn at the stress point at which the plastic deformation occurs. For each stress point, there exists a plastic strain increment vector and there exists a surface which is known as plastic potential for which this vector is orthogonal (see Figure 3.2). Accordingly, if the plastic potential function is g(p,q), then, plastic volumetric strain and plastic shear strain can be expressed as:

$$d\varepsilon_p^p = \Lambda\frac{\partial g}{\partial p} \text{ and } d\varepsilon_q^p = \Lambda\frac{\partial g}{\partial q} \qquad [3.1]$$

where Λ is the plastic multiplier. Most of the isotropic materials (metal wire, for example) and models developed for cohesive soils assume that the plastic potential curve is identical to the yield curve; this is known as associated flow rule. But this assumption is not applicable to sand – it behaves in a non-associative plastic flow manner.

The expressions developed for the plastic potential of granular materials so far relate incremental plastic strain ratio ($\frac{\partial \varepsilon_p^p}{\partial \varepsilon_q^p}$) to stress ratio ($\eta$) and not to the individual value of stresses (Wood 1990). Note that, by definition, the plastic strain increment ratio is normal to plastic potential function. This ratio is called the 'plastic dilatancy' of the soil and its relation to stress ratio is called the stress-dilatancy relationship.

Rowe (1962) derived a comprehensive stress-dilatancy relation for particulate continuum based on his experiments on an assembly of spherical balls and glass rods. In view of the gassy soil to be discussed in Chapter 4, it is appropriate to note here that for the stress-dilatancy relation expressed by Rowe (1962), the voids between the particles may be filled with air or water. In other words, the stress-dialatancy relation is governed by the effective stress of the particulates, not by the type of pore fluid that fills the pores.

3.2.3 Hardening rule

Referring to Figure 3.1, it is said that if the stress point A_1 keeps on increasing then the material is said to strain harden and if it decreases it is said to behave in a strain softening manner. The yield surface will expand when the material hardens and contracts when it softens. The hardening rule defines the evolution of the yield surface with plastic strains. Isotropic hardening is said to occur when the yield surface expands without changing its shape.

3.3 Imam's model- An overview

The model parameters used in Imam (1999)'s elasto-plastic stress strain model will be described here, so that we will have a better understanding on gassy soil modification that will be presented in chapter (4). A flow chart illustrating the model elements described in the following sections is presented in Figure 3.3.

3.3.1 Yield surface

Imam (1999) proposed the following expression for the yield surface of isotropically consolidated loose sand:

$$\eta^2 = 5M_p^2\left[1-\left(\frac{p}{p_c}\right)^{1/2}\right] \qquad [3.2]$$

where stress ratio, η=q/p; deviatoric stress, q=(σ_1-σ_3)/2; mean effective stress, p=(σ_1+σ_2+σ_3)/3; M_p= stress ratio at peak point of the yield surface (P-YS) and p_c= consolidation pressure. Parameters M_p and p_c dictate the shape and size of the yield surface respectively.

The shape of the yield surface for the above expression is shown in Figure (3.5). It agrees with experimental observations and other proposed models in that, at low stress levels, the yield surface is an ascending 'cap' surface and once the peak stress ratio (M_p) is reached, it start to decline, as denoted by 'front portion' in other models (e.g. Lade 1992). The yielding mechanism for granular materials can be explained by frictional theory as follows:

> Plastic deformations and hence yielding occurs in granular materials due to deformations at particle contacts that is governed by frictional resistance. Deformation mechanism at particle contacts differs at small strain level and high strain level (Imam 2000). At small strain level (when $\eta < M_p$), friction is not fully mobilised and minor deformations due to slippage at inter-particle contacts occurs. But, at large strain level (when $\eta > M_p$), gross slippage along a major slip plane occurs.

Based on previous studies, Imam (1999) noted that the stress ratio at the peak point of the yield surface (P-YS) can be approximated to be equal to the stress ratio measured at peak of the undrained effective stress path (P-UESP) of loose sand (note that loose sands exhibit contractive tendency or peak point in undrained response in p-q space). Figure 3.4 explains this observation. For triaxial stress space, the stress ratio at peak (M_p) and mobilised friction angle during shearing process (ϕ_m) are related by,

$$M_p = \frac{6 \sin \phi_m}{3 - \sin \phi_m}. \qquad [3.3]$$

where the mobilised friction angle (ϕ_m) is the algebraic sum of inter-particle friction angle (ϕ_μ) and average effective angle of slip (θ) with respect to minor principle stress (see Figure 3.6). It should be noted that θ is a measure of dilatancy and hence θ varies with void ratio. In other words, M_p varies with void ratio. This consistency in variation of M_p and dialatancy with void ratio has been noted by several researchers. With the analysis of experimental results available from the literature, Imam (1999) found that M_p (or $\sin \phi_m$) varies linearly with void ratio in an inverse manner: the higher the void ratio, the lower the value of M_p. This linear variation of $\sin \phi_m$ with void ratio can be expressed as (see Figure. 3.7),

$$\sin \phi_m = \sin \phi_\mu - k_m (e - e_\mu) \qquad [3.4]$$

where k_m is a constant that represents the slope of the curve and e_μ is the void ratio corresponding to friction angle, ϕ_μ. It should be noted that ϕ_μ is used as the reference value to determine the position of the line (Imam 2000). Imam (1999) pointed out that ϕ_μ is several degrees smaller than the constant volume friction angle (ϕ_{CV}) of sand.

As discussed earlier, M_p varies linearly with the consolidation void ratio. During isotropic consolidation the compression behaviour of sand (compressibility) influences the void ratio change. For sand, compressibility changes drastically from low confining stress level (<500kPa) to higher confining stress level. This results in different values of M_p for different confining pressures, though the void ratio at the start of shearing is same (for example, see Figure 3.8). Figure (3.8) shows the variation of M_p with void ratio for two different confining pressure range for Toyoura sand (Imam 1999).

To overcome this problem, Imam (1999) normalised the void ratio at a given confining pressure to a reference void ratio, e_r, at a reference confining pressure, p_r using a compression model proposed by Pestana and Whittle (1995). In this way, the reduction in void ratio due to the increase in confining pressure can be accounted for; if p_r is taken to be very small, it corresponds to formation void ratio, e_i.

In brief,

$$M_p = f(e, p_c)$$

By normalising the void ratio,

$$M_p = f(e_r)$$

The compression behaviour of sand for isotropic consolidation can be studied from the normal compression response. Establishing a normal compression line (NCL) for sand is not as easy as that for clay since slope of e vs $\ln(p)$ plot for sand is not unique; it depends on density and confining pressure. Imam (1999) used a simplified version of model proposed by Pestana and Whittle (1995) which is valid for confining pressures less than 3MPa. The simplified version expressed in terms of current void ratio is:

$$\ln\left(\frac{e}{e_0}\right) \approx -e_0^{2.5}\beta\left(\frac{p}{p_a}\right). \qquad [3.5]$$

where e_0 = formation void ratio; β = material parameter; and p_a = atmospheric pressure. Section (3.4) describes how to determine the model parameter β using data from triaxial compression.

3.3.2. Plastic potential

Rowe (1962) derived an expression for the stress-dialatancy relation which states that, for a soil sample under shear, the work done by driving stress to the work done by driven stress in any strain increment should be a constant and that constant is a function of characteristic failure friction angle ϕ_f. That is,

$$\frac{\sigma_1}{\sigma_3} = \left(1 - \frac{d\varepsilon_v}{d\varepsilon_a}\right)K \qquad [3.6a]$$

where $K = \tan^2\left(\frac{\pi}{4} + \frac{\phi_f}{2}\right)$ and $d\varepsilon_v = d\varepsilon_1 + 2d\varepsilon_3$; $d\varepsilon_1$ and $d\varepsilon_3$ are major and minor principal strain increments in triaxial space. Note that subscript '*f*' is used not to denote failure; Rowe used subscript '*f*' to denote similarity of angle to it's failure angle and ϕ_f varies between inter particle friction angle, ϕ_μ and constant volume friction angle, ϕ_{CV} depending on porosity. For dense sand, $\phi_f = \phi_\mu$ and for very loose sand ϕ_f approaches ultimate state friction angle, ϕ_{CV}.

In triaxial condition, Equation (3.6a) can be written as (Wood 1990),

$$\frac{\sigma_a d\varepsilon_a}{-2\sigma_r d\varepsilon_r} = K$$

where $K = \frac{1+\sin\phi_f}{1-\sin\phi_f}$.. Substituting $d\varepsilon_p = d\varepsilon_a + 2d\varepsilon_r$, $d\varepsilon_q = 2/3(d\varepsilon_a - d\varepsilon_r)$ and $\eta = q/p$ in the above equation results in,

$$\frac{d\varepsilon_p}{d\varepsilon_q} = \frac{3\eta(2+K-9(K-1))}{2\eta(K-1)-3(2K-1)} \qquad [3.6b]$$

Substituting $K = \frac{3+2M}{3-M}$ to Equation (3.6b) gives,

$$\frac{d\varepsilon_p}{d\varepsilon_q} = \frac{9(M-\eta)}{3+3M-2M\eta}, \qquad [3.7]$$

Like most other models, the above relation expressed by Wood (1990) assumes $\phi_f = \phi_{CV}$ and hence,

$$M = \frac{6\sin\phi_{CV}}{3-\sin\phi_{CV}}$$

For a wide range of densities, as in the case of shearing loose sand, the assumption of $\phi_f = \phi_{CV}$ may introduce error in the modeling. Imam used a variable value, ϕ_{PT} (friction angle at phase transformation), introduced by Ishihara et al. (1975) to handle the variability of ϕ_f with porosity. ϕ_{PT} is the friction angle at phase transformation where soil dilatancy changes from contractive tendency to dilative tendency. The value of this angle varies with void ratio and converges to ϕ_{CV} when the steady state is reached. In order to express the variation of ϕ_{PT} with void ratio, a state parameter (ψ) will be introduced in the next paragraph.

For sand, there exists infinite number of normal compression lines (NCL), that is, sand can exist at different void ratios for the same consolidation pressure. This limits most of the proposed models to a single initial void ratio/density and they can not be used for the same sand at different void ratio/density (e.g. Nova and Wood 1979). Jefferies (1993) handled this specific problem by introducing a state parameter (Ψ) expressed as the difference between current void ratio and 'critical void ratio' (the concept of 'critical void ratio' was proposed by Casagrande (1936) based on observations on behaviour of sand at failure (see Figure 3.9); later, Roscoe et al. (1958) proved that the concept of critical void ratio is valid for clay as well and developed 'critical state soil mechanics').

Been and Jefferies (1985) introduced a critical state framework for sand by introducing the state parameter, ψ. This parameter is a measure of how far the current void ratio is from the void ratio at constant volume shearing or at steady state.That is,

$$\psi = e_{SS} - e \qquad [3.8]$$

where e_{SS} is the void ratio at steady state/critical state. Based on critical state data of void ratio and mean stress, Been and Jefferies (1985) proposed the following equation for Critical State Line (CSL) for sand:

$$e_{SS} = \Gamma - \lambda \ln(p) \qquad [3.9]$$

where Γ and λ material parameters to describe the critical/steady state behaviour of sand. Experimental observations show that the critical state line changes from low slope to higher slope from low stress level to higher stress level. This is due to grain crushing effects at higher stress levels.

Figure (3.10) shows the variation of $\sin\phi_{PT}$ with the state parameter for Toyoura sand. From this, the linear variation of ϕ_{PT} with void ratio can be expressed as,

$$\sin\phi_{PT} = \sin\phi_{CV} + k_{PT}\psi \qquad [3.10]$$

Accordingly,

$$M = \frac{6\sin\phi_{PT}}{3-\sin\phi_{PT}}$$

where k_{PT} is the material constant that describes the slope of the above variation.

3.3.3. Hardening rule

Hardening describes the evolution of the yield surface upon shearing. Size hardening occurs when the value of p_c in yield function, as expressed by equation (3.2) changes whereas shape hardening occurs due to a change in M_p. This model assumes that M_p remains constant throughout shearing, i.e. there will not be shape hardening during the process of yielding.

During shearing, changes in the size of the yield surface occur such that p_c approaches a value p_f that corresponds to the size of the yield surface at failure. The size of the yield surface at failure, p_f can be calculated from a yield function if the stress ratio at failure (M_f) is known, where,

$$M_f = \frac{6\sin\phi_f}{3-\sin\phi_f} \qquad [3.11]$$

Been et. al. (1985) showed that the maximum attainable friction angle at failure (ϕ_f) can be related to state parameter at failure. Accordingly, Imam used the following relation to find friction angle at failure, Φ_f:

$$\sin\phi_f = \sin\phi_{CV} - k_f\psi \qquad [3.12]$$

where k_f is a material parameter that represents the slope of the variation.

The maximum attainable consolidation pressure (p_f) for the current state is obtained by assuming the current state is the failure state. This is achieved by substituting $\eta = M_f$ in equation (3.2) which then reduces to,

$$p_f = \frac{p}{\left(1-\dfrac{M_f^2}{5M_p^2}\right)^2}. \qquad [3.13]$$

where, p_f represent the size of the yield surface if the current state is the failure state.

As pointed out earlier, size hardening refers to a change in size of the yield surface, p_c in this case. Then the value, $p_f - p_c$ can be viewed as the hardening potential for the current stress state. Most of the models developed to date for sand take the plastic shear strain increment ($d\varepsilon_q^p$) as the hardening parameter (e.g. Pubela et al. 1997). Imam adopted the following form of the hardening rule, which was modified based on Jefferrie's (1993) Nor-Sand model:

$$\frac{\partial p_c}{\partial \varepsilon_q} = G_{\max}\left(\frac{p - p_c}{\left(p_f - p_c\right)_{ini}}\right) \qquad [3.14]$$

where $\left(p_f - p_c\right)_{ini}$ corresponds to the potential for hardening prior to shearing. G_{max} is the maximum plastic shear modulus, which is the slope of shear stress-strain curve at the origin.

3.3.4 Elastic response

So far only the parameters for the plastic behaviour of sand have been discussed. The elastic response of an isotropic linear elastic sand can be predicted by two parameters: Elastic bulk modulus (K) and elastic shear modulus (G). These parameters are density dependent. Imam (1999) used the following expressions proposed by Hardin and Black (1969) to find these parameters:

$$G = G_r \frac{(2.973 - e)^2}{1 + e} p^n \text{ and}$$

$$K = K_r \frac{(2.973 - e)^2}{1 + e} p^n \qquad [3.15]$$

where G_r, K_r and n are material parameters.

3.4 Determination of model parameters and calibration of the model:

A complete description of how to determine model parameters used in developing this model can be found in Imam (1999). Table (3.1) lists the model parameters used by Imam (1999) to predict the undrained behaviour of loose Ottawa sand. Imam (1999) used drained and undrained triaxial results on loose Ottawa sand reported by Sasitharan (1993) and Skopek (1994) to calibrate the model. Figure 3.11 shows the model calibration against the measured response of loose Ottawa sand in undrained triaxial condition.

A brief description on how to determine the model parameters for Fraser River delta sand (herein after referred to as FRD sand) is given in the following section:

1. The compressibility parameter (β) can be determined by curve fitting the data obtained from an isotropic compression test. As noted by Imam (1999), 'it is necessary to choose a value for this parameter that gives reasonable predictions for the range of pressures under consideration'. Since no data for FRD sand is available, a value of 0.02 has been assumed, which is the compressibility parameter for loose Ottawa sand.

2. φ_{cv} is the steady state friction angle reached when the material is sheared to large strains with no volume change experienced. This can be determined experimentally when the sample is sheared to its ultimate state. A value of $\varphi_{cv} = 35^{\circ}$ has been reported by Sasitharan (1994) for FRD sand. k_f can be determined by curve fitting failure friction angle plotted against void ratio.

3. k_p and e_μ can be obtained from an undrained triaxial compression test in which a clear peak is observed. Once φ_{cv} is known, a value of seven degrees smaller than φ_{cv} is assumed for φ_μ. From experimental observation, once M_p vs normalized void ratio (e_n) is plotted, both k_p and e_μ can be determined. Figure (3.12) shows the variation of M_p with normalized void ratio for FRD sand (Imam 1999). Assuming an intrinsic friction angle of 28° for FRD sand gives M_p=0.81 that corresponds to the void ratio e_μ =1.03. The slope of the line of M_p vs e_n, k_p = 1.14.

4. Elastic shear modulus can be obtained by drawing a tangent at the origin to the q vs ε_q plot. A typical value of Poisson ratio can be used to obtain the elastic bulk modulus. For FRD sand, G=500, K=1000, and n=0.55 is assumed.

5. The ultimate state line for FRD sand has been reported to be $e_\mu = 1.11 - 0.029 \ln(p_{ss})$ (Chillarige et al. 1997).

Accordingly, the model parameters for FRD sand have been tabulated in Table (3.1). The model performance for FRD sand using these model parameters is shown in Figure 3.13 along with observed result for loose FRD sand reported by Chillarige et al. (1997).

3.5 Summary and conclusion

Understanding the shear strength characteristics and deformation behaviour of soil requires an elasto-plastic stress-strain model that best describes the yielding behaviour of soil. Essential features of an elasto-plastic stress-strain model are: elastic parameters, yield function, flow rule and hardening rule. The existence of a unique normal consolidation line for fine-grained soils paved the way to a simple elasto-plastic model. But, for granular soil there exist infinite number of normal consolidation lines. This along with pressure and density dependency of granular soil resulted in numerous constitutive relations being proposed.

It has been observed that loose sand exhibits instability behaviour at post peak shearing during undrained loading – a phenomenon often responsible for flow liquefaction failure of loose sand. A model developed by Imam (1999) captures this behaviour well. Nine parameters are needed to describe this model and model parameters can simply be determined from laboratory tests.

Table 3.1 - Model parameters used in this study for Ottawa sand (Imam, 1999) and FRD sand.

Parameter Type	Parameter Name	Ottawa sand	FRD sand
Peak State	k_p	1.6	1.14
	e_μ	0.75	1.03
Critical state parameter	ϕ_{CV}	32	35
	k_{PT}	1	1
Failure	k_f	0.75	0.75
Compression	β	0.02	0.02
Elastic	G_r	500	500
	K_r	1000	1000
	n	0.55	0.55

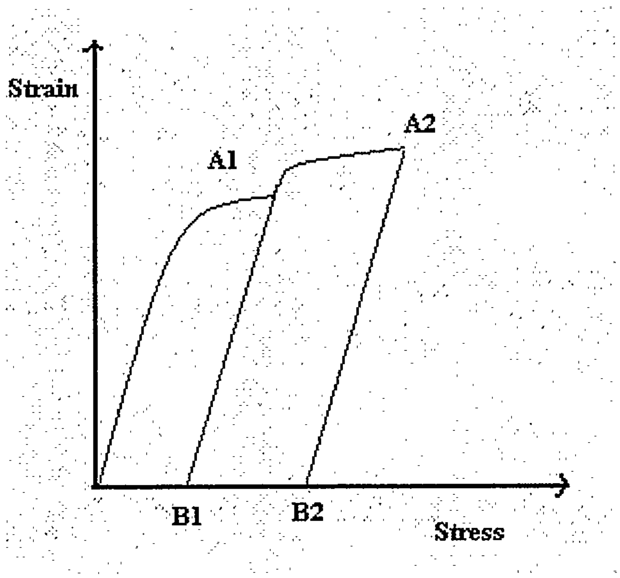

Figure 3.1 - Typical stress-strain curve for an annealed copper wire in uniaxial loading.

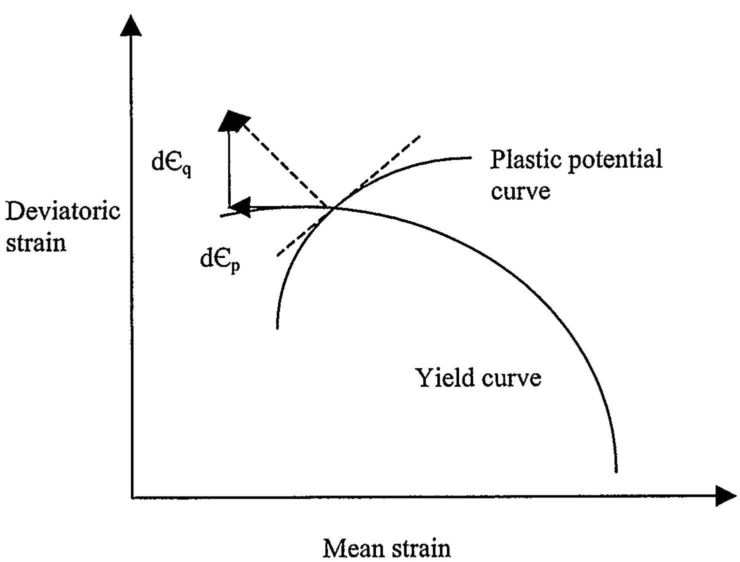

Figure 3.2 - Definition of plastic potential within the principle of co-axiality.

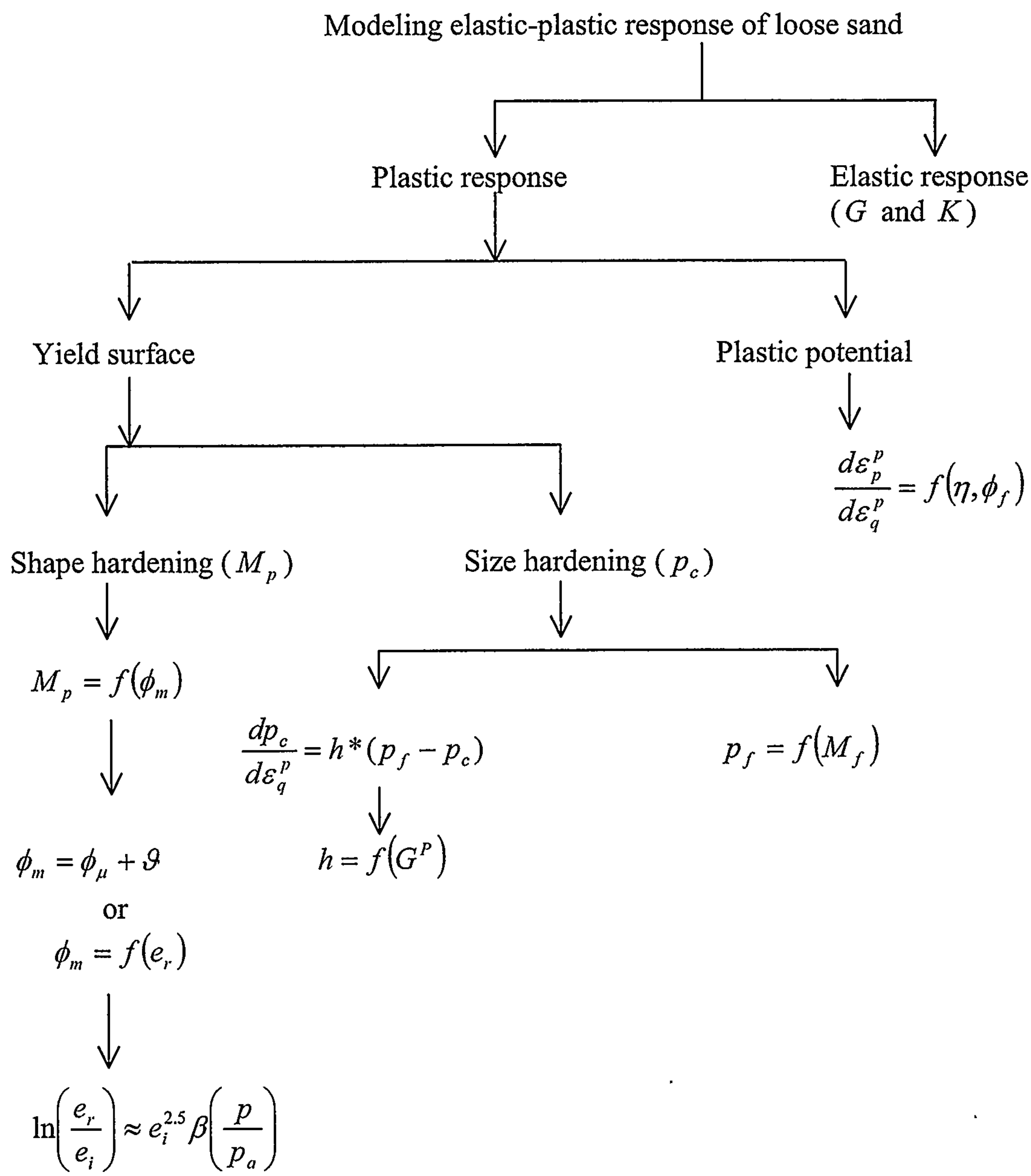

Figure 3.4 - Imam's elasto-plastic stress-strain model that captures the behaviour of loose sand – material parameters at a glance.

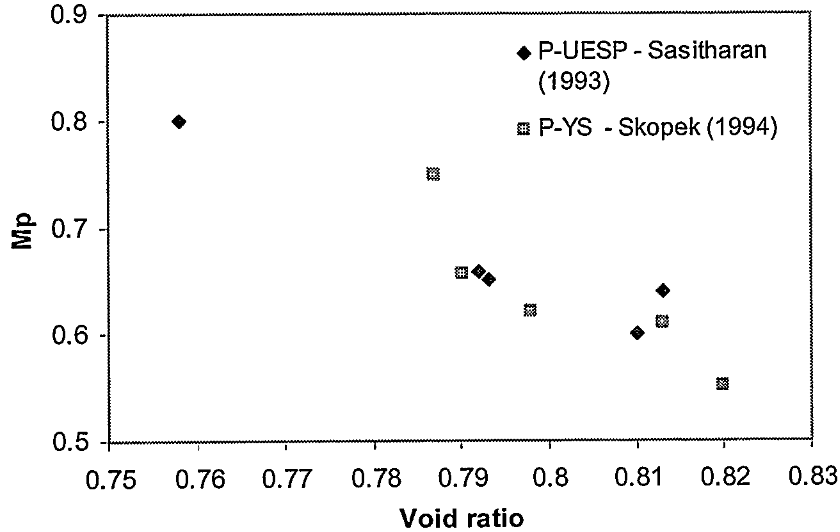

Figure 3.4 – Variation of stress ratio at peak (Mp) with void ratio for both Undrained Effective Stress Path (UESP) and Yield Surface (YS) proposed by Imam (1999) for sand. Note that, data points for P-YS had been indirectly obtained by Imam (1999) from Constant Deviatoric Stress (CDS) tests carried out by Skopek (1994). See Imam (1999) for detail.

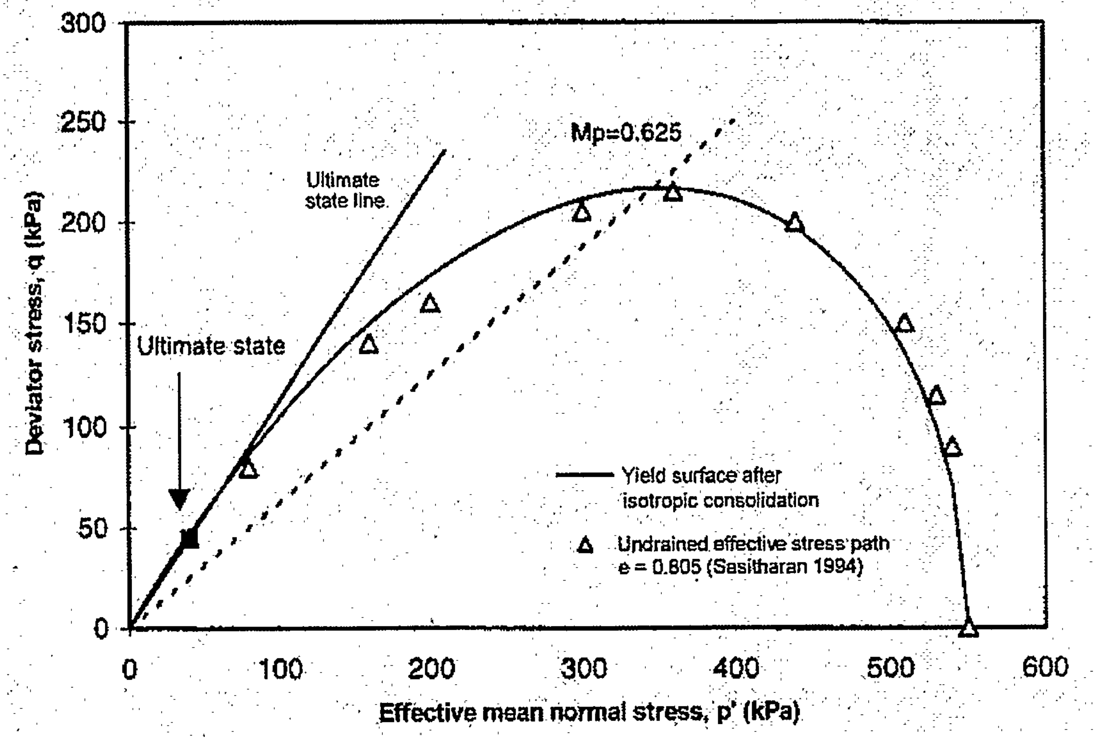

Figure 3.5 - Shape of the yield surface compared with undrained effective stress path (UESP) of Ottawa sand for isotropic consolidation pressure of 550 kPa and void ratio of 0.805, reported by Sasitharan 1994 (Imam 1999).

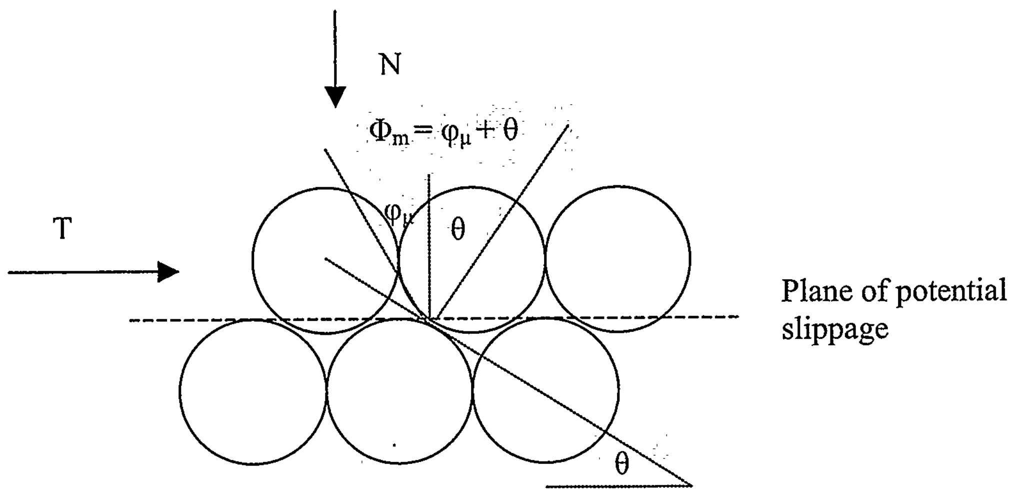

Figure 3.6 - Definition of mobilized friction angle for loose sand (adopted from Imam, 1999).

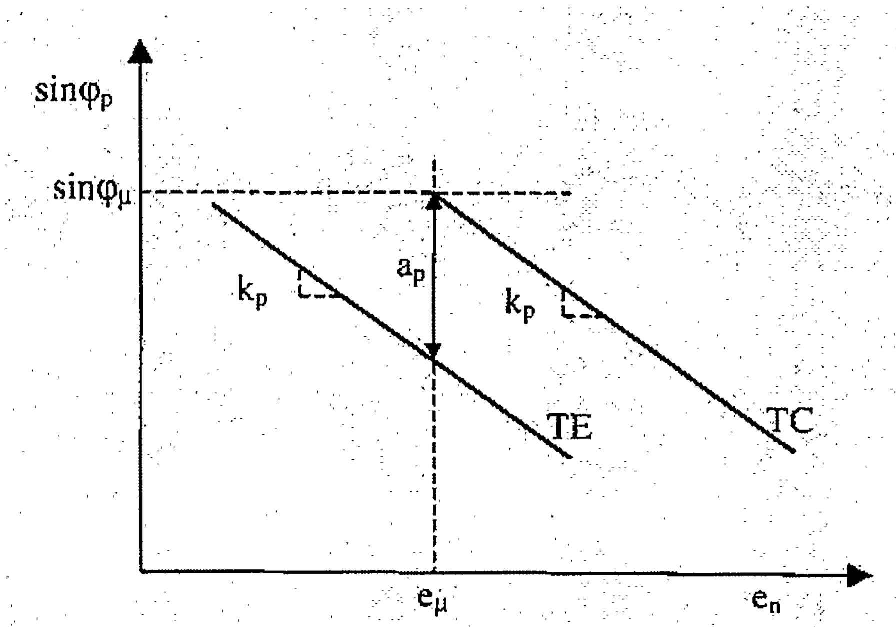

Figure 3.7 - Variation of M_p with e (adopted from Imam 1999).

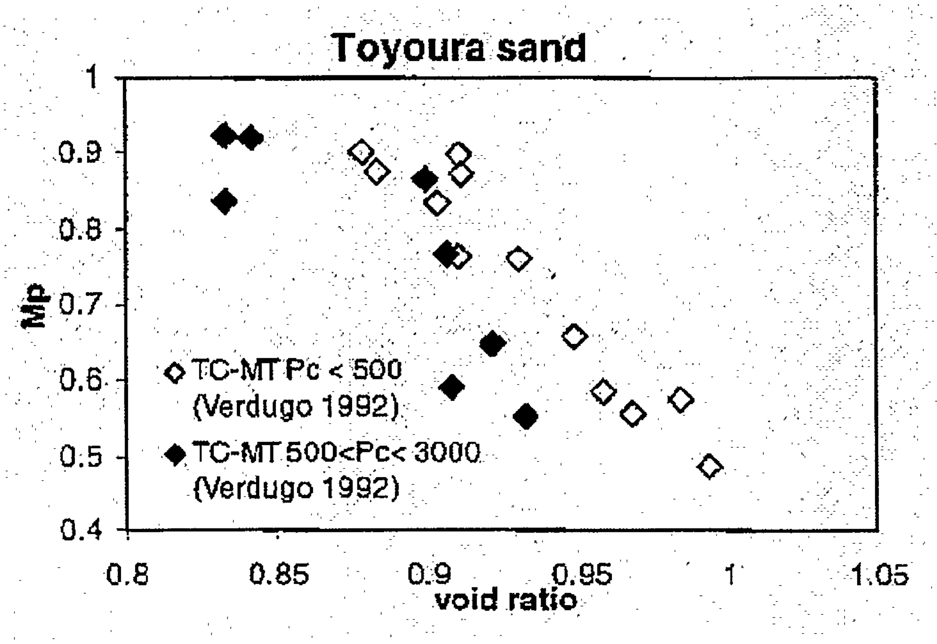

Figure 3.8 - Variation of M_p with void ratio for different confining pressure for Toyura Sand (Imam 1999).

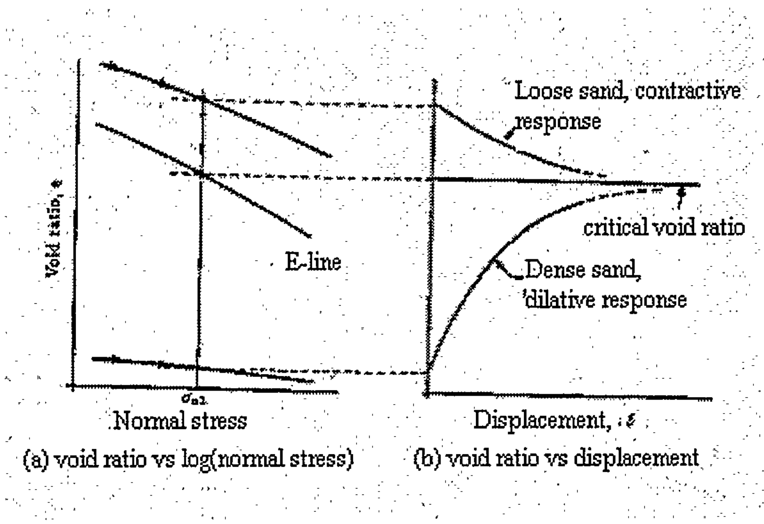

Figure 3.9 - The origin of the oncept of critical void ratio (Casagrande, 1936); this was later used in Critical state soil mechanics by Roscoe et al. (1958).

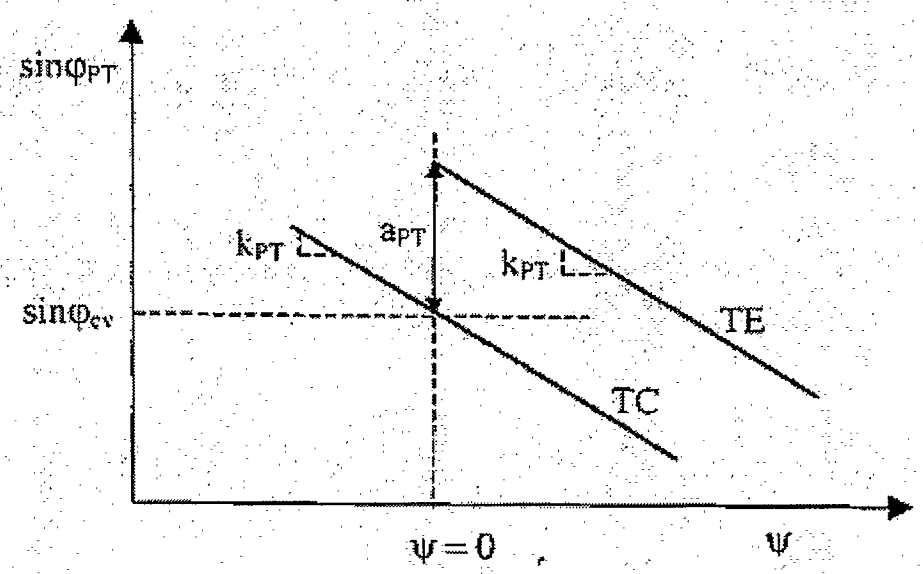

Figure 3.10 - Variation of friction angle at phase transformation with state parameter, ψ (Imam 1999).

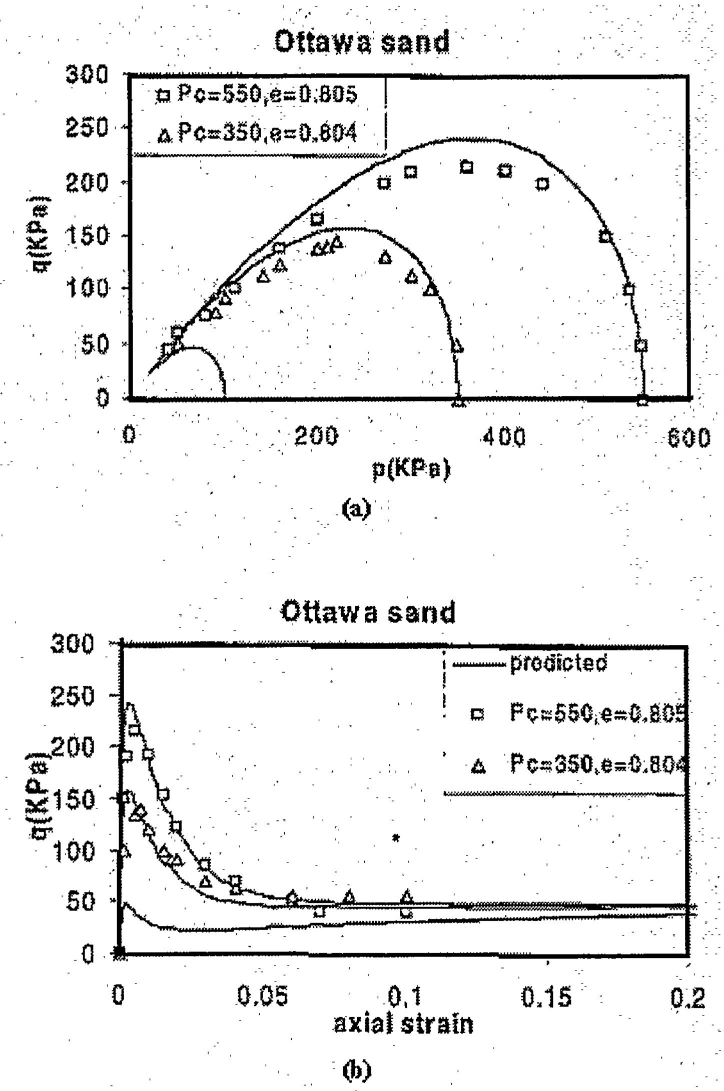

Figure 3.11 - Model calibration against measured response of very loose Ottawa sand in undrained triaxial compression test (Imam 1999).

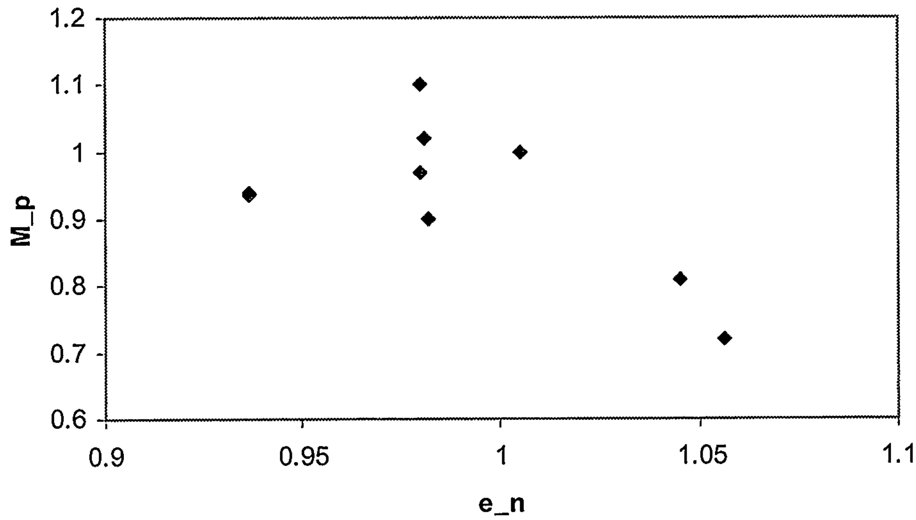

(a)

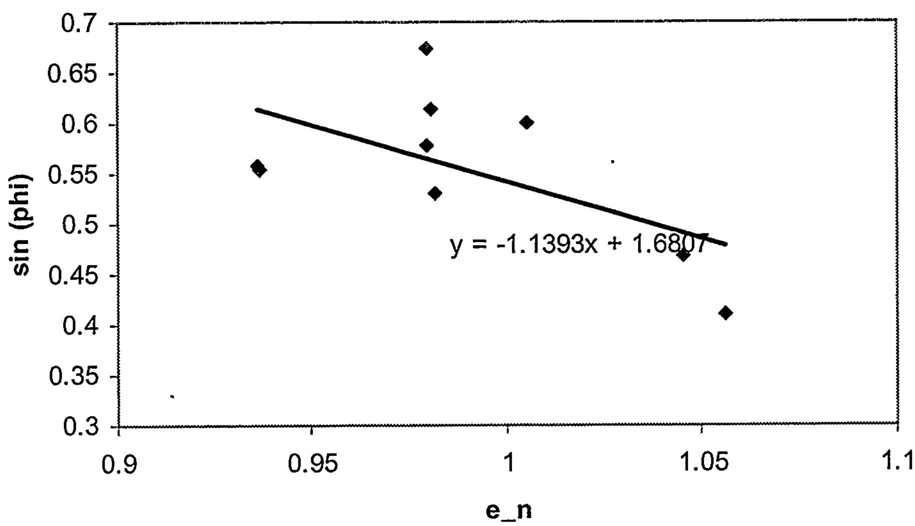

(b)

Figure 3.12 - (a) Variation of M-p and (b) variation of sin(φ) with normailsed void ratio for FRD sand (Imam 1999).

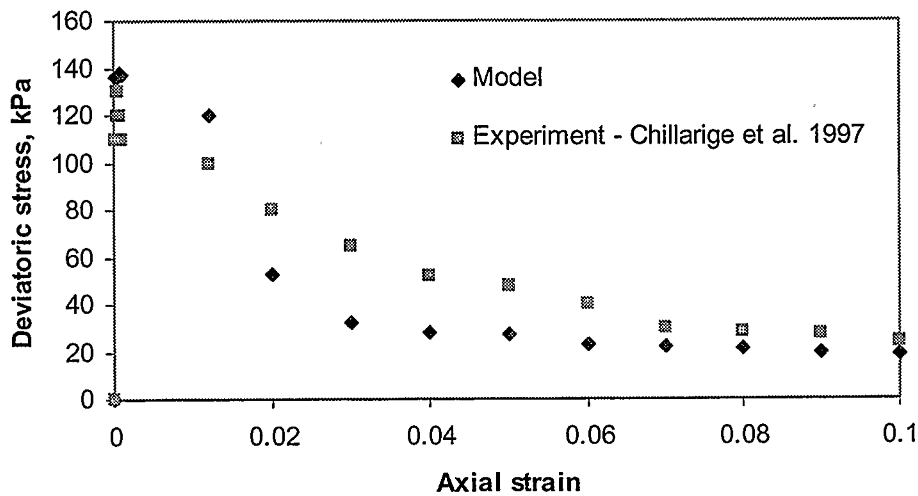

Figure 3.13 - Model performance against observed response of loose FRD sand (effective confining of 148 kPa and void ratio of 1.06) reported by Chillarige et al. (1997).

CHAPTER 4

EFFECT OF OCCLUDED GAS BUBBLES ON UNDRAINED SHEAR STRENGTH OF LOOSE SAND[1,2]

4.1 Introduction

It has been noted from Chapter 3 that loose sands are susceptible for flow liquefaction when sheared under undrained conditions. Submarine slopes like deltas predominantly contain loose sand with occluded gas bubbles that fit within voids. The bubble size of gas formed due to microbial activity (which is predominant in deltaic environments due to high organic content and anaerobic conditions) has been found to be small and remain trapped in the sediments for years (Hulbert and Bennet 1975). Studies have shown that the in situ degree of saturation of this type of soil is more than 85% (Chillarige et al. 1997; and Fourie et al. 2001).

---

[1] *Part of this chapter has been published. Mathiroban, S., and Grozic, J.L.H. 2004. A model to predict the undrained behaviour of loose gassy sand. Proceedings of the 57th Canadian Geotechnical Conference, October 25-27, 2004, Quebec City, Quebec, Canada.*

[2] *A version of part of this chapter has been submitted for possible publication on Journal of Geotechnical and Geo Environmental Engineering, American Society of Civil Engineers (ASCE).*

The presence of bubbles has been found to increase the compressibility of the soil matrix. The effect of this compressible pore fluid is referred to introduce volume change as well as pore pressure change in soil during undrained shearing. This is analogous to shearing of saturated soil under partial drainage condition, as observed by Vaid and Eliadorani (1988).

Two approaches are possible for the analysis of gassy soils. One is to consider the gassy soil as 'spherical cavities or gas voids surrounded by a saturated soil matrix' (Wheeler 1989) and the other way is to consider it as a 'saturated soil matrix with compressible pore fluid' (Thomas 1989). For gassy soil with occluded bubbles within the voids, the second postulation is considered more appropriate. Fredlund and Rahardjo (1993) argued that for degrees of saturation higher than 85%, where free gas exists in occluded form, surface tension effect can be neglected in analyzing the soil matrix for macro parameters such as effective stress and compressibility. In occluded zone (Figure 4.1), bubbles do not interact with soil matrix and the water-gas bubble mixture can be considered as one homogeneous mixture when analyzing for compressibility and effective stress.

In this chapter, the model developed by Imam (1999) for loose sand is modified to account for the effect of gas bubbles. The model has been formulated in finite difference format with plastic shear strain as the independent incremental variable.

4.2.0 Effect of gas bubbles:

4.2.1 Excess pore pressure generation

Numerous researchers have found excess pore pressure associated with gas bubbles in marine environments (e.g. Esrig and Kirby 1997, Lee et. al. 1991 and Field 1991). Growing bubbles release energy and causes the surrounding media to expand, i.e., do mechanical work on the surrounding media. A practical example of this phenomenon is the volatile expansion in magma flow during volcanic eruption. Gas ex-solution from volcanic melt causes the volume of the magma to expand by a factor of four (Linsky et al. 2002). Linsky et. al. (2002) developed a model to predict the energy dissipation during bubble nucleation and growth, assuming spherical bubbles and homogeneous bubble distribution. This was developed for situations where gas bubbles nucleate and grow by dissolution, when ambient pressure change occurs to a volatile saturated fluid. The same phenomenon is encountered in several geotechnical engineering problems such as during destabilisation of gas hydrates due to sea level change (Peter et al. 1991) and gas exsolution in heavy oil due to unloading/pressure reduction during oil and gas extraction (Wong 2003). Gas exsolution from oil sand results in the phenomenon known as 'Foamy oil flow' in oil wells that may result in the problem of 'sand production'.

Though there are no studies that relate excess pore pressure developed to gas bubble growth due to bacterial activity, the explanation above can be extended to this situation as well. No previous work has been carried out to relate degree of water saturation (*Sr*) (see page 34), in other words, presence of gas to the excess pore pressure.

Other than bubble growth that exerts pressure in surrounding soil, high sedimentation rates compared to the rate of consolidation in deltaic environments also contribute to excess pore pressure. This phenomenon is found in fine-grained granular soils that exist in sub-marine slopes (Terzaghi 1956). Terzaghi (1956) expressed the degree of consolidation in terms of excess pore pressure as,

$$U = 1 - \frac{U_w}{\gamma_S z} \tag{4.1}$$

where U_w is the excess pore pressure, z is the depth below water level and γ_S is the submerged unit weight of the sediment. To specifically denote that the value of U will be less than unity, researchers later used the term 'degree of under consolidation' (e.g. Coleman et al. 1991).

One way to look at excess pore pressure during gas exsolution/bubble growth in particulate media is to consider it as 'internal loading'. Skempton's B-parameter will be close to unity at the beginning, when the degree of saturation is 100% (fully saturated condition). Consequently, the entire load will be taken by the pore water, which is assumed to be incompressible. This increase in pore pressure occurs in the same manner whether a sample is loaded externally in an undrained condition or internally by gas exsolution and/or expansion.

The phenomenon of increase in pore fluid pressure during bubble growth can be observed in an unloading experiment on soil with gas saturated pore fluid, carried out by Sobkowikz (1982). Sobkowikz carried out this experiment in Ottawa sand (initial porosity of 0.32), saturated with carbon dioxide saturated water. Unloading was done in an incremental basis, allowing the system to come to equilibrium at each stage. Gas exsolution was observed and the pore pressure was found to be constant, close to the liquid/gas saturation pressure (510kPa in this case). That is to say, Skempton's B-parameter remained close to zero during the exsolution phase. Figure (4.2) shows the observed equilibrium behaviour of gassy soil upon unloading.

Similarly, excess pore pressure is induced in deep gas hydrate bearing sediments upon sea level reduction. When the methane-water mixture is subjected to particular temperature-pressure regime, the mixture forms a solid crystalline structure, known as gas hydrate. The reduction in sea level causes gas hydrate dissociation and releases bubble phase gas into the sediment. Hydrate will dissociate until pore pressure in the sediment is elevated to 'equilibrium phase boundary condition' (Kayen and Lee 1991). For example, Sultan et al. (2003) observed under consolidated sediments in a one dimensional consolidation test on gas hydrate bearing sediments of Zaiango area, Gulf of Guinea (see Figure 4.3).

Sobkowikz and Morgenstern (1982) used short term and long term B-parameters to handle these time dependent pore pressure parameters. Considering kinetics of gas bubble growth due to gas dissolution in super saturated oil, Wong (2003) developed a mechanistic model to predict short term and long term B-parameters. Excess pore pressures remain in marine sediments without dissipation because of high sedimentation rates and silt content in deltaic environments (Terzaghi 1956) and because of impermeable gas hydrate layer in deep sea deposits (Field 1991). Since excess pore pressure is caused by a combination of several factors, it is difficult to predict the exact level of excess pore pressure in marine sediments.

4.2.2 Increase in pore fluid compressibility

Pore fluid compressibility is defined as the change per unit volume for a unit change in pore fluid pressure. Accordingly, compressibility (β) can be expressed as:

$$\beta = -(1/V)\,(dV/dP) \qquad [4.2]$$

where V is the volume and dP is the change in confining pressure. Compressibility determines the decrease in volume for given pressure increase. Hence,

$$dV_w = -\beta_w V_w du \text{ for water and} \qquad [4.3a]$$

$$dV_T = -\beta_T V_T (d\sigma - du) \text{ for soil.} \qquad [4.3b]$$

where β_w = compressibility of water and β_T = compressibility of soil. In an undrained condition, relative values of β_w and β_T define pore pressure increase and effective stress change. In classical soil mechanics problems, water is assumed to be incompressible compared to the soil matrix, resulting in Skempton's B-parameter being equal to unity.

Even a small inclusion of gas bubbles in the pore fluid drastically changes the compressibility of the pore fluid; therefore, B-parameter is no longer close to unity. Note that the compressibility effect on the B-parameter is a different phenomenon from the short term B-parameter during gas exsolution in the undrained unloading case, as discussed in section 4.2.1. In the latter case, excess pore pressure brings B closer to zero while in the earlier case, compressibility reduces B to less than unity.

4.2.2.1 Compressibility of liquid-gas mixture

A detailed derivation for the compressibility of a gas-liquid mixture is available in Sobkowikz (1982), Fredlund and Rahardjo (1993) and Grozic (1999). Logical steps that led to the derivation are presented below for the sake of completeness:

For a miscible gas-water mixture, Boyle's law and Henry's law govern the volume change behaviour of free and dissolved gas respectively for a change in ambient pressure.

Boyle's law: In an isothermal condition, the volume of a given number of molecules of gas is inversely proportional to the absolute pressure of the gas. In mathematical form,

$$P_g V_g = k \qquad [4.4]$$

where P_g = absolute gas pressure, V_g = volume of gas and k = constant of proportionality.

Henry's law: Henry's law states that the mass of dissolved gas in a fixed volume of liquid, at constant temperature is directly proportional to the absolute pressure of the gas above the solution. i.e.,

$$M_d / P_g = k \qquad [4.5a]$$

where M_d is the mass of the dissolved gas and P_g is the absolute gas pressure. By applying the ideal gas law to the dissolved gas, it can be shown that for a fixed volume of liquid subject to a constant temperature and confining pressure P, the volume of dissolved gas is constant when the volume is measured at pressure P. This can be expressed as,

$$V_d = hV_w \qquad [4.5b]$$

where V_d and V_w are volume of dissolved gas and volume of water respectively; the constant h is referred to as Henry's volumetric coefficient of solubility (see Section 1.4b). Typical Henry's volumetric coefficient of solubility values are 0.02 for an air/water mixture and 0.82 for carbon dioxide/water mixture.

From the definition of compressibility (i.e., Equation (4.2)), the compressibility of free gas can be written as,

$$\beta_g = -\frac{1}{V_g} \cdot \frac{dV_g}{dP_g}$$

Differentiating Equation (4.4) with respect to P_g gives,

$$\frac{dV_g}{dP_g} = -\frac{k}{P_g^2}$$

Substituting this into the above equation gives the compressibility of free gas as,

$$\beta_g = \frac{1}{P_g} \qquad [4.6]$$

Note that P_g is absolute gas pressure.

Referring to phase diagram before and after loading, as shown in Figure (4.4), the compressibility of a miscible gas-liquid mixture can be derived. In deriving this equation, water is considered to be incompressible and hence the volume of water is considered to remain constant. That means the volume of dissolved gas is constant according to Henry's law. According to Figure (4.4), the total volume of gas before loading is:

$$V_{Tg}^0 = V_{fg}^0 + hV_w \text{ (at pressure } P_g^0\text{)} \qquad [4.7a]$$

The total volume of gas after loading is:

$$V_{Tg}^1 = V_{fg}^1 + hV_w \text{ (at pressure } P_g^1\text{).} \qquad [4.7b]$$

where subscript *'Tg'* refers to total gas and *'fg'* refers to free gas; superscript *'0'* refers to initial condition and *'1'* refers to final condition.

By applying Boyle's law to both the free and dissolved gas, Equation 4.7b can be written as,

$$V_{Tg}^{1} = (V_{fg}^{0} + hV_{w})\frac{P_{g}^{0}}{P_{g}^{1}} \qquad [4.8a]$$

Hence,

$$\Delta V_{fg} = V_{Tg}^{0} - V_{Tg}^{1}$$

$$= (V_{fg}^{0} + hV_{w})\left(\frac{P_{g}^{0} - P_{g}^{1}}{P_{g}^{1}}\right)$$

$$= -(V_{fg}^{0} + hV_{w})\left(\frac{\Delta P_{g}}{P_{g}^{1}}\right) \qquad [4.8]$$

where negative sign indicates decrease in volume of free gas incremental pore gas pressure change.

Suppose the compressibility of the pore fluid is denoted by β_f. Then,

$$\beta_f = -\frac{1}{V_f}.\frac{dV_f}{dP}$$

$$= -\frac{1}{V_f}\left(\frac{dV_{fg}}{dP} + \frac{dV_w}{dP}\right)$$

$$= -\frac{1}{V_f}\left(\frac{-\left(V_{fg}^0 + hV_w\right)}{P_g} - V_w\beta_w\right)$$

$$= \frac{(1 - S + Sh)}{P_g} + \beta_w S \qquad [4.9]$$

Equation (4.9) reveals that compressibility of the gas-water mixture is increased by the presence of free gas and it is pore pressure dependent. Note that the above equation has been derived when free gas is present in the sample and hence valid for degree of water saturation S<1.

---

* Throughout this thesis, degree of saturation will be referred to degree of water saturation, the ratio of volume of water voids to the volume of total voids ($S = \frac{V_w}{V_v}$) as used in classical soil mechanics. Accordingly, 'degree of gas saturation' will be,

$$1\text{-}S = \frac{V_{fg}^0}{V_v}$$

4.2.2.2 Volume change and pore pressure development:

As the compressibility of the gas-water mixture is considerably increased due to the inclusion of gas bubbles, the magnitude of the pore pressure response will depend on the relative compressibility values of the pore fluid and soil skeleton. This can easily be explained by the double spring model proposed by Duessault (1980) as shown in Figure (4.5).

Equation (4.8) gives the change in volume due to gas compression/expansion and dissolution/ex-solution of gas. Assuming change in volume (*ΔV*) is entirely due to change in free gas volume, equation (4.8) can be re-written as,

$$\Delta V = -\left(V_{fg}^{0} + hV_{w}\right)\left(\frac{\Delta P_{g}}{P_{g}}\right)$$

Dividing the entire equation by total volume (*V*) gives,

$$\frac{\Delta V}{V} = -\left(\frac{V_{fg}^{0}}{V_{v}} + h\frac{V_{w}}{V_{v}}\right)\left(\frac{V_{v}}{V}\right)\left(\frac{\Delta P_{g}}{P_{g}}\right)$$

Where $\frac{V_{fg}^{0}}{V_{v}}$ is the degrees of gas saturation, which is equivalent to $(1-S)$.

Hence,

$$\frac{\Delta V}{V} = -\left(1 - S + Sh\right)\left(\frac{\Delta P_{g}}{P_{g}}\right)n \qquad [4.10]$$

where n is the porosity and ΔP_g is the change in absolute gas pressure which is equivalent to the change in pressure (Δu) and S is the degree of water saturation. The above equation has been derived when free gas is present in the system (i.e., for degree of water saturation, S< 1). In other words, equation applies to cases where degrees of water saturation < 1.

By applying volume compatibility and considering equilibrium (with respect to gas compression and dissolution), Sobkowikz (1982) derived an expression for the change in pore fluid pressure. Accordingly, for volume compatibility,

Change in sample volume (ΔV_T) = Change in water volume (ΔV_w) +

Change in gas volume (ΔV_g)

Substituting Equations (4.3a), (4.3b) and (4.8) for the above terms respectively gives,

$$-\beta_T V_T(\Delta\sigma - \Delta u) = -\beta_f V_v \Delta u$$

Substituting Equation (4.9) for pore fluid compressibility gives,

$$-\beta_T V_T(\Delta\sigma - \Delta u) = -\left(\frac{1 - S + Sh}{P_g} + \beta_w S\right) V_v \Delta u$$

Dividing the entire equation by total volume (V_T) and re-arranging gives the quadratic equation for the change in pore water pressure as:

$$A\Delta u^2 + B\Delta u + C = 0 \tag{4.11}$$

where,

$$A = \beta_T + nS\beta_w$$

$$B = \beta_T\left(P_g - \Delta\sigma\right) + n\left(\beta_w.S.P_g + 1 - S + S.h\right)\text{and}$$

$$C = -\beta_T.\Delta\sigma.P_g$$

S in the above equation is the degree of water saturation (and hence 1-S is the degree of gas saturation). During the deformation history of an undrained shearing, degrees of water saturation changes owing to gas compression/expansion and dissolution/ex-solution. From the definition of degrees of water saturation ($S = \frac{V_w}{V_v}$), the change in degrees of water saturation can be computed as,

$$dS = \frac{V_v dV_w - V_w dV_v}{V_v^2}$$

Since there is no change in volume of water, i.e., $dV_w = 0$

$$dS = -\frac{V_w}{V_v}\frac{dV_v}{V_v} = -\frac{V_w}{V_v}\frac{dV_v}{V}\frac{V}{V_v} = -\frac{S}{n}\frac{dV_v}{V}$$

Where n is the porosity of the sample; $\frac{dV_v}{V}$ can be calculated from Equation (4.10). Negative sign indicates change in degrees of water saturation in opposite to change volume. In compressive volumetric change, dS become positive.

Hence, evolution of degrees of water saturation during shearing can be expressed as,

$$S_{i+1} = S_i + dS = S_i - \frac{S_i}{n}\frac{dV_v}{V}$$

$$= S_i\left(1 - \frac{dV_v}{nV}\right) \qquad [4.12]$$

where n is the porosity; β_T and β_w are soil and water compressibility, defined by Equation (4.2) respectively. P_0 is the initial absolute gas pressure and $\Delta\sigma$ is the incremental isotropic loading/unloading value. The compressibility of pure water (β_w) is 4.58x10^{-7} KPa^{-1} (Fredlund and Rahardjo 1993). The compressibility (β_T) of soil can be related to Compression Index (C_c) by,

$$\beta_T = C_C \frac{\log\left(1 + \frac{dp}{p}\right)}{dp(1+e)} \qquad [4.13]$$

where dp is the change in mean effective pressure and e is the void ratio; C_c is the slope of compression curve in void ratio vs log (effective stress) plot. This plot can be obtained from isotropic/hydrostatic compression test in the laboratory (see Figure 4.8). A Typical compression index value for uniform loose sand is 0.03 (Lambe and Whitman 1969). For 100 kPa to 200 kPa confining pressure range, the compressibility value can be considered as 0.000025 KPa^{-1}. β_T is a function of the confining pressure as well as back pressure, as evident from Equation 4.13.

Equation (4.11) determines the change in pore pressure for an external loading, both isotropic and anisotropic; in an anisotropic case, $\Delta\sigma$ should be changed accordingly (Sobkowikcz and Morgenstern 1984). It should be noted that, in deriving this expression it has been assumed that the pore water pressure is equal to the pore gas pressure and the change in pore water pressure is equal to the change in pore gas pressure throughout the loading process. The validity of the above assumptions has already been discussed for soil containing occluded gas bubbles in Section (4.1). Δu calculated from Equation (4.11) accounts for pore pressure change due to external loading (i.e., due to dp). Δu due to shearing characteristics of soil is computed by multiplying dp' by an appropriate assumed long term B-parameter.

The combined effect of volume change and pore pressure development has been referred to as 'partially drained condition' (Esrig and Kirby 1997). Atigh and Byrne (2003) adopted the same approach in modeling the effect of gas bubbles on undrained behaviour of loose sand.

4.3 Gassy soil modification

Gassy soil can be analysed in two ways:

1. Considering it as a saturated soil with compressible pore fluid (Thomas 1989) as shown in Figure (4.6a)
2. Considering it as large gas filled cavities surrounded by a soil matrix saturated with incompressible water (Wheeler 1989) as shown in Figure (4.6b)

While approach (1) is appropriate for granular soils with occluded bubbles within voids, approach (2) will be appropriate for the analysis of fine-grained soil with gas bubbles. The second approach considers gassy soil behaviour at the bubble level; cavity expansion/contraction and bubble flooding effects that depend on gas pressure, confining pressure and surface tension have been suggested for this approach (Wheeler 1988). In modifying the model described in Chapter (3) to incorporate effect of occluded gas bubbles in loose sand, gassy soil has been treated as saturated soil with compressible pore fluid, i.e., the conceptual model shown in Figure (4.6b) has been adopted.

Yielding in sand is entirely due to plastic deformation that occurs at the grain-to-grain contact point. According to Rowe (1969) plastic deformations, which are governed by the stress-dialatancy relation for sand, are dependent on effective stress. In other words, changing the type of pore fluid that fills the voids will not affect the yielding behaviour of sand. What should be considered is that all of the models have been proposed with model parameters that have been established for saturated soils with water as pore fluid; water is assumed to be incompressible. Compressibility behaviour should be considered in establishing model parameters when a saturated soil specimen with compressible pore fluid is analysed for yielding, as in the case of gassy soil with occluded gas bubbles.

4.3.1 Compression behaviour of gassy soil

Recall from Chapter 3 that the use of the compressibility model (Equation 3.5) is to find the 'formation void ratio' at the start of the shearing. Since gas compression is not incorporated in that model, it requires the compressibility equation (Equation 3.5) used in Imam's model to find the 'formation void ratio' of sand to be re-defined.

So far, no experimental evidence is available to understand the isotropic compression behaviour of sand that contains occluded bubbles within voids. Sills et al. (1991) reported 1-D consolidation results on cohesive soil that contains 'bubble cavities' spanning the soil skeleton. The 1-D odometer test was carried out on synthesised gassy soil using Zeolite technique. Vertical stress was increased linearly from 25 kPa to 435 kPa over a period of 4 hours, allowing one-way drainage. Pore water pressure was measured at the closed end; note that according to approach (2) in Section (4.3), pore gas pressure is not equal to pore water pressure in this experiment.

Based on the observation, Sills et al. (1991) concluded that, 'for any gas content, the void ratio of the soil matrix surrounding cavity is solely a function of 'operative stresses'*. Figure (4.7a) shows the variation of void ratio plotted against operative stress. When the water void ratio was plotted against operative stress, all curves converged to a unique curve, as shown in Figure (4.7b). This supports the idea of a unique normal consolidation line for saturated cohesive soils. If we extend the same idea to granular gassy soils, we would be able to use the compression model suggested by Pestana and Whittle (1995) to find the relation of void ratio with mean normal stress.

Since no experimental results on the compression behaviour of granular soil with gas bubbles within voids are available, a different approach has been adopted here. Once the reference void ratio for a particular initial void ratio has been found using equation (3.5), for succeeding finite difference steps, the change in void ratio that can be calculated from equation (4.10) has been subtracted to find a new reference void ratio. The following paragraph justifies this approach:

Figure (4.8) shows the typical compression behaviour of cohesionless soil over a wide range of densities. It can be noted that, within a certain pressure range, the compression

---

*Sills et al. (1991) used the term 'operative stress' defined as the difference between total stress and pore water pressure, instead of 'effective stress'. According to Terzaghi's definition of effective stress, it is the stress that controls both change in shearing resistance and distortion/deformation which is not applicable to gassy soil.

curves are parallel for any initial void ratio (e_0). This is due to the fact that, at this pressure range, the volumetric change is due to elastic compression of the soil skeleton and particle movements by sliding and/or rolling (Pestana and Whittle, 1995). Parallel compression line for different initial void ratios facilitates finding a reference void ratio at each stages of shearing by subtracting change in void ratio due to compression and dissolution of gas from reference void ratio at preceding stage. Once reference void ratio is found, in finding the mobilized friction angle from Equation (3.4), it is assumed that the gas bubble growth/shrinkage will not affect the soil fabric at a macroscopic level. Note that, some researchers have speculated that soil fabric disruption at the microscopic level is possible due to bubble nucleation and growth (Rau and Chaney 1988; and Silva and Brandes 1998). In this thesis, experimental results reported by Grozic (1999) on synthesized gassy samples have been compared with the model prediction. Grozic's gassy sample preparation was such that the soil structure was not affected by gas bubble growth.

4.3.2 Volumetric strain and pore pressure development

Equation (4.10) expresses the ratio of change in volume of voids to total volume, introduced in gassy soil matrix due to gas compression/expansion and gas dissolution/ex-solution. Referring to phase diagram (Figure 4.3), change in volume of voids (dV_{v0}) can be equated to change in volume (dV_0). Accordingly,

$$\frac{dV_{V0}}{V_0} = \frac{dV_0}{V_0} \qquad \text{which will be given by Equation (4.10)}$$

Equation (4.11) gives pore pressure development during an undrained shearing. Section (4.3.4) explains how volumetric strain interacts with the constitutive model.

4.3.3 State parameter (ψ) for gassy soil

The plot of steady state void ratio vs mean effective stress for loose gassy Ottawa sand, reported by Grozic (1999), as shown in Figure (4.9) suggests that inclusion of gas bubbles shifts the steady state line above and to the right of the steady state line for saturated soil. This supports Sills et al. (1991)'s observation that for any gas content, the void ratio of the saturated soil matrix surrounding the bubble cavity is a function of the operative stress or mean normal effective stress. The shift in steady state void ratio is simply due to gas bubble presence.

Accordingly, the state parameter (ψ) can be calculated once e_{ss} and e_0 is adjusted for the presence of bubbles as,

$$\Psi = Se - e_{ss} \qquad [4.13]$$

where S =current degree of saturation of gassy sand; and e_{ss} = steady state void ratio which can be calculated from Equation (3.9).

4.3.4 Interaction of gassy soil component with base model

Both volumetric strain and pore pressure change occurs during an 'undrained' shearing of gassy soil. Following are some procedures that highlight how the gassy soil components (volumetric strain, pore pressure development and Henry's volumetric coefficient of solubility) interact with main constitutive model for saturated sand.

1. Set up initial conditions (such as the values of mean effective stress (p), degrees of water saturation (S) and porosity (n), and initial absolute pore pressure (P)). In Imam (1999)'s model, elastic deviatoric strain is the independent incremental parameter. Calculate change in deviatoric (dq), and incremental plastic volumetric strain ($d\varepsilon_v^p$) using Imam (1999)'s model.

2. Calculate incremental developed pore pressure (Δu) due to external loading and shearing characteristics of the soil skeleton. Equation (4.11) gives the pore pressure development due to undrained shearing of soil with compressible pore fluid.

3. This incremental increase in pore pressure (Δu) will be applied to Equation (4.10) in calculating the volumetric strain ($d\varepsilon_v$) due to gas compression/expansion according to Boyle's law and gas dissolution/ex-solution according to Henry's law.

4. Hence, incremental elastic volumetric strain will be computed as:

$$d\varepsilon_v^e = d\varepsilon_v - d\varepsilon_v^p$$

where $d\varepsilon_v^p$ is given by Rowe's stress-dilatancy model (Equation 3.7).

5. In the main constitutive model, change in mean effective stress (dp) is the product of elastic volumetric strain and elastic bulk modulus. i.e.,

$$dp = K.\ d\varepsilon_v^e$$

where K = bulk modulus; $d\varepsilon_v^e$ = elastic volumetric strain for a particular finite difference increment.

6. Calculate new degree of saturation (say, S_{i+1}) from Equation (4.12) and new mean effective stress ($p_{i+1} = p_i + dp$). New porosity (n_{i+1}) will be calculated based on change in volume (Equation 4.8).

7. Consider parameters calculated in Step (6) as the initial parameters and continue to the next finite difference step starting with Step (1). Repeat the above procedure until a predetermined axial strain is reached.

At the initial stages of shearing, $d\varepsilon_v^e$ will be positive and thus, mean effective stress increases initially. There will be a stage where the plastic volumetric strain (governed by Rowe's stress-dilatancy relationship) overcomes the total volumetric strain due to gas compression and dissolution. At this stage, the mean effective stress will start to fall.

4.4 Model calibration and performance:

The model developed in section (4.3) has been applied to loose gassy Ottawa sand, with carbon dioxide as guest gas to predict the undrained response. Numerical values of the model parameters for Ottawa sand are available from Imam (1999) and tabulated in Table (3.1). For calibration purposes, an undrained triaxial compression experiment result reported by Grozic (1999) for loose gassy Ottawa sand has been selected, where carbon dioxide- water mixture was the compressible pore fluid (Henry's law constant = 0.82). The compressibility of Ottawa sand is taken to be 0.00002 kPa^{-1}.

Grozic (1999) prepared loose gassy sand by reducing the backpressure of the sample below the liquid-gas saturation pressure of the carbon dioxide- water mixture, thereby allowing gas bubbles to form within the soil matrix. It is appropriate at this stage to discuss the gassy soil preparation methods available for laboratory research purposes and the impact of preparation method on analysis of gassy soil response for undrained loading.

4.4.1 Gassy soil preparation methods:

There are several reasons for dissolved gas to come out of the solution in the field. Gasses may exsolve due to biogenic activities, destabilization of gas hydrates, reduction in confining pressure of gas saturated pore fluid etc. Researchers have applied various methods to mimic the field condition of bubble growth: Zeolite technique (Wheeler 1998), culturing selective micro-organisms (Sills and Gonzalez 2000) and by reducing back pressure of gas saturated pore fluid (Grozic 1999) are some methods adopted in the past.

Wheeler (1998) used the Zeolite technique to generate gas bubbles in Combwich mud. Zeolite has a strong affinity to water; hence, when methane saturated Zeolite is introduced to the soil sample, the methane is replaced by water molecules and methane is released to the surrounding. Wheeler (1998) noted that this preparation method mimics the bubble nucleation and growth in offshore environment, where bubbles nucleate around bacteria.

Rad et al. (1994) utilised the dilative tendency of dense sand to prepare gassy soil. When dense sand is sheared, pore pressure decreases due to the expansive tendency of dense sand; when the pore pressure reduces to the gas-liquid saturation pressure, gas bubbles nucleate and expand. On the other hand, Grozic (1999) prepared gassy sand by reducing the backpressure below the gas-liquid saturation pressure and thereby achieved gas exsolution and isotropic consolidation of the sample simultaneously. In this case, there was not excess pore pressure, since bubble growth occurred under 'drained' conditions, though bubble growth and excess pore pressure are inter related in the field.

Grozic (1999) prepared the samples using the moist tamping method, which gives the loosest possible soil structure (Sasitharan 1994). The moist tamping method can produce void ratios higher than the maximum void ratio obtained using ASTM (American Society for Testing of Materials) method. A complete step-by-step description of sample preparation using moist tamping technique is also available from Sasitharan (1994). One of the finding of Canadian Liquefaction Exmeriment (CANLEX) project study is that the existence of sand in the field (mostly in deltaic environment) is looser than if prepared using the water puluviation method. Therefore, the moist tamping method, adopted by Grozic (1999) is a valid method to study loosest possible soil structure.

4.4.2 Model calibration and comparison:

Figure 4.10 (a) and (b) shows the model calibration for the undrained response of loose gassy Ottawa sand, calibrated against experimental results reported by Grozic (1999). Test #25 has been taken from Grozic's (1999) experimental result for which the effective consolidation pressure at the start of the shearing = 272 kPa, void ratio = 0.85 and the degree of saturation at the start of the shearing = 91%. Though there is a slight deviation from the experimental result, the trend at the small strain level is predicted by the model. The model agrees with experimental result as long as the degree of saturation is above 85%. It is speculated that bubbles are no longer in occluded form and the assumptions discussed in Chapter (2) are no longer valid when the degree of saturation falls below 85%. Figure 4.10(b) compares the model prediction with the experimental result in stress-strain space. A lower axial strain to reach peak strength has been predicted during the loading of gassy samples. This is because the model assumes only volumetric strain due to the presence of gas bubbles and that shape of the bubbles remains spherical even after deformation. However, Thomas (1987) noted that gas bubbles deform to an ellipsoidal shape upon deviatoric loading.

The modified model for loose gassy sand has the ability to predict saturated soil response if the degree of saturation is equated to 100% and Henry's coefficient of solubility is set to zero; i.e., model acts as Imam(1999)'s original model. Figure 4.11 shows the model prediction for saturated soil compared with Test #11 from Grozic (1999) for saturated loose sand, where initial consolidation pressure = 266 kPa and void ratio = 0.896.

No other experimental data is available other than for loose gassy Ottawa sand except that reported by Grozic (1999). Hence, for comparison purpose, another test result (test # 10) from Grozic (1999) which was not used to calibrate the model has been considered to verify the model performance. Figure 4.12 shows the model prediction compared with the experimental observation. This figure illustrates that the model is able to capture the general trend of the gassy sand.

4.4.3. Model simulation:

Figure 4.13a shows the model prediction for the undrained response of loose gassy sand in p-q space for different initial degrees of saturation, but for the same initial pore pressure of 470 kPa. It can be noted that the gassy soil's response deviates from the saturated loose sand's response at the early stages of loading. As the degree of saturation decreases, more deviation is observed from the saturated loose sand. Figure (4.13b) shows the response in stress-strain space. It can be noted that gassy soil needs to experience more axial strain to reach peak undrained shear strength; the presence of gas bubbles increases the strain. It can be concluded that presence of occluded bubbles within pore voids of loose sand increases the undrained shear strength. This has been suggested by several other researchers such as

Fourie et al. (2002) and Esrig and Kirby (1997). These observations might be of particular importance in designing marine structures for both strength and deformation.

Note: The trend of increase in mean stress (p) with deviatric stress (q) during early stages of shearing has been reported experimentally by Grozic (2000) (see figure (2.9a) and Nadim & Kvalstad (2003)). Grozic (1999) did the experiment on synthesized loose gassy Ottawa sand while Kvalstad et al. (2003) carried out experiment on Laponite- an artificial specimen that resembles gassy soil and on marine clay from Congo slope.

It was mentioned earlier that there exists excess pore pressure in marine sediments because of various factors, one of which is gas bubble nucleation and growth. The existence of excess pore pressure means a reduction in effective confining pressure (and hence less undrained shear strength) compared to a zone in the same depth without gas bubbles. In other words, the presence of gas bubbles causes stability problems by reducing the effective confining stress (Erig and Kirby 1997).

In addition to lowering effective confining pressure, excess pore pressure changes the compression behaviour of the gas – water mixture (see Equation 4.9). The higher pore pressure means a stiffer response of free gas, according to Boyle's law and hence a higher pore pressure response during undrained shearing. The model prediction shown in Figures 4.14 (a) and (b) captures this trend where the model predicted the undrained response of loose gassy Ottawa sand at different pore pressure levels of u=370 kPa, 570 kPa, and 770 kPa (with the same initial degree of saturation of Sr=90%). Rad et al. (1994) observed the same trend for dense gassy sand.

Figure 4.15 simulates the behaviour of loose gassy Ottawa sand for different guest gases (carbon dioxide and methane in this case). This shows the role of the volumetric coefficient of solubility on the gassy soil response. It influences the compressibility of the pore fluid mixture; the relative compressibilities of the pore fluid and soil skeleton determines both the pore pressure change and the volumetric strain. This has been experimentally observed by Rad et al. (1994), see Figure 2.7.

Grozic (1999) observed that there exists a minimum (or cut off) initial degree of saturation that a sample must be greater than to strain soften and this is 90%. Further investigation and analysis is needed to establish this minimum saturation level and to investigate whether this cut off value depends on mean effective pressure, void ratio etc. One possible explanation for the existence of a minimum degree of saturation below which gassy soil behaves in strain hardening manner upon shearing is ‘bubble flooding’ (Wheeler, 1989). At this saturation level, bubbles might make contact with solid particles and the assumption made of occluded bubbles is no longer valid. Bubble flooding can be considered as an ‘internal’ drainage effect.

4.4.4 Analysis for Fraser River sand:

As reported in Chapter (2), deltaic environments contain loose sand with occluded gas bubbles within the pore voids. An in situ measurement in Fraser River Delta, British Columbia indicates the existence of free gas (mostly methane). Sediment load to the delta is fed by the main channel and a net work of distributory channels where the main channel carries approximately 88% of the sediment bearing water (Mckenna et al. 1992) with average sedimentation rate of 2.16 cm/year (Moslow et al. 1991). A mean tidal variation of 5.4 m has been reported.

Figure (3.13) shows the undrained response of loose, re-constituted, saturated Fraser River Delta sand (FRD sand) prepared using moist tamp technique (Chillarige et al. 1997). In a strain controlled loading at a constant strain rate of 0.15 mm/minute, all three samples showed peak behaviour. Table (3.1) lists the model parameters used in modeling FRD sand for undrained shearing. For FRD sand, compressibility value of 0.0002 kPa^{-1} is assumed and for methane in fresh water, Henry's volumetric coefficient of solubility is 0.034.

The behaviour of loose FRD sand that contains occluded gas bubbles has been analysed with methane as the guest gas; Figure (4.16) shows the predicted response. Note that the presence of gas bubbles prevents peak response of FRD sand; experimental observation shows a definite peak response of saturated FRD sand upon undrained shearing (Chillarige et al. 1997; see Figure 3.13). This agrees with Grozic (1999)'s conclusion that presence of gas bubbles decreases the liquefaction susceptibility of marine sediments under loading stress path. This has been noted by Atigh and Byrne (2004) as well.

4.5 Summary and conclusion

Several views have been given as to the role of gas bubbles in submarine slope failures. The presence of even a small amount of the gas increases the compressibility of gas-liquid mixture drastically. In an undrained condition, this causes volumetric strain as well as pore pressure change in gassy sample. In addition to increased compressibility, bubble growth in 'undrained' conditions causes excess pore pressure in the pore fluid that influences the volume change behaviour of gassy soil. Two different approaches are being suggested to analyse gassy soil depending on the structure of the gassy soil. Gassy sand that contains occluded bubbles within voids can be analysed as saturated soil with compressible pore fluid while cohesive gassy soils can be analysed as bubble cavities surrounded by a saturated soil matrix.

The effect of gassy soil on the model described in Chapter 3 is incorporated by coupling the volumetric strain introduced during undrained shearing with plastic and elastic volumetric strain during the yielding process. Unlike the models proposed in the past, this model accounts for both the effect of excess pore pressure and the effect of gas type on gassy soil response (as observed by Rad et al. 1994). This is achieved by incorporating pore pressure dependent compressibility of pore fluid and Henry's volumetric coefficient of solubility into the model.

The model that accounts for above phenomena predicts that presence of gas bubbles increases the undrained shear strength and hinders the liquefaction potential. The axial strain needed to mobilize the peak strength is increased due to gas bubbles, which might be a concern in designing marine structures for deformation.

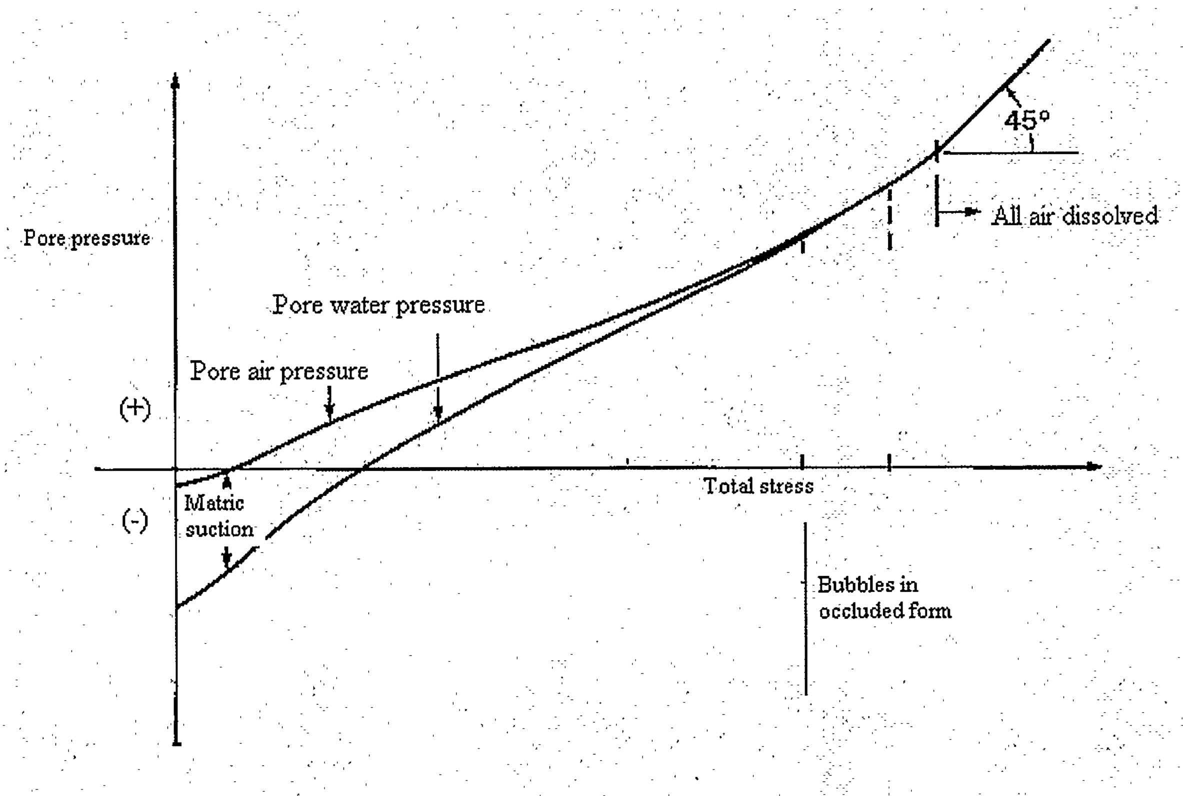

Figure 4.1 – Pore gas and pore water pressure response to a change in total stress in undrained compression (adopted from Fredlund and Rahardjo 1993). When bubbles are in occluded form, gas-water mixture can be considered as one homogeneous mixture for the analysis of macro parameters such as compressibility and effective stress.

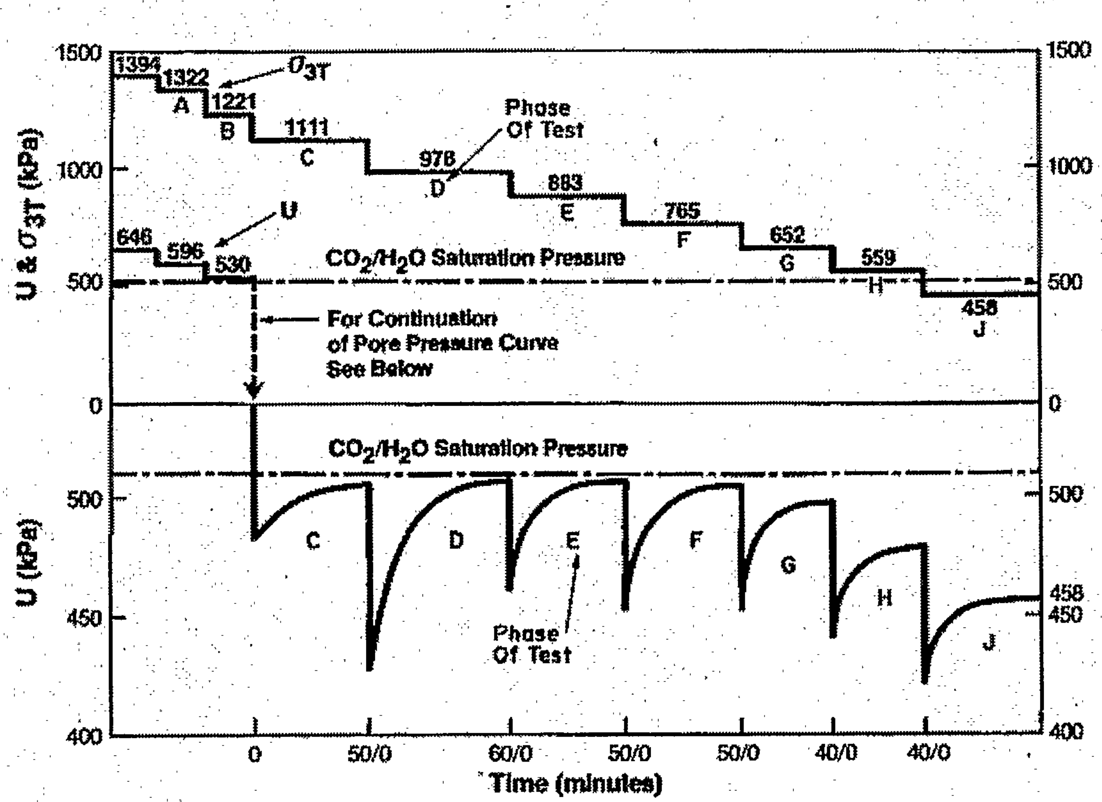

Figure 4.2 - Result of an unloading experiment on soil with gas saturated pore fluid. Pore pressure increase up to gas-liquid saturation pressure of 500 kPa can be noticed during unloading. (adopted from Sobkowikz, 1982).

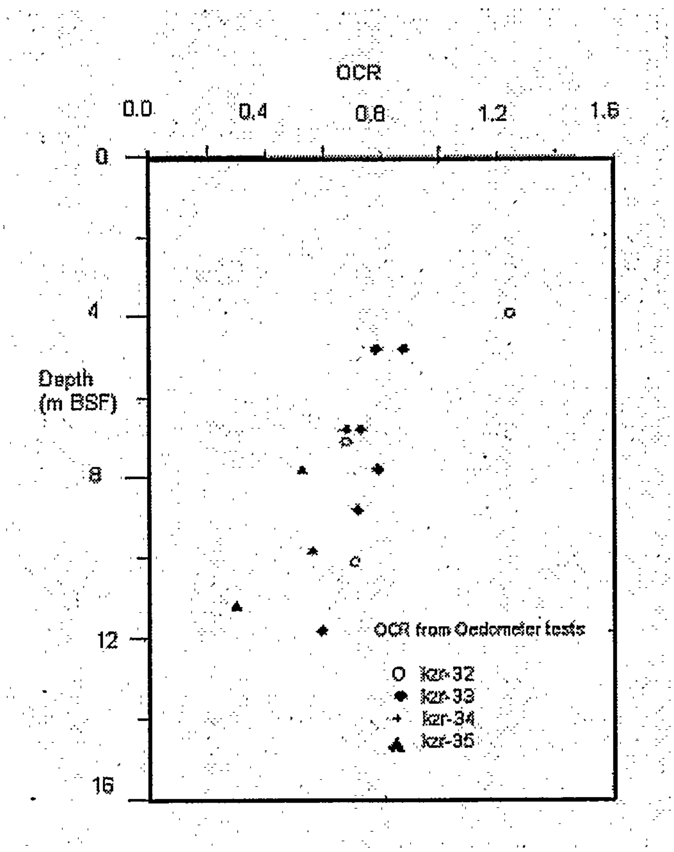

Figure 4.3 - Over consolidation values as a function of depth below Base Sea Floor (BSF) in gas hydrate laden Zaiango study area, Gulf of Guinea (Sultan et al. 2003).

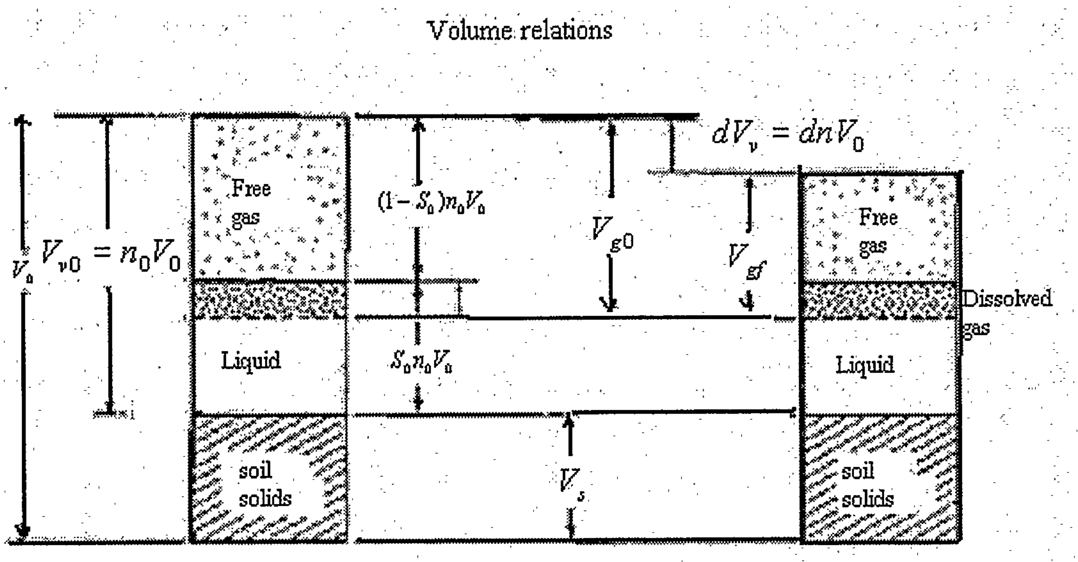

Figure 4.4 - Pressure and volume before and after application of external load to a gassy soil (modified from Fredlund and Rahardjo, 1993).

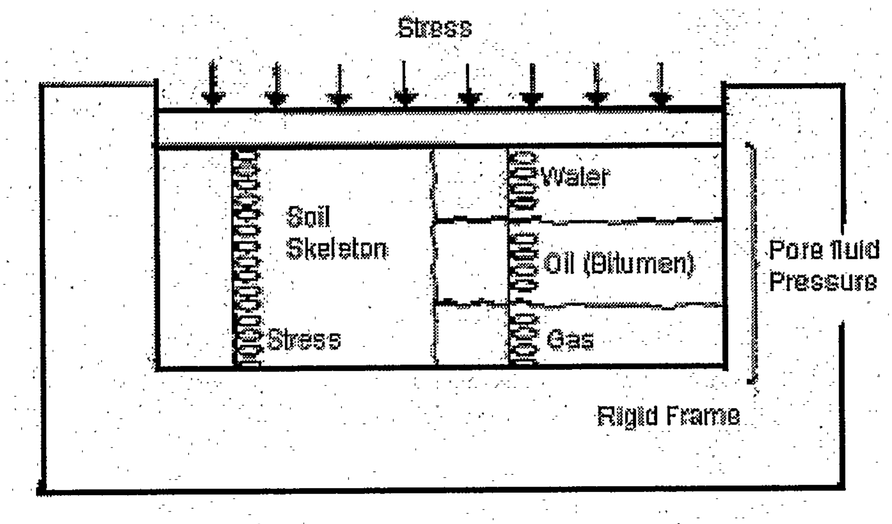

Figure 4.5 - A conceptual double spring model of oil sand that can be used to explain undrained behaviour (adopted from Dessault 1979).

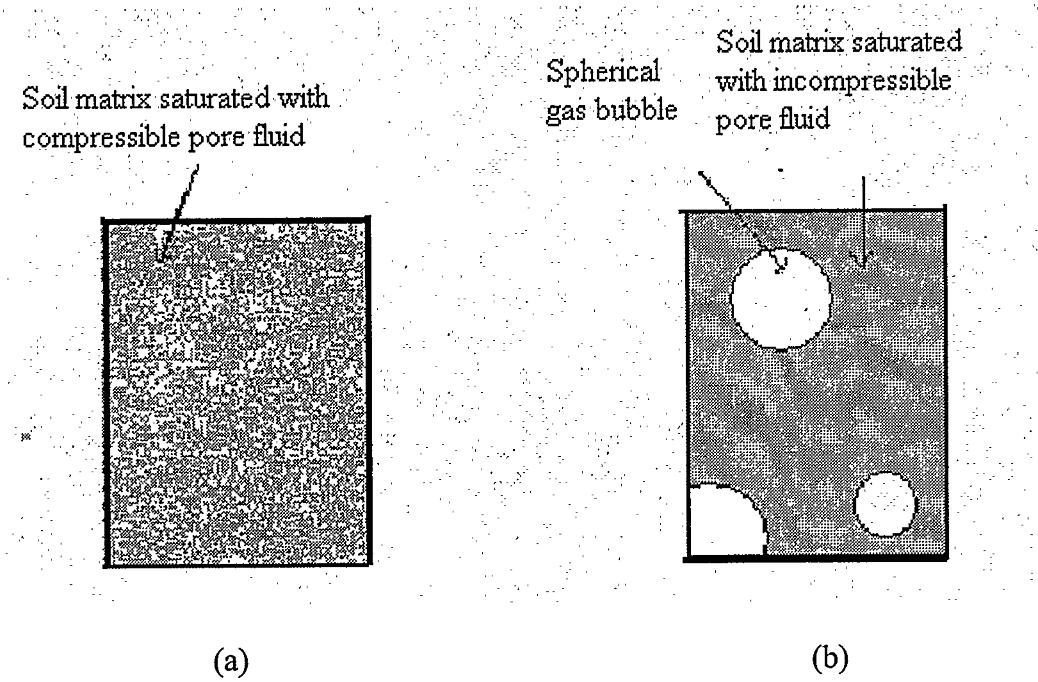

Figure 4.6 - Conceptual models for (a) Type C gassy soil (Thomas 1989) and (b) Type D gassy soil (Wheeler 1988).

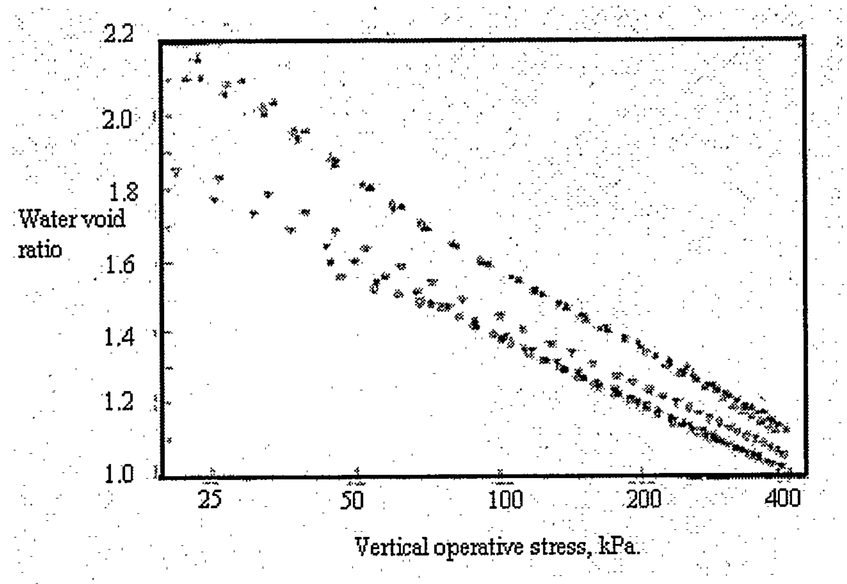

(a)

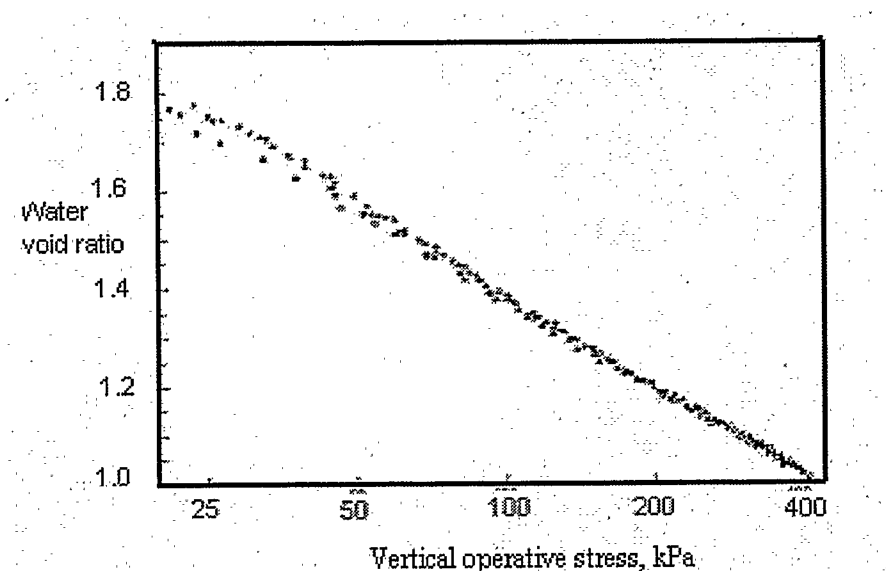

(b)

Figure 4.7 – (a) Total void ratio plotted against vertical operative stress for a 1-D consolidation test of cohesive gassy soil, prepared using Zeolite technique. (b) Water void ratio plotted against vertical operative stress for a 1-D consolidation test of cohesive gassy soil, prepared using Zeolite technique; note the convergence of all lines in fig. (4.4a) to a single line (adopted from Sills et al., 1991).

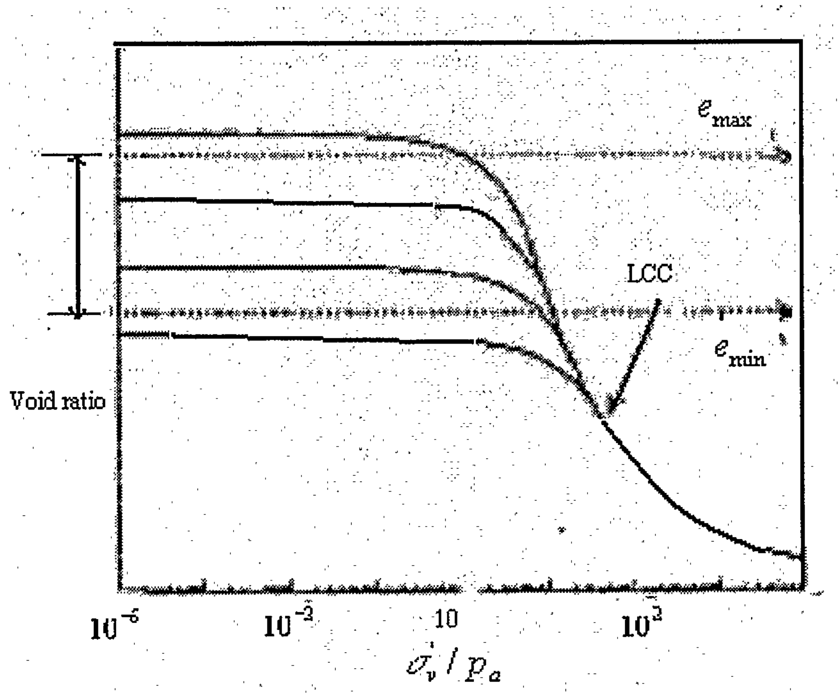

Figure 4.8 - Conceptual model of isotropic and one dimensional compression of cohesionless soil at different formation void ratio; note the convergence of all compression to one curve (Limiting Compression Curve) once a particular stress level is exceeded (From Pestana and Whittle 1995).

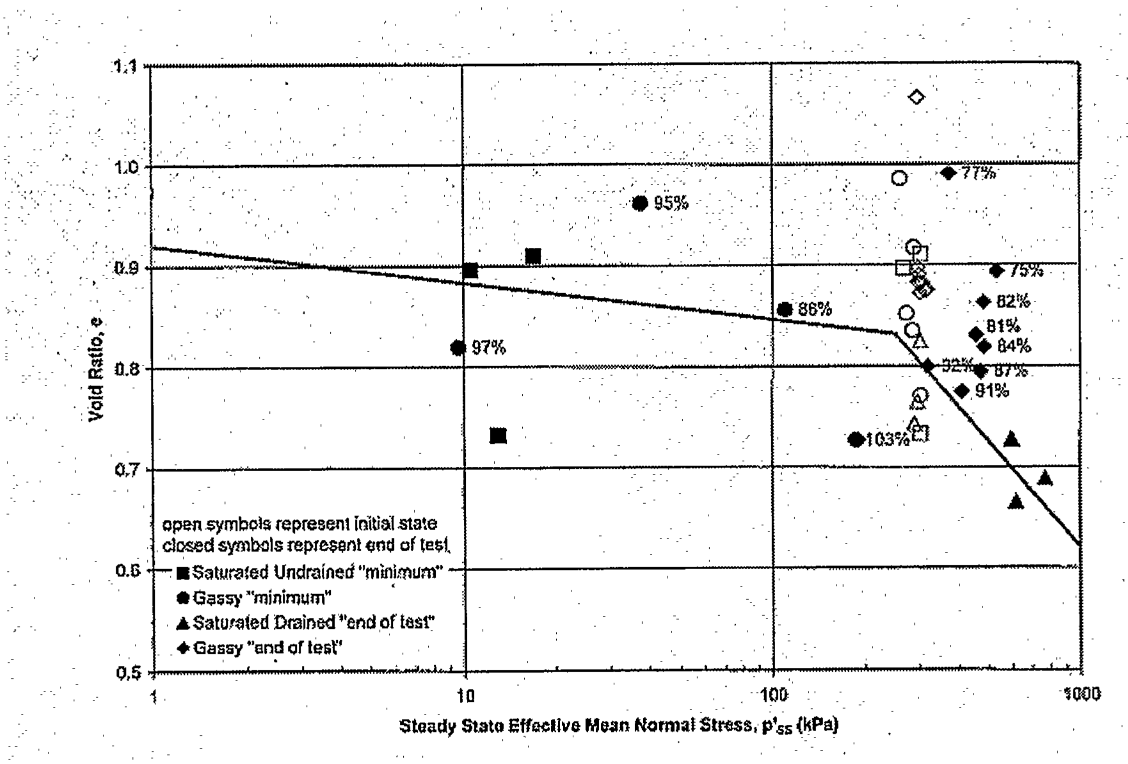

Figure 4.9 - Steady state line for granular gassy Ottawa sand in e-ln(p) space, showing initial and final states; numerical values represent the final degree of saturation at steady state (adopted from Grozic 1999).

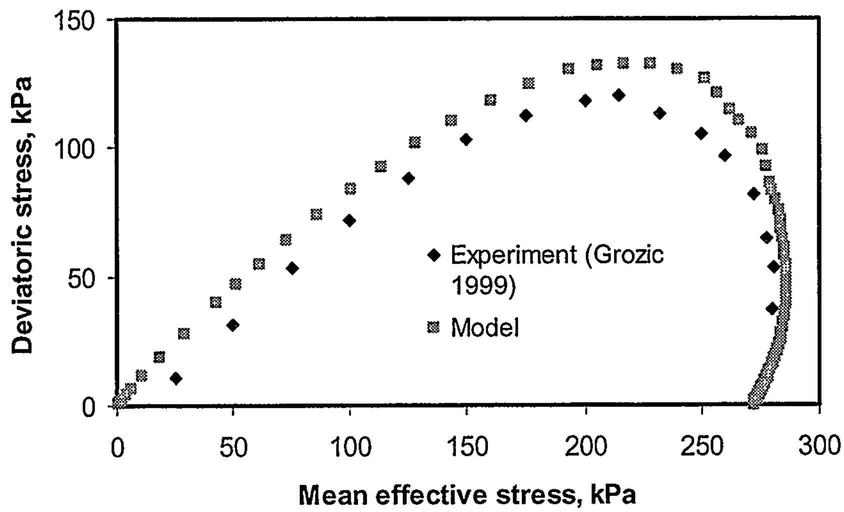

(a)

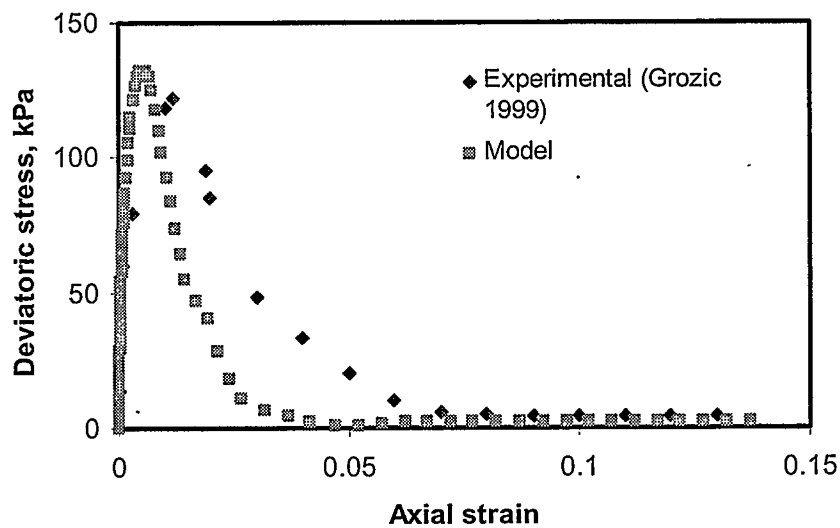

(b)

Figure 4.10 - Calibration of the model against experimental observation for loose gassy Ottawa sand (Grozic 1999), sheared at consolidation pressure of 272 kPa, degree of saturation of 91% and formation void ratio of 0.85 (Test #25). Pore pressure was assumed to be liquid-gas saturation pressure, (a) Deviatoric stress-effective mean stress curve and (b) stress-strain curve.

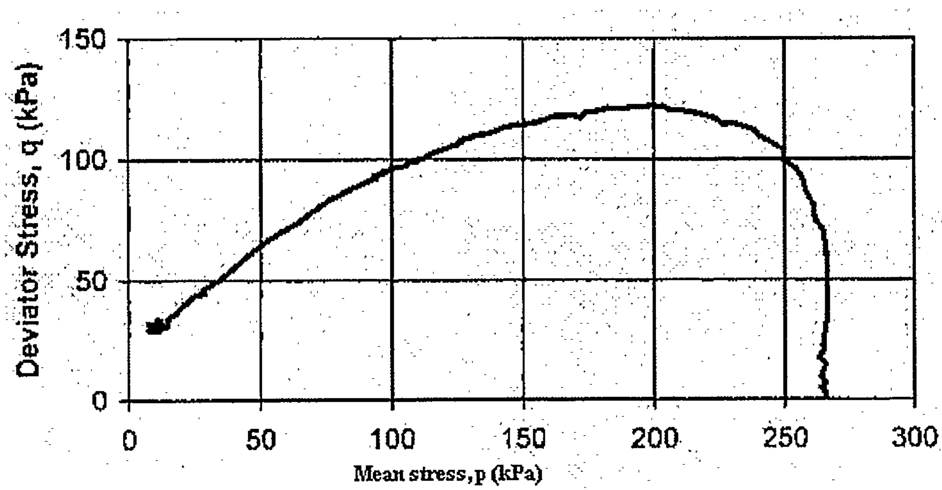

(a)

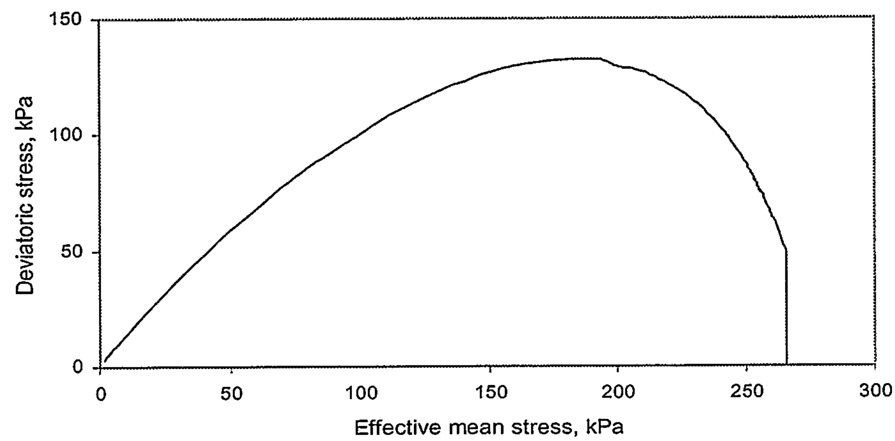

(b)

Figure 4.11 – Performance of the gassy soil model for saturated soil compared against undrained response of saturated loose Ottawa sand, reported by Grozic (1999) for Test #11; this has been achieved by making Degree of saturation = 100% and Volumetric coefficient of solubility = 0. (a) Experimental observation for Test #11; (b) Model prediction.

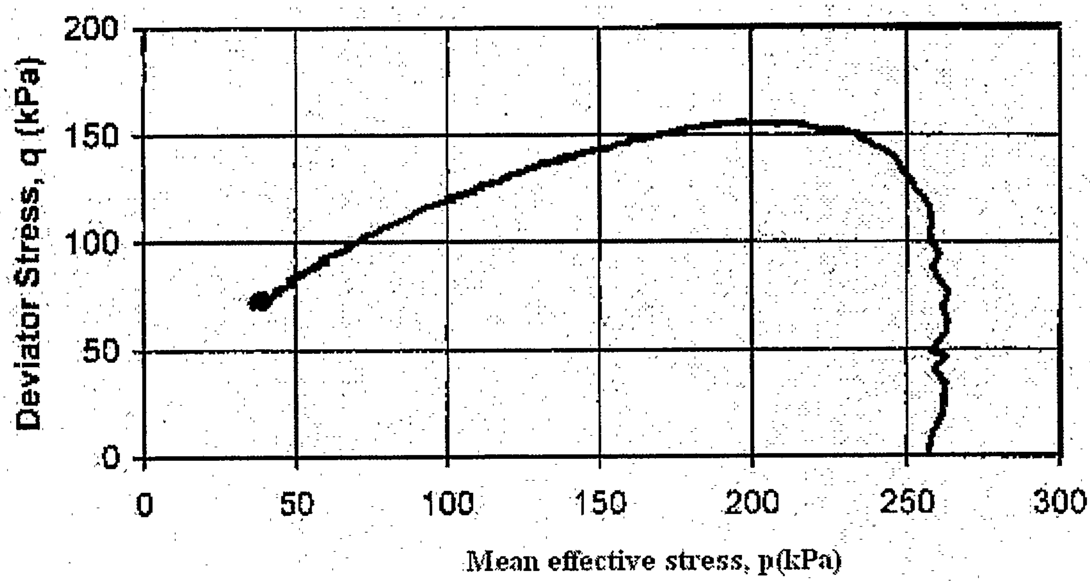

(a)

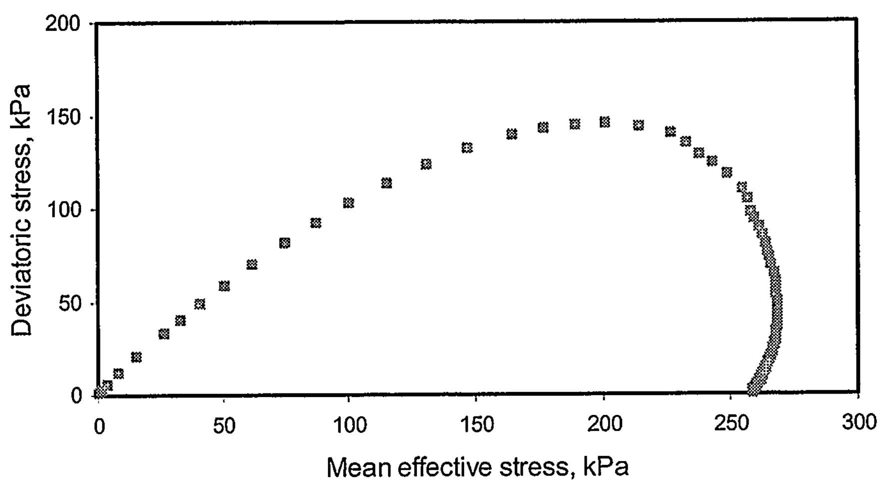

(b)

Figure 4.12 – Comparison of model prediction with experimental observation for loose gassy Ottawa sand reported by Grozic (1999). (a) Experimental observation for Test # 10; (b) Model prediction, with CarbonDioxide as the guest gas.

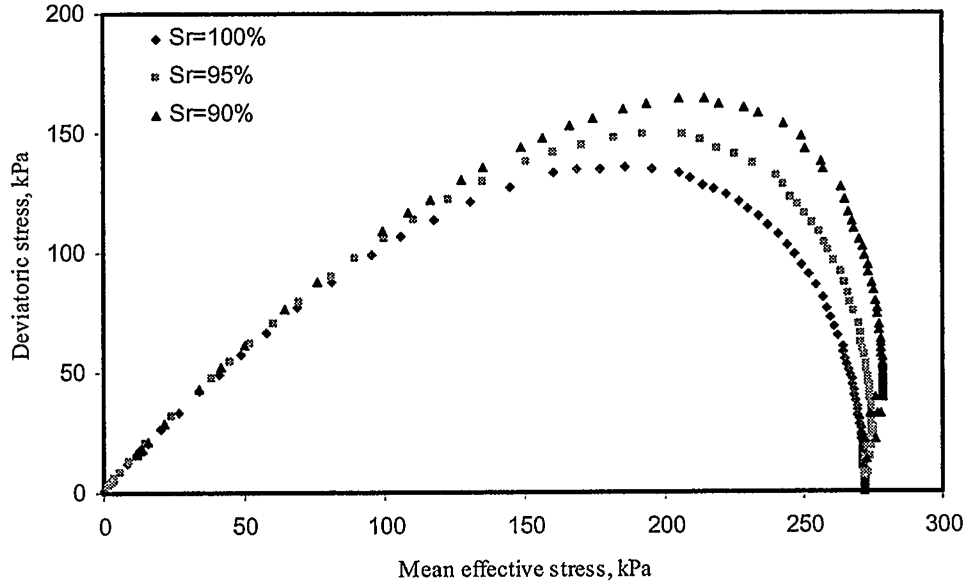
200
150
100
50
0
Deviatoric stress, kPa
0
50
100
150
200
250
300
Mean effective stress, kPa
Sr=100%
Sr=95%
Sr=90%

(a)

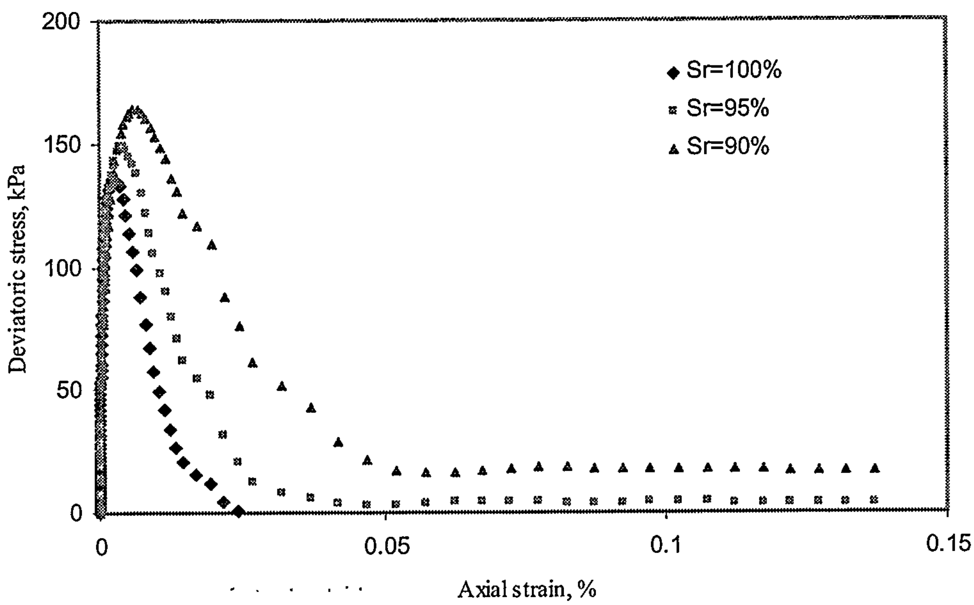
200
150
100
50
0
Deviatoric stress, kPa
0
0.05
0.1
0.15
Axial strain, %
Sr=100%
Sr=95%
Sr=90%

(b)

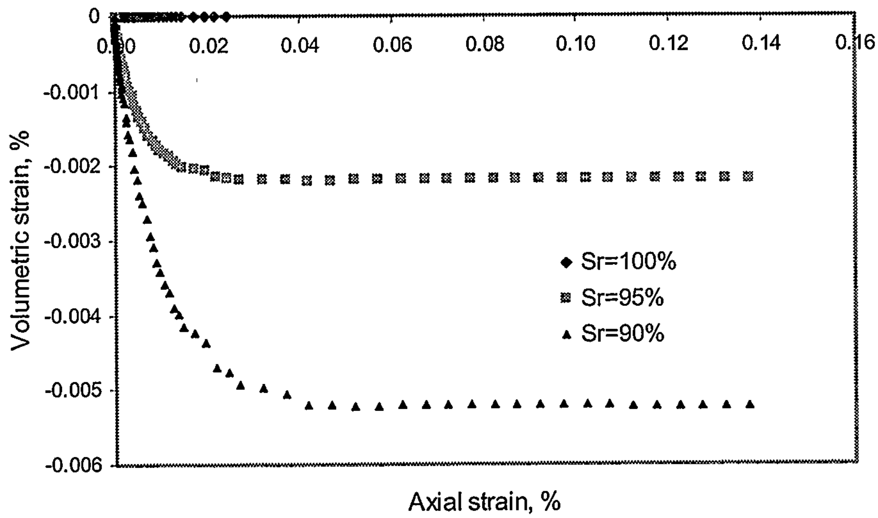

(c)

Figure 4.13 - Model prediction for loose gassy Ottawa sand at different initial degrees of saturation and pore pressure of 470 kPa, (a) in q-p space; (b) in stress-stain space; and (c) volumetric strain vs axial strain (note that long term B-parameter = 3 is assumed irrespective of gas content.

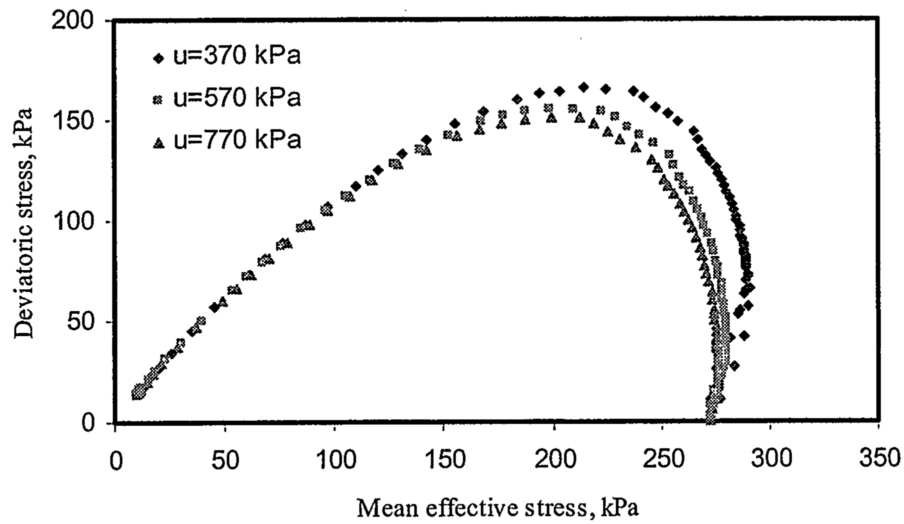

(a)

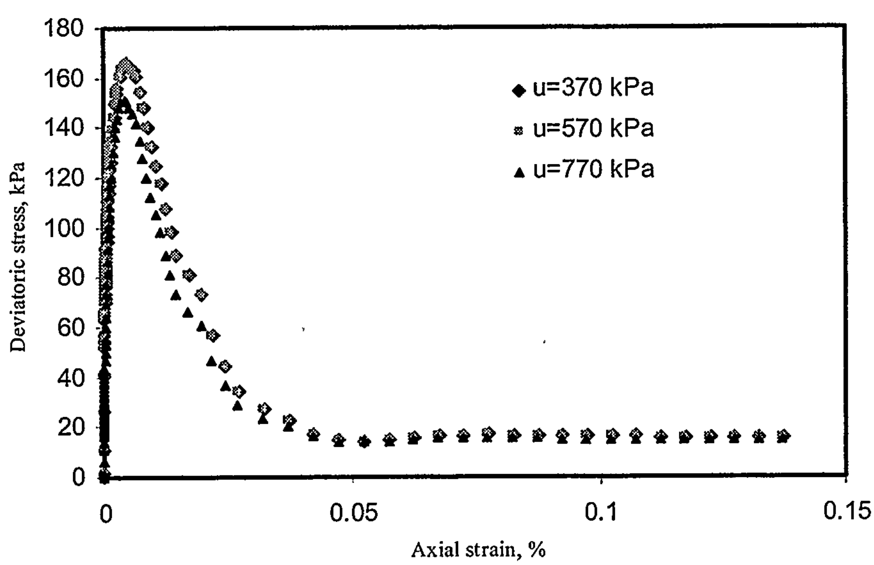

(b)

Figure 4.14 - Model simulation for loose gassy Ottawa sand at different pore pressure level and initial degree of saturation of 90% (a) in p-q space and (b) in stress-strain space.

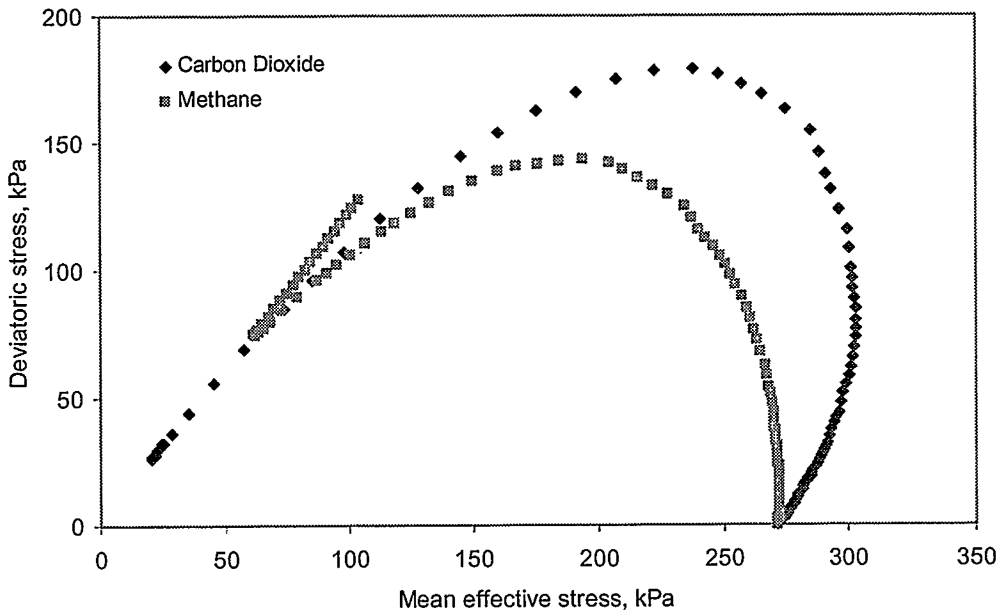

Figure 4.15 – Model simulation for loose gassy Ottawa sand for different gas types. This shows the importance of gas type in analysis. Volume change behaviour of gassy soil is influenced by type of gas and compressibility of soil skeleton.

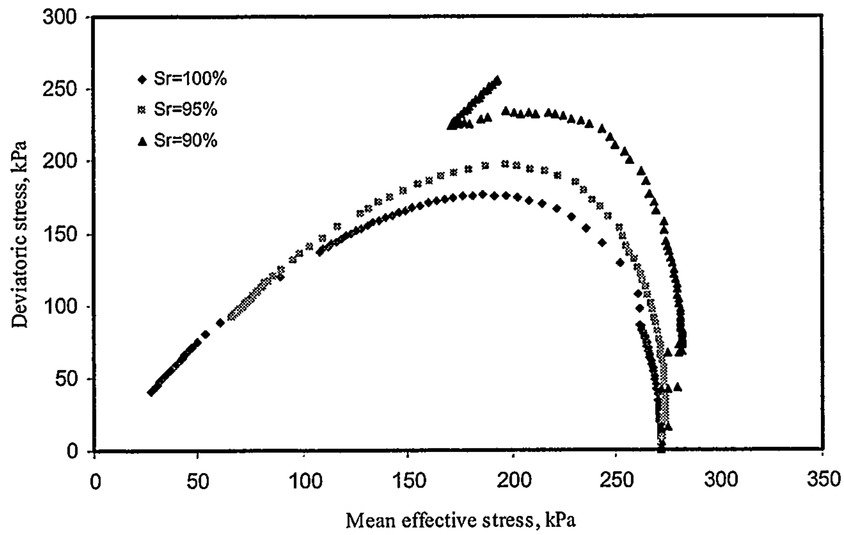

(a)

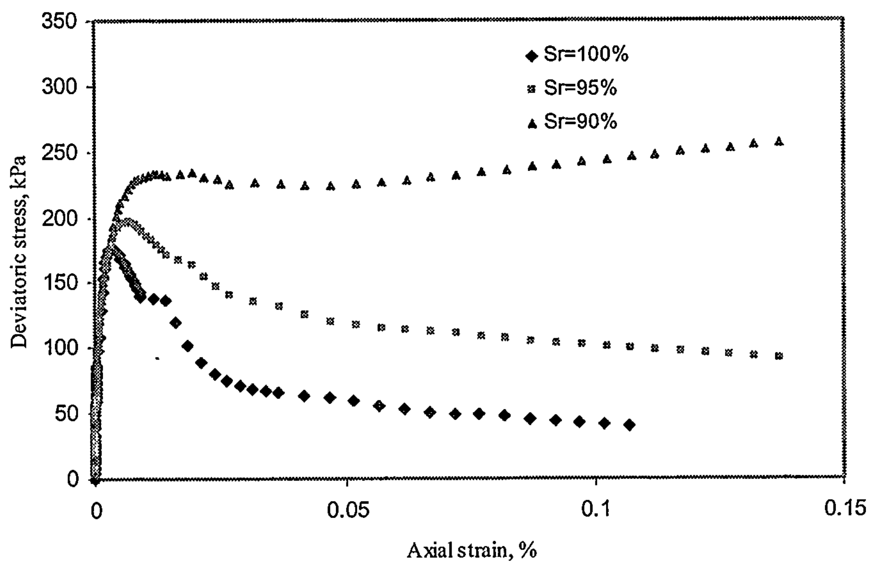

Figure 4.16 - Undrained response of loose gassy Fraser River sand, with methane (Henry's law constant = 0.034) as the guest gas, for different initial degrees of saturation in (a) p-q space; (b) in stress-strain space. Model parameters for FRD sand has been tabulated in Table (3.1).

CHAPTER 5

SUMMARY AND CONCLUSION

5.1 Introduction

Gas in soil, commonly found in oil sand tailings and marine sediments, alters the engineering properties of soil; it influences both shearing resistance and volume change behaviour. Gas found in marine sediments is of particular concern for marine development. Above all, the presence of gas bubbles in marine sediments has been thought to cause slope instability problems. This thesis studies the effect of gas bubbles on loose sand for undrained loading and incorporates this effect into a model for saturated sand developed by Imam (1999).

Marine sediments in deltas and deep sea beds contain gas bubbles in occluded form either within the voids or spanning the soil skeleton. Gas found in marine sediments under high confining pressure is mostly methane, which is soluble in water and speculated to be one of the causes of submarine slope instability problems. Chapter 1 discusses some of the submarine slope failures where the presence of gas bubbles has been found in the vicinity of the failure area (e.g. Fraser River delta, British Columbia; and Storregga submarine slide, Norwegian continental margin). Anaerobic oxidation of organic sediments in deltaic environment and decomposition of gas hydrates in deep seabeds are the two major sources of gas in marine sediments. Other than that, petrogenic processes and volcanic action contribute to gas in marine sediments to a lesser degree.

Researchers studying subaqueous slope failure mechanisms speculated that presence of gas bubbles would have been one of the causes of slope failure. However, the exact role of gas bubbles has not been fully understood. The following conclusions (some of which are contradictory) on the role of gas bubbles on undrained shear strength from several researchers indicate the perplex nature of the subject matter:

- Whelan et al. (1977) - Reduction in grain to grain contact due to gas bubbles results in low in-situ shear strength of marine sediments.
- Fourie et al. (2001) - Liquefaction potential of sand is reduced due to the presence of gas bubbles (i.e. undrained shear strength of gassy sand is increased).
- Esrig & Kirby (1997) - Increased compressibility enhances the stability of gas laden soil, but also speculated that excess pore pressure associated with gassy soil causes stability problem.
- Lee et al. (1991) - Excess pore pressure causes instability problems in fjords.
- Silva & Branndes(1988) - Disruption of sediment fabric during gas exsolution results in lower undrained shear strength.

5.2 Model development

In this thesis, the effect of gas bubbles in loose sand is studied and incorporated into an existing model for loose sand. In fine grained soil, bubbles are larger than the average pore size and span the soil skeleton. Surface tension is said to influence the engineering property of this type of soil and the pore gas pressure will not be equal to the pore water pressure. In coarse grained soil, which is commonly found in deltaic environments, gas bubbles are smaller than pore voids and exist within the voids. Pore gas pressure can be assumed to be equal to pore water pressure; this simplifies the analysis to a greater extent.

Coarse grain soils found in deltaic environments are very loose; in-situ void ratios higher than that can be obtained from ASTM (American Society for Testing of Materials) method have been found in some instances. Very loose sands are susceptible to liquefaction failure upon undrained loading because of their high contractive volume change that results in an increase in pore pressure. An elasto-plastic stress-strain model developed by Imam (1999) has been chosen as the base model to incorporate into the effect of gassy soil, as gas bubbles in deltaic environments exist in very loose sand. Chapter 3 describes the basic elements of an elasto-plastic constitutive model with particular emphasis on Imam (1999)'s model.

It has been shown that the presence of gas bubbles, even in a small amount, greatly affect the compressibility of the soil matrix as a whole. In this sense, gassy soil can be viewed as a saturated soil with compressible pore fluid, as opposed to incompressible water in classical saturated soil mechanics. Dessault (1980)'s double spring model implicitly assumes this concept which is suitable for Type C gassy soil (bubbles are smaller than average pore void and pore gas pressure is assumed to be equal to pore water pressure). Fredlund and Rahardjo (1993) proved the validity of this assumption for Type C soil when the degree of saturation is greater than 85%.

The effect of this compressible pore fluid on the undrained behaviour of gassy soil is to introduce volumetric strain as well as pore pressure change in gassy sample. This phenomenon has been coupled with a saturated soil matrix response, predicted by Imam's model, by coupling incremental bulk volumetric strain ($d\varepsilon_v$) due to gas compression and dissolution with the plastic and elastic volumetric strain during yielding process. The pore pressure dependency of the bulk volumetric strain (Equation 4.10) suggests that excess pore pressure undermines the undrained shear strength of gassy sand in addition to reducing the effective confining pressure. In this analysis, the gas ex-solution/dissolution process has been assumed to be instantaneous. In other words, only the equilibrium gassy soil response has been considered. It has been assumed that any change in pore gas pressure is equal to the change in pore water pressure.

A model that simulates strain controlled tests on a triaxial system is considered. The following is the step by step procedure that has been followed in the finite difference formulation of the gassy soil effect:

- Apply incremental plastic shear strain and calculate deviatoric stress (q).

- Compressible pore fluid means sample exhibits both volumetric strain and pore pressure change. Equation (4.10) determines the volumetric strain ($d\varepsilon_v$) due to gas compression and/or dissolution. Pore pressure development depends on both external loading (Equation 4.13) and shearing characteristics of the soil skeleton. A suitable assumed value of the long term B-parameter is needed to calculate the total pore pressure development.

- Couple volumetric strain ($d\varepsilon_v$) with Imam's model by incorporating elastic volumetric strain, which is the difference between total volumetric strain (Equation 4.10) and plastic volumetric strain (Equation 3.7).
- Change in mean effective stress is the product of elastic volumetric strain and elastic bulk modulus.

It is the pore pressure response that causes the deviation of the gassy soil response from a saturated soil. The material parameters that describe yielding are assumed not to be affected by the pore fluid compressibility. In reality, there are suggestions that gas exsolution would alter the micro fabric of the soil skeleton (Whelan et al. 1977; Rau and Chaney 1988; and Pietrusczak and Pande 1996). The model has been compared with experimental results on loose gassy sand reported by Grozic (1999). The deviation of the gassy soil response from a saturated soil response at small strain level, as noted by Grozic (1999) and Kvalstad et al. (2004) has been captured by this model.

In the course of the model development, the following assumptions/considerations have been made:

1. Equilibrium behaviour of gassy soil is considered or gas ex-solution/dissolution process is considered instantaneous. In fact, the gas dissolution process is time dependent. To handle this time dependent behaviour of gassy soil, researchers use short term and long term pore pressure response parameters (e.g. Wong 2003)

2. Surface tension effect has been neglected. Fredlund and Rahardjo (1993) justified the validity of above assumption for occluded gas bubbles within pore voids (Type C soil), which has been studied in this thesis.

3. It is further assumed that the change in pore gas pressure is equal to the change in pore water pressure during shearing. This assumption is valid for Type C soil. Assumptions 1 and 2 lead us to consider the pore fluid as one continuum in the context of compressibility. Dessault (1979)'s compressibility model proposed for oil sand considers this assumptions. Accordingly, Type C soil has been considered as a saturated soil with a compressible pore fluid.

4. It is assumed that the micro soil structure is not affected due to gas nucleation and bubble growth.

5.3 Significance and contributions

The research work described in this thesis has made a significant contribution to the field geotechnical engineering, particularly for the analysis of submarine slope instability problems. Important observation from the model simulation is that the undrained response of gassy soil is pore pressure as well as gas type dependent. This emphasizes the importance of considering excess pore pressure associated with gassy soil in submarine environments.

Effect of gas on undrained behaviour of loose sand has been incorporated by coupling volumetric strain introduced in gassy soil due to gas compression/expansion (according to Boyle's law) and gas dissolution/ex-solution (according to Henry's law) with Imam (1999)'s model, as explained in Section (4.3.4)

5.4 Limitations

Some important features and limitations of this modified model for gassy soil are:

1. The model predicts the undrained behaviour of loose gassy sand for initial degrees of saturation above 85%; assumptions 1 and 2 limit the model performance to this cut-off saturation level. Note that this cut off level is not an exact value. The model has the capability to predict the gassy soil response for different degrees of saturation. Comparison with experimental observation shows closer agreement for gassy soils

than has been previously predicted as long as degree of saturation falls within the limits discussed above. This again emphasizes that the model is valid for Type C gassy soil only.

2. The gassy soil response for different pore pressure levels (but same effective confining pressure and void ratio) can be predicted by this model. Excess pore pressure exists in marine sediments associated with gas bubbles and due to several other reasons.

3. The model also predicts the response of gassy soil for different gas types. Differing Henry's law constant values for different gas types alters the compressibility and volume change behaviour of gassy soil.

5.5 Conclusion and recommendations:

1. The model suggests that presence of gas bubbles increases the undrained shear strength of loose gassy sand. In other words, the liquefaction potential of loose gassy sand is reduced. This is due the increased compressibility of the gas-water mixture; the higher the degree of saturation, the greater the compressibility effect and the greater the undrained shear strength.

2. Pore pressure dependency of compressibility and volume change behaviour (according to Boyle's law) in this model suggests that the excess pore pressure plays an important role in the behaviour of gassy soil. A higher pore pressure means a stiffer response of

gas-water mixture; this results in reduction of the undrained shear strength compared to the undrained shear strength of a gassy soil with the same degree of saturation, but with a lower initial pore pressure.

3. The volumetric coefficient of solubility plays an important role in the behaviour of gassy soil. Even if the guest gas is air (h=0.02), the effect is prominent when the compressibility of the soil is high.

The following recommendations are made for further study on gassy soil:

1. More experimental based study is needed to further modify the gassy soil model. For example, whether the Henry's law effect is prominent in dense/impermeable soil needs to be investigated. In addition, understanding the compressibility characteristics of gassy sand is important in determining the state parameter (ψ) of sand.

2. As the degree of saturation is increased, at one stage, experimental observation shows strain hardening response of very loose sand (Grozic 1999). Further experimental observation and analytical study is needed to establish the critical degree of saturation at which gassy soil exhibits this shift in response. It is logical to say that this critical degree of saturation will depend on various factors such as void ratio, pore pressure and confining pressure.

3. To better understand the role of gas bubbles in submarine slope failures, experimental study with unloading stress paths that mimic actual situations are necessary. This can be

achieved by performing Constant Deviatoric Stress (CDS) experiments on gassy samples.

4. The behaviour of Type D gassy soil in which gas bubbles are larger than the average pore size of the soil needs to be investigated, both experimentally and numerically.

REFERENCES

Atigh, E., and Byrne, P.M. 2003. Liquefaction Flow of Submarine Slopes Under Partially Undrained Conditions: An Effective Stress Approach. Canadian Geotechnical Journal, **41**: 154-165.

Been. K., and Jefferies, M.G. 1985. A State Parameter for Sands. Geotechnique, **41**(2): 99-112.

Bishop, A.W. 1966. The Strength of Soils as Engineering Materials. 6th Rankine lecture. Geotechnique, **16**(2): 91-121.

Bjerrum, L. 1971. Subaqueous Slope Failures in Norwegian Fjords. Norwegian Geotechnical Institute Publication. No.88, pp. 1-8.

Bugge, T., Befring, S., and Belderson, R.H. 1987. A Giant Three-stage Submarine Slide off Norway. Geo-marine letters, **7**:191-198.

Byron, J.M. 1974. Pathways and Environmental Requirements for Biogenic Gas Production in the Ocean. *In* Natural gases in marine sediments, *Edited by* Kaplan, I.R. Plenum Press, New York.

Carpenter, G. 1981. Coincident slump/clathrate complexes on the U.S. Atlantic continental slope. Geo-Marine Letters, **1**:29-32.

Casagrande, A. 1936. Characteristics of Cohesionless Soils Affecting the Stability of Slopes and Earth Fills. Journal of Boston Society of Civil Engineers.

Chillarige, A.V., Robertson, P.K., Morgenstern, N.R., and Christian, H.A. 1997. Evaluation of the in situ state of Fraser River sand. Canadian Geotechnical Journal, **34**(4): 510-519.

Chillarige, A.V., Robertson, P.K., Morgenstern, N.R., and Christian, H.A. 1997. Sea bed instability due to flow liquefaction in the Fraser River delta. Canadian Geotechnical Journal, **34**(4): 520-533.

Christian, H.A., Woeller, D.J., Robertson, P.K., and Courtney, R.C. 1997. Site investigations to evaluate flow liquefaction sides at Sand Heads, Fraser River delta. Canadian Geotechnical Journal, **34**: 384-397.

Claypool, G.E., and Kaplan, I.R. 1974. The origin and distribution of methane in marine sediments. *In* Natural gases in marine sediments, *Edited by* Kaplan, I.R. Plenum Press, New York.

Coleman, J.M., Prior, D.B., Garrison, L.E., and Lee, H.J. 1991. Slope failures in area of high sedimentation rate: Offshore Mississippi River delta. *In* Submarine landslides: Selected studies in the U.S Exclusive Economic Zone, *Edited by* Schwab, W.C., Lee, H.J. and Twichell, D.C.

Dessault, M.B. 1979. Undrained volume and stress change behaviour of unsaturated very dense sands. Canadian Geotechnical Journal, **16**(4): 627-640.

Dessault, M.B., and Morgenstern, N.R. 1978. Characteristics of natural slopes in the Athabassca oil sands. Canadian Geotechnical Journal, **15**(2): 202-215.

Dittrich, J.P. 2002. Analysis of the 1990's excavation of the Sarnia approach for the new st.Clair tunnel project. 55th Canadian Geotechnical Conference, Niagara Falls, Ontario, pp.299-306.

Esrig, M., and Kirby, R.C.1997. Implications of gas content for predicting the stability of submarine slopes. Marine Geotechnology, **2**(2): 81-100.

Field, M.E. 1991. Liquefaction of continental shelf sediment: The Northern California earth quake of 1980. *In* Submarine landslides: Selected studies in the U.S Exclusive Economic Zone, *Edited by* Schwab, W.C., Lee, H.J. and Twichell, D.C.

Field, M.E., and Barber, J.H, Jr. 1991. A submarine landslide associated with shallow sea floor gas and gas hydrates off Northern California. *In* Submarine landslides: Selected studies in the U.S Exclusive Economic Zone, *Edited by* Schwab, W.C., Lee, H.J. and Twichell, D.C.

Field, M.E., and Jennings, A.E. 1987. Sea floor gas seeps triggered by a northern California earthquake. Marine Geology, **77**: 39-51.

Fourie, A.B., Hoffman, B.A., Mikula, R.J., Lord, E.R.F., and Robertson, P.K. 2001. Partially saturated tailings sand below the phreatic surface. Geotechnique, **51**(7): 577-585.

Fredlund, D.G., and Morgenstern, N.R. 1977. Stress state variables for unsaturated soils, Journal of Geotechnical Engineering, **103**: 447-466.

Fredlund, D.G., and Rahardjo, H. 1993. Soil mechanics for unsaturated soils. John Wiley & Sons, Inc., New York, New York.

Grozic, J.L.H. 1999. The behaviour of loose gassy sand and its susceptibility to liquefaction. Ph.D. Thesis, University of Alberta, Edmonton, Alberta, Canada.

Hardin, B.O. and Black, W.L. 1969. Closer to vibration modulus of normally consolidated clay. Journal of Soil Mechanics and Foundation Engineering Division, ASCE, **95** (SM6): 1531-1537.

Hardy, R.M., and Hemstock, R.A. 1963. Shearing strength characteristics of Athabassca oil sands. K.A.Clark Volume, Research Council of Alberta, Information Series No. 45, pp.109.

Hilf, J.W. 1948. Estimating construction pore pressures in rolled earth dams. Proceeding of the 2nd International conference on Soil mechanics and Foundation engineering, Rotterdam, The Netherlands. **3**:234-240.

Hulbert, M.H., and Bennett, R.H. 1975. Electrostatic cleaning technique for fabric SEM samples. Clays and Clay minerals, **23**:331.

Imam, S.M.R. 1999. Modeling the constitutive behaviour of sand for the analysis of static liquefaction. Ph.D. Thesis, University of Alberta, Edmonton, Alberta, Canada.

Ishihara, K., Tatsuoka, F., and Yasuda, S. 1975. Undrained deformation and liquefaction of sand under cyclic stresses. Soils and Foundation, **15**(1): 29-44.

Kayen, R.E., and Lee, H.. 1991. Pleistocene slope instability of gas hydrate-laden sediment on the Beaufort sea margin. Marine Geotechnology, **10**:125-141.

Kvalstad, T.J., Nadim, F., Dyvik, R., Grozic, J.L.H., and Sandbakken, G. 2003. Evaluation of deep water soil instability – Phase 2: Tests on artificial clay (Laponite) and triaxial tests on clay from Congo slope. Norwegian Geotechnical Institute Report No: 20001 108-05.

Lade, P.V. 1978. Prediction of undrained behaviour of sand. Journal of Geotechnical Engineering. ASCE, GT6, **104** : 721-735.

Lade, P.V. 1992. Static instability and liquefaction of loose fine sandy slopes. Journal of Geotechnical Engineering. ASCE. **118**(1): 51-70.

Lade, P.V., and Duncan, J.M. 1976. Stress-path dependent behaviour of cohesionless soil. Journal of Geotechnical Engineering, ASCE, GT1, **102**: 1019-1036.

Lee, H.J., Schwab, W.C., and Booth, J.S. 1991. Submarine landslides: An introduction. *In* Submarine landslides: Selected studies in the U.S Exclusive Economic Zone, *Edited by* Schwab, W.C., Lee, H.J. and Twichell, D.C.

Linsky, N.G., Lyakhovsky, V., and Navon, O. 2002. Expansion dynamics of volatile-supersaturated liquids and bulk viscosity of bubbly magmas. Journal of Fluid Mechanics, **460**: 39-56.

McKenna, G.T., Luternauer, J.L., and Kostaschuck, R.A. 1992. Large scale mass wasting events on the Fraser River delta front near Sand Heads, British Columbia. Canadian Geotechnical Journal, **29**: 151-156.

Mienert, J., Andreasson, K., and Bunz, S. 2003. Gas hydrate at Storegga slide, *In* European margin sediment dynamics; side-scan sonar and seismic images, *Edited by* Mienert, J., and Weaver, P. Springer-Verlag. Berlin, Federal Republic of Germany.

Morgenstern, N.R. 1967. Submarine slumping and the initiation of turbidity currents. *In* Marine Geotechnique, *Edited by* A.F.Richards. University of Illinois Press, Urbana, III., pp. 189-210.

Nova, R., and Wood, D.M. 1979. A constitutive model for sand in triaxial compression. International Journal for Numerical and Analytical methods in Geomechanics, **3**: 255-278.

Pestana, J.M., and Whittle, J.A. 1995. Compression model for cohesionless soils. Geotechnique, **45**(4): 611-631.

Pietruszczak, S., and Pande, G.N. 1996. Constitutive relation for partially saturated soils containing gas inclusions. J.of Geotech.Engrg. ASCE. **122**(1): 50-59.

Popene, P., Schmuck, E.A., and Dillon, W.P. 1991. A submarine landslide associated with shallow sea floor gas and gas hydrates off Northern California. *In* Submarine landslides: Selected studies in the U.S Exclusive Economic Zone, *Edited by* Schwab, W.C., Lee, H.J. and Twichell, D.C.

Pubela, H., Byrne, P.M., and Phillips, R. 1997. Analysis of CANLEX liquefaction embankments: prototype and centrifuge models. Canadian Geotechnical Journal, **34**: 641-657.

Rad, N.S., Vianna, A.J.D., and Berre, T. 1994. Gas in soils. II: Effect of gas on undrained static and cyclic strength of sand. J.of Geotech.Engrg. ASCE. **120**(4): 716-737.

Rau, G., and Chaney, R.C. 1988. Triaxial testing of marine sediments with high gas content. Advanced Triaxial Testing of Soil and Rock, ASTM STP 977, pp-338-352.

Robertson, P.K. 1994. Suggested terminology for liquefaction. Proceedings of the 47th Canadian Geotechnical Conference, Halifax, September 1994. 277-286.

Roscoe, K.H., Schofield, A.N., and Wroth, C.P. 1958. On the yielding of soils. Geotechnique, **8**:22-53.

Rowe, P.W. 1962. The stress-dilatancy relation for static equilibrium of an assembly of particles in contact. Proceeding of the Royal society of London, A269, pp-500-527.

Schuurman, I.E. 1966. The compressibility of an air-water mixture and a theoretical relation between the air and water pressures. Geotechnique. **16**: 269-281.

Sills, G.C. Drained triaxial testing of gassy soils. Final report on SERC grant No. GR/D/67064.

Sills, G.C., Wheeler, S.J., Thomas, S.D., and Gardner, T.N. 1991. Behaviour of offshore soils containing gas bubbles. Geotechnique, **41**(2): 227-241.

Sills, G.C., and Gonzalez, R. 2001. Consolidation of naturally gassy soft soil. Geotechnique, **51**(7): 629-639.

Silva, A.J., and Brandes, H.G. 1998. Geotechnical properties and behaviour of high-porosity, organic-rich sediments in Eckernforde Bay, Germany. Continental Shelf Research.

Sobkowikz , J.C. 1982. The mechanics of gassy sediments. Ph.D. thesis, University of Alberta, Alberta, Canada.

Sobkowikz, J.C., and Morgenstern, N.R. 1984. The undrained equilibrium behaviour of gassy sediments. Canadian Geotechnical Journal, **21**: 439-448.

Sultan, N., Vanoudheusden, E., and Cochonat, P. 2003. Evaluation of deep water soil instability – Phase 2, NGI reference: 20001108.

Terzaghi, K. 1936. The shearing resistance of saturated soils and the angle between the planes of shear. Proceedings of the 1st International Conference on Soil Mechanics, Harvard, **1**:54-56.

Terzaghi, K. 1956. Varieties of submarine slope failures. *In* Proceedings of the 8th Texas conference on soil and foundation engineering, University of Texas, Austin, pp. 1-41.

Thomas, S.D. 1987. The consolidation behaviour of gassy soil. Ph.D. Thesis, University of Oxford.

Thomas, S.D. 1989. A finite element model for the analysis of wave induced stresses, displacements and pore pressures in an unsaturated sea bed. Computers and Geotechnics. **8**: 1-38.

Vaid, Y.P., and Eliadorani, A. 1988. Instability and liquefaction of granular soils under undrained and partially drained states. Canadian Geotechnical Journal. **35**: 1053-1062.

Wheeler, S.J. 1988a. A conceptual model for soils containing large gas bubbles. Geotechnique. **38**: 389-397.

Wheeler, S.J. 1988b. The undrained shear strength of soils containing large gas bubbles. Geotechnique. **38**: 399-413.

Whelan, T. III, Coleman, J.M., Suhayda, J.N., and Roberts, N.H. 1977. Acoustical penetration and shear strength in gas charged sediments. Marine Geotechnology. **2**: 147-159.

Wong, R.C.K. 2003. Kinetics of gas exsolution in oil sands under undrained unloading. *Submitted to* Canadian Geotechnical Journal.

Wood, D.M. 1990. Soil behaviour and critical state soil mechanics. Cambridge University Press, Cambridge.